Formulation and Development of

Recombinant Protein Vaccines

By

Brooke S. Barrett

Submitted to the Department of Pharmaceutical Chemistry and the Faculty of the Graduate School of the University of Kansas in partial fulfillment of the requirements for the degree of Doctor of Philosophy.

Dissertation Committee

_____

Chairperson

_____

_____

_____

_____

Dissertation defended on April 2, 2009

©2009
Brooke S. Barrett

The Dissertation Committee for Brooke S. Barrett certifies that this is the approved version of the following dissertation:

Formulation and Development of

Recombinant Protein Vaccines

Dissertation Committee

_____

Chairperson

_____

_____

_____

_____

Date approved: April 2, 2009

ABSTRACT

Recombinant protein vaccines are fast becoming the focus of the vaccine industry due to their increased safety. Here we examine the development of several recombinant protein vaccines and the challenges involved. Once an antigen is identified, and a process to recombinantly produce the protein established, the first step is to perform a biophysical characterization of the macromolecule. The proteins were stressed with respect to variables such as temperature and pH and monitored for perturbations in physical structure indicating potential sources of instability. Next, we examined aspects of formulation such as excipient screening and adjuvant adsorption which may enhance the antigen immunogenicity and stability. The third step involved evaluating the working formulation in an animal model to establish dose dependency and the effect of the adjuvant. Finally, accelerated and real-time stability studies are being completed, and the formulations adjusted accordingly.

We begin with three analogous mutant proteins from the pathogenic bacteria *Shigella flexneri, Burkholderia pseudomallei and Salmonella typhimurium.* All three species rely on a type III secretion system (TTSS), commonly referred to as a supramolecular injectisome, for virulence. This macromolecular complex is composed of 25 or more proteins which form basal and extracellular domains, and shares gross architectural similarities with bacterial flagella. The extracellular component or 'needle complex', previously identified as a potential vaccine target, is primarily composed of a single monomeric subunit organized in a helical array to form a hollow pore which

protrudes from the bacterial membrane. Results of the biophysical characterization studies indicate that the secondary structure is largely α-helical in all three proteins, and surprisingly thermally labile with transition midpoints in the range of 35-50 ^{o}C over the pH range of 3-8. Second derivative UV absorbance spectroscopy data indicates some disruption of the protein's tertiary structure occurs at temperatures in the range of 29-46 ^{o}C. It appears, that at physiological temperatures, all three proteins experience intermediate nonnative molten globule like states in which they display significant secondary structure in the absence of extensive tertiary interactions. These antigens are found to be thermally stabilized by the presence of carbohydrates and polyols, and additionally all adsorb readily to aluminum hydroxide apparently through hydrogen bonds and/or Van der Waals forces. We have found that the interaction of the proteins with the adjuvant changes with time resulting in varying extents of irreversible binding. Peptide maps of desorbed protein, however, suggest that chemical changes are not responsible for this irreversibility. We also demonstrate the ability of MxiH$^{\Delta 5}$ and PrgI$^{\Delta 5}$ to elicit strong humoral immune responses in a murine model when administered as three intramuscular injections. When administered as monomers, the needle components exhibited strong dose dependent behavior, while the polymerized version (shown only for MxiH) was exceptionally immunogenic at low doses.

The second system described here is a recombinant ricin vaccine. There is an urgent need for the development of protective countermeasures against the use of ricin toxin as a bioterrorism agent due to its ease of access and distribution as well as its low lethal dose. We describe here the characterization of the stability of RiVax®, an

aluminum salt adsorbed recombinant ribotoxin A-chain double mutant, and optimization of adjuvant-antigen interactions which has allowed us to produce a stable vaccine that displays strong immunogenicity in mice. We used front face fluorescence as a physical measure of protein stability and monitored the adsorbed product upon storage at various temperatures. Indications of protein unfolding were observed and in the most extreme cases correlated with a decrease in immunogenicity of the vaccine. By adding phosphate anion, we are able to prevent the conformational changes, and maintain immunogenicity of the vaccine during long term storage.

Dedicated to:

My parents,
Helen Krause and Tim Barrett

ACKNOWLEDGEMENTS

This work would not have been possible without the continued guidance and support of my graduate advisor Dr. Russ Middaugh. Russ's passion for science is truly extraordinary and his dedication to teaching students is genuinely appreciated. I want to specifically thank Russ for his patience, and for recognizing when I actually needed help and when I just thought I did. I would also like to thank our lab director, Dr. Sangeeta Joshi, for her friendship and scientific guidance throughout the years. I am also grateful for each of my colleagues, both past and present, in the Middaugh lab. The camaraderie and humor were critical to getting through long days of research, and the scientific discussions were helpful too. Specifically, I would like to thank Aaron Markham for being a fantastic partner and for bringing humor into all our ventures.

I would also like to express thanks to Drs. Cory Berkland, Susan Lunte, Teruna Siahaan and Bill Picking for taking the time out of their full schedules to serve on my dissertation defense committee.

I would like to acknowledge the NIH Biotechnology Training Grant as well as Pharmaceutical Research and Manufacturers of America (PhRMA) for their generous financial support of my graduate research.

In addition, I would like to thank our collaborators Dr. Robert Brey of DOR Biopharma Inc. and the entire RiVax® team for the opportunity to contribute to the development of a ricin vaccine. Also, sincere thanks to Drs. Bill and Wendy Picking for their scientific insight and support of the needle protein project.

I would also like to recognize and thank the distinguished faculty and staff of the Department of Pharmaceutical Chemistry. This department has been, and continues to be, regarded as one of the premiere institutions in the field because of your hard work and commitment. I am both honored and proud to have studied here and I thank you for that opportunity.

I am genuinely thankful for the friendship of all past and present graduate students in the department. In particular, I would like to thank Dr. Laura Peek for teaching me 'the ropes' before leaving, and also for her friendship since. Our monthly dinners have been an true blessing, and I hope we can continue both our scientific discussions and personal friendship long-distance. I would also like to thank Courtney Kuhnline, Diana Sperger, Maria Thorson and Natalie Ciaccio for all the fun they brought to my graduate school experience. I would like to more specifically thank Courtney for being my study buddy, my lunch buddy and my stamping buddy. I will really miss seeing you everyday! I also want to thank my roommates and friends for their endless encouragement and support. Sneha, you have been an amazing friend to me and I will always cherish all the time we've spent studying together and procrastinating studying together!

Last, but certainly not least, I would like to thank my family and my boyfriend for their continuous encouragement and infinite patience. Mom, there are no words to express how fortunate I feel to have you as my mother. You are truly my best friend and I can say with absolute certainty that I would not have made it through this without you as my 'number one fan'. Dad, you have taught me the true value of hard work and taking

pride in what I do. I will miss our family dinners more than you know, and promise to come back to Kansas someday! Gus, I am amazed and grateful for your ability to 'bring me down a level' and remind me that life isn't meant to be so serious. I am looking forward to our adventure in Pennsylvania and whatever else comes our way! And finally, I would like to thank GOD for blessing my life with health, education and wonderful people.

TABLE OF CONTENTS

INDEX OF FIGURES

INDEX OF TABLES

LIST OF ABBREVIATIONS

A	Alanine
Å	Angstrom
ACS	American Chemical Society
Al	Aluminum Hydroxide
ANS	8-Anilino-1-napthalene sulfonate
APBS	Adaptive Poisson-Boltzmann Solver
APC	Antigen Presenting Cell
AU	Absorbance Unit
CD	Circular Dichroism
CDC	Centers for Disease Control
Da	Dalton
DSC	Differential Scanning Calorimetry
ELISA	Enzyme Linked Immunosorbent Assay
EPD	Empirical Phase Diagram
FDA	Food and Drug Administration
ff-Fluor	Front Face Fluorescence
FTIR	Fourier Transform Infrared Spectroscopy
GRAS	Generally Regarded As Safe
HiB	*Haemophilus influenzae* type b
HPLC	High Performance Liquid Chromatography

HRP	Horseradish Peroxidase
IACUC	Institutional Animal Care and Use Committee
IC	Immune Correlate
Ipa	Invasion Plasmid Antigen
ITC	Isothermal Titration Calorimetry
LD_{50}	Lethal Dose, 50%
LPS	Lipopolysaccharide
M	Methionine
MWCO	Molecular Weight Cut-off
NMR	Nuclear Magnetic Resonance
NRC	National Research Council
PBS	Phosphate Buffered Saline
PhRMA	Pharmaceutical Researchers and Manufacturers of America
Phe	Phenylalanine
pI	Iso-electric Point
PZC	Point of Zero Charge
RIP	Ribosome Inactivating Proteins
RNA	Ribonucleic Acid
RTA	Ribotoxic A Chain
RTB	Ribotoxic B Chain
rRTA	Recombinant Ribotoxic A Chain

RT	Room Temperature
Soln	Solution
TD	Thymus Dependent
TI	Thymus Independent
T_m	Midpoint of Thermal Melting
TMB	3,3',5,5'-tetramethylbenzidine
Trp	Tryptophan
TTSS	Type Three Secretion System
Tyr	Tyrosine
UV	Ultraviolet
V	Valine
VLS	Vascular Leak Syndrome
WHO	World Health Organization
Y	Tyrosine

Chapter 1

Introduction

1.1 History

The initial origin and continued development of the field of vaccinology is truly remarkable. The earliest practice of variolation is attributed to a group of 7th century Indian Buddhists who drank the venom of poisonous snakes, which may have been a toxoid-like product, to become immune to its effect [1]. Some time later, in 11th century China, it was observed that prior smallpox exposure often protected humans against future acquisition of the disease and thus it became common practice to place variola scabs in the nose as a preventative measure [2, 3]. Other sources attribute the original smallpox variolation practices to India, but despite the origin it quickly spread to many nations as noted by Voltaire below [2, 3].

> "The Circassians perceived that of a thousand persons hardly one was attacked twice by full blown spallpox; that in truth one sees three or four mild cases but never two that are serious and dangerous; that in a word one never truly has that illness twice in life."
>
> -Voltaire, "On Variolation," Philosophical Letters, 1734.

The same practice was in fact used by George Washington, who insisted that the men of his Continental Army undergo smallpox variolation treatment prior to encounters with their largely immune English opponents [4]. Although revolutionary, variolation practices were quite crude and involved intentionally transmitting disease in order to confer protection. As a result, a number of people died from the 'protective' treatment [5].

The next major discovery in vaccinology was made by Edward Jenner in 1798, when he discovered that immunity against smallpox could be produced in those inoculated with cowpox, a mild illness in humans [6]. He also discovered that cowpox could be transmitted from person-to-person thereby enabling mass protection against deadly outbreaks [6]. Louis Pasteur succeeded Jenner in the summer of 1879 when he discovered an alternative to person-to-person vaccination strategies based on a similar concept of using a weakened form of the disease to induce immunity [7]. He was working on the chicken cholera bacterium at the time and discovered that an aged attenuated culture was protective [7]. He further concluded that this type of vaccination was safer because it was less likely, relative to treatment with a related organism, to transmit other disease. He also applied this approach to anthrax and rabies illnesses in 1885 [8]. Despite success, Pasteur was met with resistance in attempting to transfer this application from animals to humans because of the public fear of injecting a 'weakened' toxic material [9]. Pasteur's expertise was developed further in 1886 by Daniel Elmer Salmon and Theobald Smith who used heat to kill typhoid, cholera and plague organisms and proposed the resulting material as vaccines with increased safety because they were no longer virulent [10]. The rights to the discovery of this technique however were disputed due to similar yet subsequent discoveries in the laboratory of Pasteur, who was widely famous at the time [3]. Then, in the early 1900's, toxoids against diphtheria and tetanus, which could be prepared by treating the toxins with formalin at 37 ^{o}C, were found to be protective by a number of scientist including Gaston Ramon who created the first human vaccination [11, 12].

In the roughly 100 years following Jenner's 1798 discoveries, the field of vaccinology flourished, and the ensuing 100 years were no different. The application of cell culture and a greater understanding of immunology supplemented a rapidly growing field that saw the invention of vaccines against Yellow Fever, Pertussis, Influenza, Typhus, Polio, Measles, Mumps, Adenovirus, Varicella, Japanese Encephalitis, Hepatitis A, Meningitis, Pneumococcus and *Haemophilius influenzae* type b [5]. Additionally, mass vaccination campaigns led by the World Health Organization (WHO) completely eliminated naturally occurring smallpox in the year 2005 and are currently focused on the eradication of polio [3,13,14]. It is now well recognized that the prevention of disease through vaccination, if possible, is far more effective than post-infection treatment. This sentiment is well stated by vaccinologist Stanley Plotkin:

> "The impact of vaccination on the health of the world's peoples is hard to exaggerate. With the exception of safe water, no other modality, not even antibiotics, has had such a major effect on mortality's reduction and population growth."

1.2 Definition

By definition, a vaccine is a biological preparation which may include peptides, proteins, polysaccharides, polynucleotides, viruses and other whole organisms that establishes or improves immunity to a particular disease [15]. The word carries with it a deliberate history as it was adapted from Edward Jenner's 1798 discovery that when administered to humans, cow pox (*variolæ vaccinæ)* would protect against smallpox [15]. As indicated above, there are many different types of routinely used vaccines, and many

more in various stages of development. Each vaccine type has noted advantages and disadvantages associated with both its application to certain organisms as well as its use in humans.

1.2.1 Live, Attenuated

Vaccines composed of live attenuated organisms contain the entire disease causing organism and thus are intrinsically extremely potent. These vaccines are able to stimulate both the humoral and cellular immune systems often resulting in life-long protection after just one dose [3]. Although the vaccine has been attenuated through exposure to heat, chemicals or radiation, there is a small likelihood that the agent may not be completed altered or may revert to its virulent form [3, 15]. For this reason, attenuated vaccines are some of the most dangerous and are rarely given to immuno-compromised patients who are the most likely to contract the illness from a small number of untreated or reverted organisms [15]. Another disadvantage of live attenuated vaccines is the common requirement that they be refrigerated before use to maintain biological activity [15]. This is extremely problematic for developing countries where a cold-chain may not be available for the entire transport route.

1.2.2 Killed, Inactivated

Vaccines which are referred to as killed or inactivated typically consist of formaldehyde or heat treated organisms or toxoids which cannot revert to their virulent form [15]. This type of vaccine is known to generate a weaker immune response relative

to live attenuated versions because only the humoral immune system is stimulated. They are notably safer, but may require administration of several doses to ensure protection [15]. Killed inactivated vaccines are regarded as being easier to store relative to live attenuated vaccines because they can often be lyophilized [15].

1.2.3 Conjugated

A conjugate vaccine refers to one in which a poor immunogen is covalently linked to a carrier protein. The antigen is typically a bacterial polysaccharide such as that seen on the surface of *Haemophilus influenzae* B (HiB), *Streptococcus pneumoniae* or *Nesseria meningitis* which are considered poor antigens in children because they are Thymus cell independent (TI) and therefore do not induce the necessary opsinizing antibodies [3]. Through their association with a Thymus cell dependent (TD) carrier protein, the most common of which are tetanus and diptheria toxoids, they confer the proper protective response [3].

1.2.4 Subunit

Subunit vaccines are considered the safest; however they are also far less immunogenic than attenuated or killed vaccines because they represent only a portion of the organism and therefore do not stimulate the immune system to the extent that a whole organism vaccine does [3, 15]. Subunit vaccines are composed of purified antigens which have been identified for their ability to stimulate the immune system, but are not infectious and thus are far less likely to induce unfavorable immune related side effects.

FDA approved examples of this approach are the Hepatitis B and Human Papillomavirus Vaccines; however a great number of vaccines using this approach are currently under investigation. Recently, the vaccine industry has focused largely on subunit vaccines due to their increased safety profile and the ability to manufacture them recombinantly in large quantities in a reproducible manner [3, 15]. One major challenge associated with their use, however, is their decreased antigenicity relative to whole cell vaccines which is often insufficient for protection. As a result, several booster doses are often required and may decrease patient compliance. Additionally, a vaccine adjuvant is almost always required.

1.3 Subunit Vaccine Development

Discussion herein will pertain to the development of several recombinant protein subunit vaccines. Therefore, we will discuss in greater detail those problems commonly encountered in this arena of vaccinology and the strategies used to overcome them. For example, as mentioned above, recombinant subunit vaccines are typically only weakly immunogenic relative to their whole cell counterparts due to their inability to stimulate both humoral and cellular immune responses. Their intrinsic immunogenicity is humoral in nature and mainly represented by the production of specific opsinizing antibodies [3]. Production of a protective response by a recombinant subunit vaccine often requires administration of several doses as well as the presence of an adjuvant [3]. A second challenge stems from the intrinsic instability of biomolecules as well as the criticality of antigen conformation to generate proper immune recognition. Close attention must be

paid to the stability of subunit vaccine antigens to ensure biological activity is sustained throughout storage until the point of administration.

1.3.1 Adjuvant Use

As a result of their decreased immunogenicity, subunit vaccines typically require the presence of adjuvant to elicit a protective immune response. When co-administered with an antigen, an adjuvant increases the specific immune response to the antigen without having any specific antigenic activity itself. Currently, only two adjuvants, both aluminum salts, are approved by the United States Food and Drug Administration (FDA) for human use, although novel adjuvants are a hot topic of current research and are in clinical development [16-18]. Aluminum salt adjuvants are suspensions of particles with highly charged surfaces which have been precipitated in the presence of selected anions. Aluminum hydroxide is described in the literature as consisting of aggregates of poorly crystalline material approximately 3 μm in size [19-21]. Its point-of-zero (PZC) charge is approximately 11 which means that at neutral pH, the particle surface is characterized by a net positive charge [21, 22]. Aluminum phosphate, precipitated in the presence of phosphate ions, is amorphous in nature and is slightly larger in size at approximately 4-5 μm [19-21]. Its corresponding PZC is lower than that observed for aluminum hydroxide, but can range from 5-7 [21, 22]. As a result, at neutral pH the material is negatively charged. The charged surface character of these substances facilitates an electrostatic interaction with proteins of the opposite charge, although forces such as hydrophobic

interactions, hydrogen bonds and Van der Waals forces may also be involved in their surface interactions [22].

Aluminum salts are commonly referred to as immunopotentiators due to their ability to prime the immune system. After nearly 100 years of investigation and use, however, their exact mechanism of action is still unclear. Several mechanisms have been suggested, and it appears that their actual complex course of action may be a combination of several factors and may be dependent on both the injection route as well as the antigen.

The two most widely accepted mechanisms of action are that of depot formation and enhanced targeting to antigen presenting cells (APCs). When injected, aluminum adsorbed vaccines disperse slowly from the site of injection due to their particulate nature resulting in a depot which produces sustained release of antigen [23-27]. Additionally, the adsorbed antigens are more likely to be targeted for uptake by APCs due to their increased size relative to soluble antigens [23-26, 28]. Aluminum salt particles are in the range of 5 μm and macrophages are known for their ability to target and phagocytose particulate material up to 10 μm [29].

The third mechanism is broadly referred to as immunopotentiation, and over time many groups have hypothesized and investigated specific mechanisms of such proposed activity. More specifically, one group found that aluminum salts are toxic to nearby cells causing them to induce the secretion of uric acid, resulting in recruitment of monocytes to the site of injection. This is suggested to result in more efficient antigen processing [30, 31]. Similarly, others proposed that aluminum salts induce a local inflammatory immune response that attracts immunocompetent cells and thereby enhances the antigen specific

immune response [32-34]. Still another group hypothesized that aluminum salts activate the complement system. Studies in which the aluminum salt and antigen were administered separately, at locations remote from one another were presented as support for this systemic theory [35].

Historically, the major disadvantage to the use of aluminum salt adjuvants is their inability to stimulate the cell mediated responses. Several groups have, however, proposed that by adding selected interleukins, both humoral and cellular responses can be initiated [36, 37]. Additionally, the instability of aluminum salts to lyophilization has limited their use in a number of formulations. It has been shown recently, however, that provided an optimized cycle is developed, it is possible to lyophilize aluminum salts without observing gross aggregation of the product [38]. Other disadvantages include stimulation of IgE (allergic) mediated responses, erythema and/or contact hypersensitivity and the inability of the adjuvants to boost responses for all antigens [19].

The most widely recognized advantage to the use of aluminum salt adjuvants is the induction of higher, faster and longer antibody responses to a primary immunization using small, antigenically weak synthetic or recombinant antigens [39]. It is also recognized that the presence of an aluminum salt adjuvant may reduce the amount of antigen or number of injections required to elicit a protective response [17, 19, 25]. Thus, drug companies can include less antigen per dose enabling production of a greater number of doses. Additionally, aluminum salt adjuvants are recognized for their ability to improve efficacy of vaccines in newborns, elderly and otherwise immuno-compromised patients [17, 19, 25].

It is currently unclear exactly which formulation factors, degree of adsorption, dose of adjuvant and/or strength of this interaction, are the most important for immunogenicity of adsorbed antigen. It is hypothesized that optimal conditions may vary depending on the antigen. For example, FDA regulations require that adult tetanus and diptheria toxoid be >75% adsorbed [40], however vaccines with low adsorption (<50%) have been used effectively and meet all regulatory requirements [19]. Additionally, some research suggests that in order to attain an optimal effect, excess free adjuvant must be present [41,42]. There appears, however, to be a critical maximum level above which the antigen specific immune response is decreased [43-45]. This phenomenon may be a result of antigen masking [25] or perhaps macrophage toxicity [46]. More recently, it has been established that the strength of adsorption affects the immunogenicity [47, 48]. Specifically, results from these studies indicate that immunogenicity is decreased if the antigen is too tightly bound to the adjuvant. Thus, there are a number of factors influencing efficacy of an adsorbed antigen, and each must be evaluated thoroughly to ensure optimal efficacy of each vaccine product.

1.3.2 Protein Stability

Proteins and peptides are the most common constituents of subunit vaccines. Although simple in structure relative to whole virus vaccines, proteins are associated with an array of both chemical and structural problems due to their dynamic character and the presence of higher order structure. Biomolecules used in vaccines must remain within established stability parameters to eliminate the potential for adverse effects on

antigenicity. A loss in biological activity is often the result of aggregation or adsorption to the walls of the storage container, epitope loss, or decreased uptake and processing by the immune system. By studying the physical and chemical stability of proteins we can learn about their potential sources of instability and take pro-active formulation steps to prevent them.

Proteins are charged polymers with distinct primary, secondary, tertiary and sometimes quaternary structure. Primary structure involves the amino acid sequence, while the secondary structure involves local interactions of the peptide backbone leading to structures such as helices and sheets. Tertiary structure describes the interaction of secondary structural elements to form a distinct three dimensional shape while quaternary structure defines the interaction among protein monomers, each with tertiary structural elements. Every aspect of structure is influenced by changes in solution conditions such as pH, ionic strength and temperature. The pH of a solution, for example, impacts the charge state of individual amino acid side chains and therefore their interaction with other residues and the solvent to form secondary, tertiary and possibly quaternary structure. Additionally, pH can affect chemical degradation reactions which can alter the protein primary sequence and therefore higher order structural elements. Changes in ionic strength can alter solubility and can also directly affect protein structure and stability by weakening electrostatic interactions which contribute to protein structure through charge pair formation. The effects of temperature on protein folding and stability are also important. As temperature is increased, bonds responsible for maintaining protein structure may be weakened leading to either reversible or irreversible protein unfolding.

Additionally, just as in the case of pH, some chemical degradation reactions are promoted by elevated temperatures and may result in protein degradation. As mentioned above, it is critical to vaccine efficiency that the stability profile for a proposed vaccine antigen be thoroughly characterized and well understood in order to propose formulation conditions which can reproducibly maintain antigenicity.

In many cases, biological assays such as immunogenicity in animals are key to studying vaccine stability. While necessary, biological assays do not provide information regarding the source or origin of instability. Thus, it is imperative that chemical and physical techniques be used to enable the development of formulations based on specific case-by-case behavior.

The chemical integrity of a protein is often examined using high-performance liquid chromatography (HPLC) in one of several formats (reversed phase, hydrophobic interaction, ion-exchange or size exclusion). These techniques allows for the sensitive detection of changes in polarity, charge or size, which are often the result of chemical modifications. Additionally, one can couple HPLC columns to mass spectrometers to identify the nature of the chemical change as well as its location in the protein primary structure.

Biophysical techniques enable one to evaluate various structural aspects of proteins which often result in unfolding, aggregation or other adverse events. X-ray crystallography and NMR are commonly used to elucidate high resolution three dimensional structures which greatly aide studies of structural stability. It is also possible to obtain structures under various solution conditions to investigate the effects of solute

concentration, pH or other variables. The drawback is that these methods are often rather time extensive and usually require large amounts of highly purified antigens which are not always available during early stages of vaccine development. Other spectroscopic techniques of potential utility in biophysical studies of macromolecular systems are static and dynamic light scattering, circular dichroism, intrinsic and extrinsic fluorescence, UV absorbance, infrared and Raman spectroscopies and differential scanning and isothermal titration calorimetry. Each technique can be utilized under a range of solution conditions to monitor subtle changes in protein conformation and thereby enable analysis of stability related phenomenon. For example, if upon an increase in temperature a protein displays a decrease in structural elements, one can presume that unfolding major structural alterations are occurring. Although this represents a somewhat simplistic use of spectroscopic techniques, the same approach can be applied in more complex scenarios. Light scattering techniques are often used to determine size or molecular weight of a protein and thus can be used to monitor unfolding and/or aggregation events. Circular dichroism spectroscopy is used to monitor secondary structure based on the chiral nature of secondary structural elements. Ultraviolet absorbance and fluorescence emission spectroscopies are used to define changes in tertiary structural elements by using aromatic residues as probes of their surrounding environments. Infrared and Raman spectroscopies focus on characterizing aspects of secondary and tertiary structure based on vibrational properties of peptide bonds and side chains. Calorimetry permits the study of the thermal properties of vaccine components in terms of thermally induced structural changes (DSC) and interaction between molecular components (ITC).

There are several approaches available to prevent or slow changes in protein structure during storage and to preserve biological activity. The most common is the addition of compounds such as organic osmolytes which stabilize antigens based on their preferential hydration [49]. This phenomenon forces surrounding water molecules to pack in a more ordered fashion around the protein surface and thereby discourages protein unfolding. Surfactants can also be used as excipients by interfering with protein aggregation and/or surface adsorption [50, 51]. Another commonly utilized stabilization technique is lyophilization or freeze drying. Many biomolecules exhibit enhanced stability as dry powders where dynamic motions are restricted. It is also possible in some cases to eliminate the source of instability by point mutating specific residues or deleting regions of protein primary structure. It is important, however, to verify that critical epitopes have not been altered if this is necessary. Another option for protein stabilization is to restrict the conformational mobility through disulfide bonds or chemical crosslinking. In all cases, it is imperative to ensure that alterations made do not alter antigenicity.

1.4 Specific Aims

In this work, I will examine the task of developing several recombinant subunit proteins as vaccine antigens. These studies can be divided into several sections each of which builds upon previous work. The first effort was to thoroughly characterize the solution stability of a previously selected group of antigens using biophysical methods. This was done to identify potential formulation problems as well as define conditions

under which the antigen was most stable and therefore suitable for formulation. The second step, which is referred to as pre-formulation, involved the examination of formulation parameters such as excipient stabilization adjuvant adsorption. The third portion involved the use of animal models to evaluate the antigenicity of preliminary formulations upon which adjustments and improvements were made. Finally, the final step evaluated the stability of the adsorbed formulation using real time and accelerated models and correlated the results with animal immune responses. Final adjustments were made based on the results obtained, and clinical work was initiated by collaborators.

I will present data from each of the steps indicated above. The data, however, pertain to more than one antigen. The first three chapters present work done on a series of analogous mutant proteins, $MxiH^{\Delta 5}$, $PrgI^{\Delta 5}$ and $BsaL^{\Delta 5}$ from three different bacterial pathogens while data in the last chapter pertains to rRTA, a single mutated chain from ricin toxin. All antigens discussed here share in common their recombinant subunit nature and the need for an adjuvant.

1.4.1 Biophysical Characterization of Needle Proteins

The data presented in Chapter 2 is related to the first step in the development process described above. Through the use of several spectroscopic techniques, we compiled a set of data representative of the conformational behavior of several antigens under conditions of thermal stress and over a pH range of 3-8. Then, using a previously established approach [52-55], we converted the individual data points at each pH and temperature condition into a series of vectors and assigned them arbitrary color

representations. When summed, the vectors are represented in the form of a multi-colored phase diagram which enables the identification of solution conditions under which the antigen remains stable, and those which induce structural changes.

1.4.2 Pre-formulation of Needle Proteins

Chapter 3 details pre-formulation experiments which were designed using information acquired in the biophysical characterization step. We screened each of the antigens for thermal stabilization by a group of "generally regarded as safe" (GRAS) compounds and then investigated the strength and nature of their interactions with both aluminum phosphate and aluminum hydroxide adjuvants. We also established accelerated and real time stability studies of the adsorbed formulation to examine the effect of storage temperature and duration on the adsorbed material.

1.4.3 Immunogenicity of Needle Proteins

In this chapter (4), we present data obtained from several murine immunogenicity studies. The purpose of this work was to confirm the hypothesized immunogenicity of the antigens, investigate the effect of dose on the magnitude of the response as well as examine the adjuvant affect, if any.

1.4.4 Adsorbed stability studies of rRTA

Chapter 5 describes a number of accelerated and real-time stability studies, and the exploration of a correlation between a physical and a biological assay. This chapter also contains work on the optimization of adjuvant-antigen interactions through modulation of the adjuvant surface.

1.4.5 Summary and Conclusions

The last chapter (6) serves as a summary of concepts and findings discussed herein. Suggestions for future work are also discussed.

1.5 Bibliography

[1] deBary W. The Buddhist Tradition in India, China and Japan. New York: Vintage Books, 1972.

[2] Fenner F, Henderson D, Arita I, Jezek Z, Ladnyi I. Early efforts at control: variolation, vaccination, and isolation and quarantine. In: Fenner F, Henderson D, Arita I, Jezek Z, Ladnyi I, editors. History of International Public Health. Geneva: World Health Organization, 1988: 245-76.

[3] Plotkin SL, Plotkin SA. A Short History of Vaccination. In: Plotkin SA, Orenstein WA, editors. Vaccines. 4th Ed. ed. Philadelphia: W.B. Saunders, 2004: 1-15.

[4] Fenn EA. Pox Americana: The Great Smallpox Epidemic of 1775-1782. New York: Hill and Wang, 2001.

[5] Parish HJ. A History of Immunization. London: E & S Livingstone, 1965.

[6] Jenner E. An Inquiry into the Causes and Effects of the *Variolae Vaccinae*. London: Low, 1798.

[7] Pasteur L. De l'attenuation du virus du cholera des poules. CR Acad Sci Paris 1880;91:673-80.

[8] Pasteur L. Methode our prevenir la rage apres morsure. CR Acad Sci Paris 1885;101:765-72.

[9] Geison GL. The Private Science of Louis Pasteur. Princeton: Princeton University Press, 1995.

[10] Salmon DE, Smith T. On a new mehtod of producing immunity from contageous diseases. Am Vet Rev 1886;10:63-9.

[11] Ramon G. Sur le pouvoir floculant et sur les proprietes immunisantes d une toxine diptherique redue anatoiquie. CR Acad Sci Paris 1923;177:1338-40.

[12] Ramon G, Zoeller C. L'anatoxine tetanique et immunisation active de l'homme vis-a-vis du tetanus. Ann Inst Pasteur Paris 1927;41:803-33.

[13] Fenner F, Henderson D, Arita I, Jezek Z, Ladnyi I. Smallpox and its eradication. Geneva: World Health Organization, 1988.

[14] Smith J, Leke R, Adams A, Tangermann R. Certification of polio eradication: process and lessons learned. Bull World Health Org 2004;82(1):24-30.

[15] Understanding Vaccines: What they are and how they work. [cited March 10, 2009]; Available from: http://www3.niaid.nih.gov/topics/vaccines/PDF/undvacc.pdf

[16] Harandi AM, Davies G, Olesen OF. Vaccine adjuvants: scientific challenges and strategic initiatives. Expert Review of Vaccines 2009;8(3):293-8.

[17] Petrovsky N, Aguilar JC. Vaccine adjuvants: Current state and future trends. Immunol Cell Biol 2004;82(5):488-96.

[18] Peek LJ, Middaugh CR, Berkland C. Nanotechnology in vaccine delivery. Advanced Drug Delivery Reviews 2008;60(8):915-28.

[19] Gupta RK, Rost BE. Aluminum Compounds as Vaccine Adjuvants. In: O'Hagan DT, editor. Vaccine Adjuvants: Preparation Methods and Research Protocols. Totowa: Humana Press, Inc., 2000: 65-89.

[20] Hem SL, White JL. Structure and Properties of Aluminum-Containing Adjuvants. In: Powell MF, Newman MJ, editors. Vaccine Design: The Subunit and Adjuvant Approach. New York: Plenum Press, 1995.

[21] Shirodkar S, Hutchinson RL, Perry DL, White JL, Hem SL. Aluminum Compounds Used as Adjuvants in Vaccines. Pharmaceutical Research 1990;7:1282-8.

[22] Al-Shakhshir RH, Regnier FE, White JL, Hem SL. Contribution of electrostatic and hydrophobic interactions to the adsorption of proteins by aluminium-containing adjuvants. Vaccine 1995;13(1):41-4.

[23] Edelman R. An Overview of Adjuvant Use. In: O'Hagan DT, editor. Vaccine Adjuvants: Preparation Methods and Research Protocols. Totowa: Humana Press, Inc., 2000: 1-27.

[24] Gupta RK. Aluminum compounds as vaccine adjuvants. Advanced Drug Delivery Reviews 1998;32(3):155-72.

[25] Gupta RK, Rost BE, Relyveld E, Siber GR. Adjuvant Properties of Aluminum and Calcium Compounds. In: Powell MF, Newman MJ, editors. Vaccine Design: The Subunit and Adjuvant Approach. New York: Plenum Press, 1995: 229-48.

[26] Mendez R, Ilia Z., Shi Y, HogenEsch H, Hem SL. Potentiation of the immune response to non-adsorbed antigens by aluminum-containing adjuvants. Vaccine 2007;25(5):825-33.

[27] Glenny AT, Buttle GAH, Stevens MF. Rate of disappearance of diphtheria toxoid injected into rabbits and guinea - pigs: Toxoid precipitated with alum. The Journal of Pathology and Bacteriology 1931;34(2):267-75.

[28] Morefield GL, Sokolovska A, Jiang D, HogenEsch H, Robinson JP, Hem SL. Role of aluminum-containing adjuvants in antigen internalization by dendritic cells in vitro. Vaccine 2005;23(13):1588-95.

[29] Eldridge JH, Staas JK, Meulbroek JA, Tice TR, Gilley RM. Biodegradable and biocompatible poly(DL-lactide-co-glycolide) microspheres as an adjuvant for staphylococcal enterotoxin B toxoid which enhances the level of toxin-neutralizing antibodies. Infect Immun 1991 September 1, 1991;59(9):2978-86.

[30] Kool M, Soullie T, van Nimwegen M, Willart MAM, Muskens F, Jung S, et al. Alum adjuvant boosts adaptive immunity by inducing uric acid and activating inflammatory dendritic cells. J Exp Med 2008 April 14, 2008;205(4):869-82.

[31] How alum works. J Exp Med 2008 March 24, 2008;205(4):742.

[32] White R, Coons A, Connolly J. Studies on antibody production. III. The alum granuloma. J Exp Med 1955;102(1):73-82.

[33] Ramanathan VV, Badenoch-Jones P, Turk JL. Complement activation by aluminum and zirconium compounds. Immunology 1979;37:881-8.

[34] Walls RS. Eosinophil response to alum adjuvants: involvement of T cells in non-antigen-dependent mechanisms. Proc Soc Exp Biol Med 1977;156:431-5.

[35] Flebbe LM, Braley-Mullen H. Immunopotentiating effects of the adjuvants SGP and Quil A. I. Antibody responses to T-dependent and T-independent antigens. Cell Immunol 1986;99:119-27.

[36] Jankovic D, Caspar P, Zweig M, Garcia-Moll M, Showalter SD, Vogel FR, et al. Adsorption to aluminum hydroxide promotes the activity of IL-12 as an adjuvant for antibody as well as type 1 cytokine responses to HIV-1 gp120. J Immunol 1997 September 1, 1997;159(5):2409-17.

[37] Pollock KGJ, Conacher M, Wei XQ, Alexander J, Brewer JM. Interleukin-18 plays a role in both the alum-induced T helper 2 response and the T helper 1 response induced by alum-adsorbed interleukin-12. Immunology 2003;108(2):137-43.

[38] Clausi AL, Merkley SA, Carpenter JF, Randolph TR. Inhibition of aggregation of aluminum hydroxide adjuvant during freezing and drying. Journal of Pharmaceutical Sciences 2008;97(6):2049-61.

[39] Volk VK, Bunney WE. Diphtheria Immunization with Fluid Toxoid and Alum-Precipitated Toxoid. Am J Public Health Nations Health 1942 July 1, 1942;32(7):690-9.

[40] Health NIo. Tetanus and diptheria toxoids combined precipitated, adsorbed (for adult use). In: Health USDo, editor. United States Minimum Requirements; 1956; Bethesda, MD; 1956.

[41] Cooper PD, McComb C, Steele EJ. The adjuvanticity of algammulin, a new vaccine adjuvant. Vaccine 1991;9:408-15.

[42] Jensen OM, Koch C. On the effect of $Al(OH)_3$ as an immunological adjuvant. Acta Pathol Microbiol Immunol Scand 1988;96:257-64.

[43] Hennessen W. The mode of action of mineral adjuvants. Prog Immunobiol Stand 1965;2:71-9.

[44] Holt LB. Quantitative studies in diptheria prophylaxis: An attempt to derive a mathematical characterization of the antigenicity of diptheria prophylactic. Biometric 1955;11:83-94.

[45] Schmidt G. The adjuvant effect of aluminum hydroxide in influenza vaccine. Symp Ser Immunobiol Stand 1967(275-282).

[46] Munder PG, Ferber E, Modolell M, Fischer H. The influence of various adjuvants on the metabolism of phospholipids in macrophages. Int Arch Allergy Appl Immunol 1969;36(1):117-28.

[47] Hansen B, Belfast M, Soung G, Song L, Egan PM, Capen R, et al. Effect of the strength of adsorption of hepatitis B surface antigen to aluminum hydroxide adjuvant on the immune response. Vaccine 2009;27(6):888-92.

[48] Hansen B, Sokolovska A, HogenEsch H, Hem SL. Relationship between the strength of antigen adsorption to an aluminum-containing adjuvant and the immune response. Vaccine 2007;25(36):6618-24.

[49] Lee JC, Timasheff SN. The stabilization of proteins by sucrose. J Biol Chem 1981 July 25, 1981;256(14):7193-201.

[50] Bam NB, Cleland JL, Yang J, Manning MC, Carpenter JF, Kelley RF, *et al.* Tween protects recombinant human growth hormone against agitation-induced damage via hydrophobic interactions. Journal of Pharmaceutical Sciences 1998;87(12):1554-9.

[51] Jones LS, Cipolla D, Liu J, Shire S, Randolph TW. Investigation of Protein-Surfactant Interactions by Analytical Ultracentrifugation and Electron Paramagnetic Resonance: The Use of Recombinant Human Tissue Factor as an Example Pharm Res 1999;16(6):808-12.

[52] Fan H, Kashi RS, Middaugh CR. Conformational lability of two molecular chaperones Hsc70 and gp96: Effects of pH and temperature. Arch Biochem Biophys 2006;447(1):34-45.

[53] Fan H, Ralston J, Dibiase M, Faulkner E, Middaugh CR. Solution behavior of IFN-γ-1a: an empirical phase diagram based approach. J Pharm Sci 2005;94(9):1893-911.

[54] Peek LJ, Brey RN, Middaugh C. A rapid, three-step process for the preformulation of a recombinant ricin toxin A-chain vaccine. J Pharm Sci 2007;96(1):44-60.

[55] Rexroad J, Talia T. Martin David McNeilly Simon Godwin C. Russell Middaugh. Thermal stability of adenovirus type 2 as a function of pH. Journal of Pharmaceutical Sciences 2006;95(7):1469-79.

Chapter 2

The Response of Type Three Secretion System Needle Proteins MxiH$^{\Delta 5}$, BsaL$^{\Delta 5}$ and PrgI$^{\Delta 5}$To Temperature and pH

2.1 Introduction

A variety of gram negative bacterial pathogens including *Shigella flexneri*, *Salmonella typhimurium*, *Burkholderia pseudomallei*, *Yersinia enterocolitica*, and *Pseudomonas aeruginosa* are responsible for an array of diseases including dysentery, gastroenteritis, typhoid fever and mellioidosis ranging in intensity from mild to lethal. Such diseases are common in developing nations where sources of food and water are commonly contaminated, but have also been implicated in cases of intentional exposure within the United States [1]. Despite attempts, there is currently no commercially available vaccine for any of the aforementioned pathogens. Each year, *Shigella* alone continues to infect more than 165 million people resulting in greater than 1.1 million deaths (http://www.who.int/vaccine_research/diseases/shigella/en/).

Essential to the virulence of these bacteria is their multi-component type III secretion system (TTSS), which mediates the specific secretion and translocation of virulence factors via a supramolecular structure. This surface localized protein complex is evolutionarily related to bacterial flagella [2,3]. Morphologically, this "syringe-like" structure consists of 25 or more unique proteins, and spans the bacterial membranes, extracellular space and host cellular membrane [2]. Direct physical contact between the bacterium and target cell allows the specific secretion and translocation of effector proteins into the cytosol of the target cell to interfere with host cell signaling processes [4, 5]. Although the syringe apparatus is morphologically similar and functionally conserved among the aforementioned bacteria, the constituent and secreted proteins vary among the different species [3].

The exposed filamentous portion of the TTSS, commonly referred to as the "needle", is approximately 60 nm long, and is comprised of approximately 120 copies of a monomeric subunit arranged in a superhelical array [6-8]. A pore approximately 2-3 nm in diameter lines the needle, and effectively connects the bacterial cytoplasm to the target host cell membrane [4-5]. The tip of the needle is composed of an invasion plasmid antigen (Ipa) protein unique to each bacterium [9]. Upon exposure to bile salts, this tip protein has been shown to specifically recruit a second unique Ipa protein which localizes distal to the needle tip [10]. It is possible that direct contact with the host cell by the distal protein represents the initiation of an activation pathway for the virulent invasion of the target cell. Transmission of the activation signal is suspected to pass through the helical needle structure, occurring by an unknown mechanism which may involve slight changes in the packing of the needle while maintaining the helical parameters defining the structure [6].

The monomeric subunits of the helical needle are small (~10 kDa), hydrophilic proteins with low isoelectric points (<5). Recent developments in structural studies of the acidic needle proteins indicate that their surfaces are characterized by distinct patches of positive and negative charge (Figure 2.1) [11]. This observation suggests that electrostatic interactions might be intimately involved in needle assembly, and consequently that changes in pH and/or ionic strength might affect this process [11]. Despite significant conservation in primary sequence (Figure 2.2), however, the three proteins do not share similar distributions of surface charge [11].

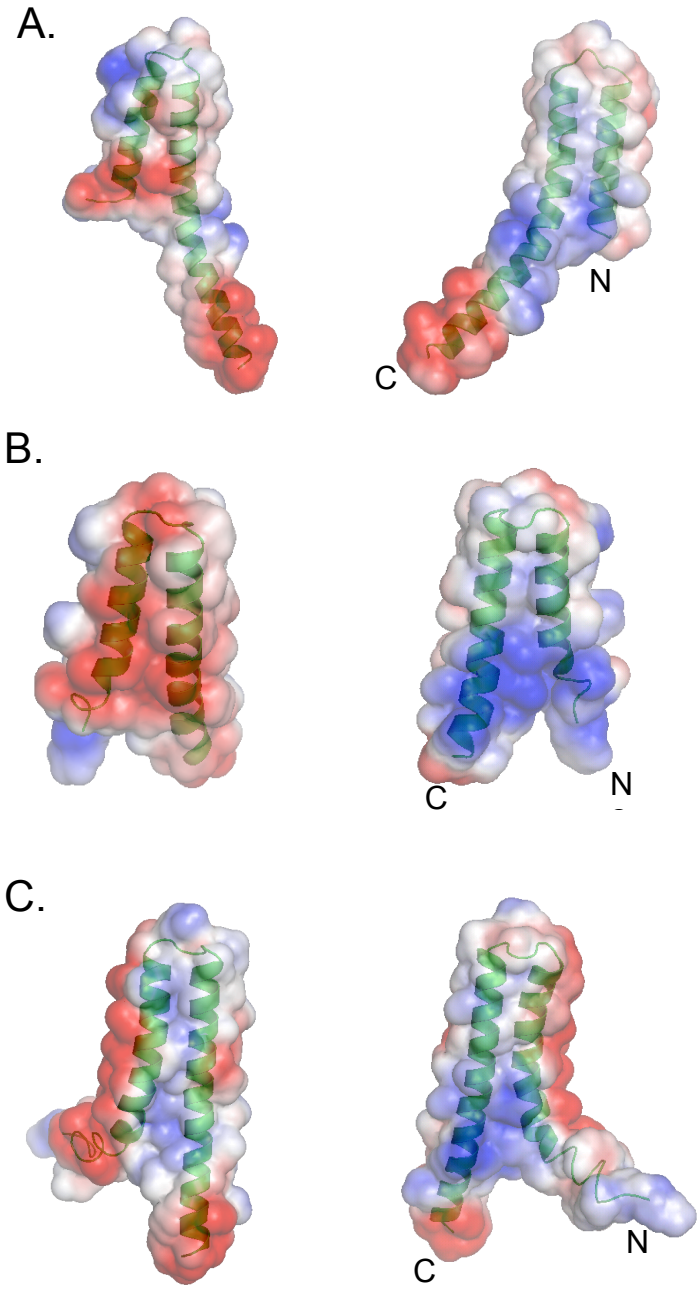

Figure 2.1 Shown for (A) MxiH$^{\Delta 5}$ (PDB # 2CA5), (B) BsaL$^{\Delta 5}$ (PDB # 2G0U) and (C) PrgI$^{\Delta 5}$ (PDB # 2JOW) is a protein ribbon structure overlaid with a solvent accessible surface map colored according to electrostatic potential where the color red denotes negatively charged regions and blue positively charged. Structures on the right panel represent a 180 degree rotation about the y axis. The surface electrostatic potential maps were calculated using APBS [44], and visualized using PyMol (http://pymol.sourceforge.net).

```
MxiH    MSVT----VPNDDW--TLSSLSETFDDGTQTLQGELTLALDKLAKNPSNPQLLAEYQSKL 54
PrgI    MATP----WSG-----YLDDVSAKFDTGVDNLQTQVTEALDKLAAKPSDPALLAAYQSKL 51
BsaL    MSNPPTPLLADYEWSGYLTGIGRAFDDGVKDLNKQLQDAQANLTKNPSDPTALANYQMIM 60

MxiH    SEYTLYRNAQSNTVKVIKDVDAAILEHHHHHH 86
PrgI    SEYNLYRNAQSNTVKVFKDIDAAILEHHHHHH 83
BsaL    SEYNLYRNAQSSAVKSMKDIDSSILEHHHHHH 92
```

Figure 2.2 Primary sequence alignment of MxiH, BsaL and PrgI as acquired from the ClustalW server.

This suggests that the protein-protein interactions responsible for needle formation may differ from bacterium to bacterium [11]. For example, while all three proteins form similar two helix bundles, the electrostatic potential seen in $PrgI^{\Delta5}$ is such that positively charged regions are located ~90 degrees from the oppositely charged face, whereas for $BsaL^{\Delta5}$ and $MxiH^{\Delta5}$, the orientational difference is approximately ~180 degrees (Figure 2.1). Furthermore, the negative face is oriented along the surface of the two helix bundle in $BsaL^{\Delta5}$ and $MxiH^{\Delta5}$ while in $PrgI^{\Delta5}$ the most significant region of negative charge is located away from the helix interface along the side of the structure (Figure 2.1). The presence of significant basic character on the surface of acidic proteins such as $MxiH^{\Delta5}$, $BsaL^{\Delta5}$ and $PrgI^{\Delta5}$ further suggests that electrostatic interactions may be an integral component of needle polymerization, although higher resolution structures of polymerized needles will be necessary to confirm this [11].

Needle formation is suspected to take place in a stepwise manner in which, upon receiving the proper signal, subunits are secreted through the central channel of the basal body and polymerize at the growing distal tip [2,12]. The channel passing though the basal body and extending into the needle complex has an inner diameter of approximately 20-30 Å, and therefore does not appear able to accommodate fully folded proteins [4, 6, 13]. Thus, it probably secretes proteins in structurally altered forms [6].

Both the monomeric and oligomerized needle forms of the subunit proteins are promising vaccine candidates due to their presence on the bacterial membrane surface during the initial stages of infection by the pathogens. It is suspected that an oligomerized form of the protein will initiate a more robust immunological response as

compared to the monomeric subunits. This hypothesis is supported by literature concerning protein aggregates in which a correlation between increased antigen molecular weight and repetitive organization of the structure results in an enhanced immune response [14-17]. Furthermore, recent studies indicate that immunization of mice with the recombinant YscF needle protein provide protection against challenge with *Yersinia pestis* [18].

In their full length form, the monomeric proteins have a strong tendency to oligomerize and self-associate. Consequently, a soluble C terminal truncated variant which maintains native secondary structure while inhibiting needle polymerization was used for spectroscopic work shown here [19]. Even with this modification, however, both YscF (*Yersinia pestis*) and PscF (*Pseudomonas aeruginosa*) rapidly self associate upon expression and purification (unpublished results), and as a result were not suitable for characterization using the methods described in this paper.

Here we report a detailed study of the effect of temperature and pH on the mutated monomeric subunit proteins $MxiH^{\Delta 5}$ (*Shigella*), $PrgI^{\Delta 5}$ (*Salmonella*), and $BsaL^{\Delta 5}$ (*Burkholderia*). Additionally, the behavior of the needle proteins under such conditions may shed light on the mechanism of needle assembly. To facilitate a detailed characterization of the three non-polymerizing proteins, an empirical phase diagram (EPD) technique was employed [20-27]. In this method, proteins are represented as vectors in a highly dimensioned experimental space. As previously shown, EPDs are useful tools when large quantities of data are required for a comprehensive analysis of stability behavior.

2.2 Materials and Methods

2.2.1 Materials

Expression of the C terminal truncated versions of the needle proteins has been described previously [8, 19, 28]. The plasmid for each of the soluble variants was expressed in E. coli BL21 (DE3), and induced for overexpression [29]. Recombinant proteins were purified by means of a C terminal His_6 tag according to previously documented methods [30, 31]. The C terminal Δ5 variants were dialyzed against 20 mM citrate-phosphate buffer in preparation for spectroscopic analysis. The citrate-phosphate buffer (20 mM) was prepared over a pH range of 3-8 using citric acid monohydrate (Fisher Scientific, Pittsburgh, PA) and anhydrous dibasic sodium phosphate (Sigma, St. Louis, MO). The ionic strength of each buffer solution was not adjusted to a constant value across the pH range. All spectroscopic studies employed protein concentrations of 0.15 to 0.25 mg/mL based on extinction coefficients of 9,970, 11,460 and 12,950 $M^{-1}cm^{-1}$ at 280 nm for MxiH, PrgI and BsaL respectively. Extinction coefficients were obtained using Protparam on the Expasy server (http://www.expasy.ch/tools /protparam.html).

2.2.2 High Resolution UV Absorbance Spectroscopy

Ultraviolet absorbance temperature studies were conducted over a pH range of 3-8 at one unit intervals using an Agilent 8453 UV-Visible diode array spectrophotometer. Individual spectra were collected every 2.5 ^{o}C from 10 to 80 ^{o}C following a 5 min. equilibration at each temperature, sufficient for equilibrium to be reached. Solution

turbidity was simultaneously analyzed by monitoring the optical density at 350 nm as a function of temperature. All second derivative UV absorbance and optical density data are presented as mean values (N=3). Chemstation software (Agilent) was employed to generate second derivatives of the zero-order UV spectra from 200 to 400 nm using a nine-point data filter. The resulting spectra were fit to a third-order polynomial using the Savitsky-Golay method, and smoothed with 99 points of interpolation to obtain effective high resolution (+/- 0.01 nm). The resultant spectra contained six negative peaks, representing well established contributions from the three aromatic amino acids (Phe, Tyr, and Trp) [24]. Peak positions were identified as a function of temperature and plotted in Microcal Origin (version 7.0) as previously described [31]. When applicable, midpoints of thermal transition were determined using the sigmoidal fit function in the Microcal Origin software.

2.2.3 Intrinsic Tryptophan (Trp) Fluorescence Spectroscopy

Using a Photon Technology International (PTI) spectrofluorometer (Lawrenceville, NJ), samples were excited at 295 nm (>95% Trp emission), and the resulting fluorescence emission was collected from 300 to 400 nm. Spectra were obtained following a 5 min thermal equilibration period every 2.5 ^{o}C from 10 to 80 ^{o}C. Data were acquired in triplicate and subsequently averaged. The resulting spectra were imported into Microcal Origin (version 7.0) where the buffer background was subtracted, and the spectra were smoothed using an 11-point second order Savitsky-Golay polynomial. The wavelength of the emission maximum was determined using the first

derivative of the smoothed data, and the corresponding peak position and intensity were plotted with respect to temperature. Additionally, the fluorescence intensity at 295 nm was also recorded as a measure of light scattering.

2.2.4 ANS Binding

Apolar sites characteristically buried in the core of proteins often become more accessible with structural alterations. Such changes were probed through the use of the fluorescent dye 8-Anilino-1-napthalene sulfonate (ANS), although the presence of the negative charge on the dye always requires qualification concerning potential electrostatic components of binding [32]. An optimized 10-fold molar excess of ANS to protein (0.2 mg/mL) was prepared and excited at 375 nm. Emission spectra were collected from 400-600 nm every 2.5 ^{o}C, from 10-80 ^{o}C following a 5 min thermal equilibration. Prior to data analysis, a spectrum of the negligible ANS emission in the absence of protein was subtracted from the corresponding spectrum at the same temperature and pH. The intensity of fluorescence emission at 485 nm was plotted as a function of temperature to assess changes in ANS binding upon thermal perturbation.

2.2.5 Far-UV Circular Dichroism Spectroscopy

The secondary structure of the three proteins was characterized over the pH range of interest using a Jasco J-720 spectropolarimeter equipped with a six position sample holder. Temperature was regulated with a Peltier control device (Easton, MD). Far-uv spectra were initially recorded at 10 ^{o}C from 260 to 190 nm in a 0.1 cm path length cell.

Subsequently, samples were heated from 10-80 ^{o}C and monitored at 222 nm following a five min. thermal equilibration period at each 0.5 ^{o}C interval. Using the instrument software, the resulting data were converted to molar ellipticity as a function of temperature. Midpoints of thermal transition were determined using Microcal Origin sigmoidal fit graphing tools.

2.2.6 Analysis of Thermal Unfolding Data

Thermodynamic unfolding values were calculated using molar ellipticity thermal unfolding curves at the various pH values. Assuming a two state model, a sigmoidal Van't Hoff plot of the fraction unfolded with respect to temperature was generated using equation 1 shown below. The equilibrium constant at each data point was then determined from the relationship shown in equation 2, and subsequently used in equation 3 to arrive at an experimentally determined value for the Gibbs free energy (ΔG_U). A Gibbs free energy plot was generated and fit to a linear equation (4) to obtain the entropic and enthalpic contributions to the thermal unfolding event at each pH.

$$f_U = \Theta_N\text{-}\Theta/\Theta_N\text{-}\Theta_U \quad (1)$$

$$K_U = [U]/[N] = f_U /1\text{-} f_U \quad (2)$$

$$\Delta G_U = -RT\ln K_U \quad (3)$$

$$\Delta G_U = \Delta H_U - T\Delta S_U \quad (4)$$

2.2.7 Empirical Phase Diagrams

An empirical phase diagram was constructed to combine data acquired using the multiple spectroscopic techniques described above [20-27]. This permits a comprehensive comparison of the response of each protein to temperature and pH in terms of secondary and tertiary structure change as well as any association/dissociation events present. Each plot was generated using MatLab software, employing combined data from each technique to create a multi-component vector at each temperature-pH condition. Together, the vectors form an *n x n* density matrix where *n* represents the number of variables used in the data set. Subsequently, *n* sets of eigenvalues and eigenvectors are derived from the data and normalized, and the three with the greatest magnitude are assigned to arbitrarily selected red, blue or green color. Regions of the diagram with similar color represent related physical states of the protein, and therefore permit the identification of "apparent" phase boundaries which represent structural or size changes in the protein. Note that these diagrams are not the commonly encountered thermodynamic phase diagrams and thus, no equilibrium is implied between the empirically defined phases. Further discussion of this approach is presented elsewhere [20-27, 33].

2.3 Results

2.3.1 High Resolution UV Absorbance Spectroscopy

The second derivative UV absorbance spectra of $MxiH^{\Delta 5}$, $BsaL^{\Delta 5}$ and $PrgI^{\Delta 5}$ were de-convoluted to display the individual contributions from the three aromatic residues, Phe, Tyr and Trp. Six negative peaks were observed, and at 10 ^{o}C their approximate wavelengths were: 253 nm (Phe), 259 nm (Phe), 270 nm (Phe/Tyr), 277 (Tyr), 284 nm (Tyr/Trp), and 290 nm (Trp) [24]. Information regarding structural changes in the protein's tertiary structure was obtained by monitoring shifts in peak position with varying pH and increasing temperature. This method serves as a sensitive conformational probe given the unique distribution of the aromatic amino acids throughout the core and terminal domains of the proteins. For example, the sole Trp residue found in each of the three proteins is located in its N terminal region. As a result, changes seen in the Trp specific absorbance can be primarily attributed to changes in the N terminal region of the protein. Similarly, the mutant proteins contain only one Phe residue, with the exception of PrgI, which is positioned in the N terminal alpha helix. Alternatively, multiple Tyr residues are dispersed throughout the alpha helix core, and therefore do not permit such unambiguous interpretations.

Phe spectral peaks, which demonstrate absorption maxima at approximately 253 (data not shown) and 259 nm (Figure 2.3), experienced 1-2 nm red shifts in peak position with increasing temperature. Phe residues are typically found within the apolar core of proteins, and are consequently the last to undergo a change in environment as structure is altered. For all three proteins, it appears that the shift in Phe peak position at pH 3-6 is relatively linear and continuous, and therefore probably reflects the intrinsic effect of temperature on the aromatic side chains

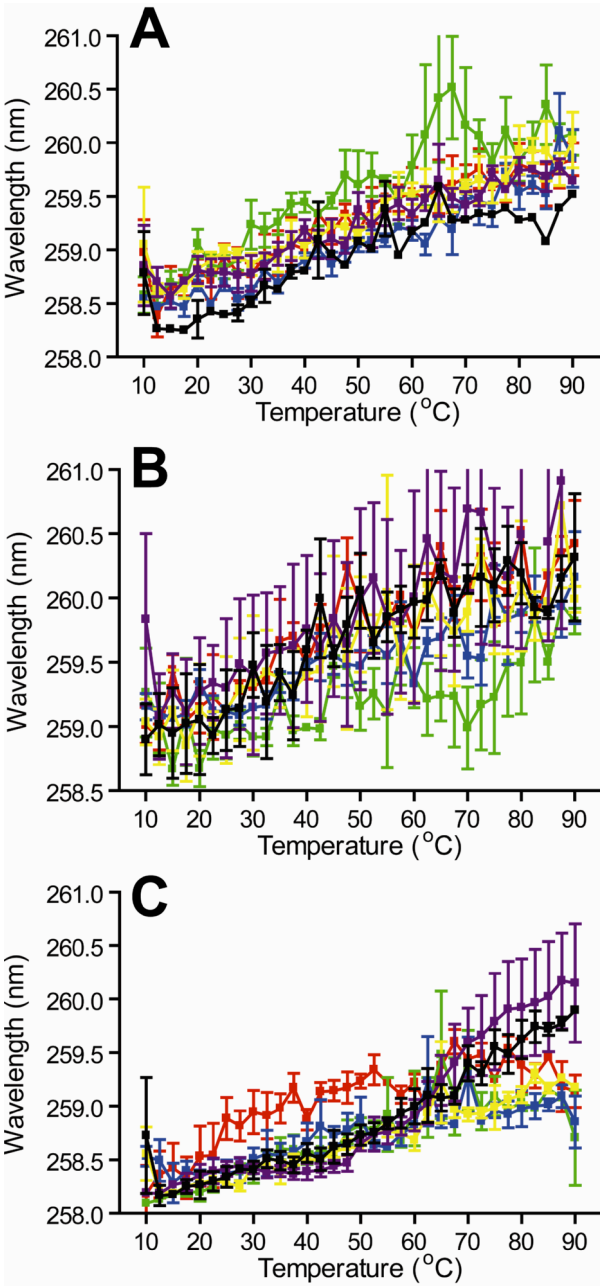

Figure 2.3 Effect of temperature on MxiH$^{\Delta 5}$ (A), BsaL$^{\Delta 5}$ (B) and PrgI$^{\Delta 5}$ (C) as observed by a shift in second derivative near-UV absorbance peak position representing the contribution made by Phe residues at pH 3.0 (red), 4.0 (green), 5.0 (blue), 6.0 (yellow), 7.0 (purple), and 8.0 (black).

[24]. At pH 7 and 8, however, the shift becomes increasingly nonlinear in nature, and therefore presumably represents alterations in structure induced by thermal perturbation.

The Tyr peak at 277 nm exhibits a blue shift of approximately 1 nm over the temperature ramp, and demonstrates a distinct sigmoidal response with a clear transition in all cases (Figure 2.3a, d, g). As mentioned above, the mutant proteins contain several Tyr residues in the alpha helical regions, and consequently the resultant data are a summation of polarity changes in numerous micro-environments throughout the proteins. For each of the three proteins studied, the midpoint of the thermal transition (T_m) varied with respect to pH, and the pH at which the highest T_m was seen varied among the three proteins. For all three proteins, however, the lowest T_m occurred at pH 3. With respect to MxiH$^{\Delta 5}$, peak shifts at pH 3 and 4 appear to be slightly blue shifted compared to the other pH conditions. Additionally, it appears that the onset temperature defining the transition occurs at slightly lower temperatures than at the higher pH conditions. In the case of BsaL$^{\Delta 5}$ and PrgI$^{\Delta 5}$, this trend was not observed.

The negative peak seen near 290 nm at 10 ^{o}C which represents contributions solely from the single Trp residue did not display any significant shifts in its absorption maximum peak position for any of the three proteins indicating that the local environment of this particular residue did not undergo major alterations upon thermal stress or changes in pH, presumably due to its surface exposure in the truncated version (data not shown) [8, 11, 34]. The remaining two peaks represent a combination of aromatic contributions, (Phe/Tyr and Tyr/Trp at approximately 253 and 270 nm at 10 ^{o}C, respectively), both of which display blue shifts of approximately 1 nm with transition

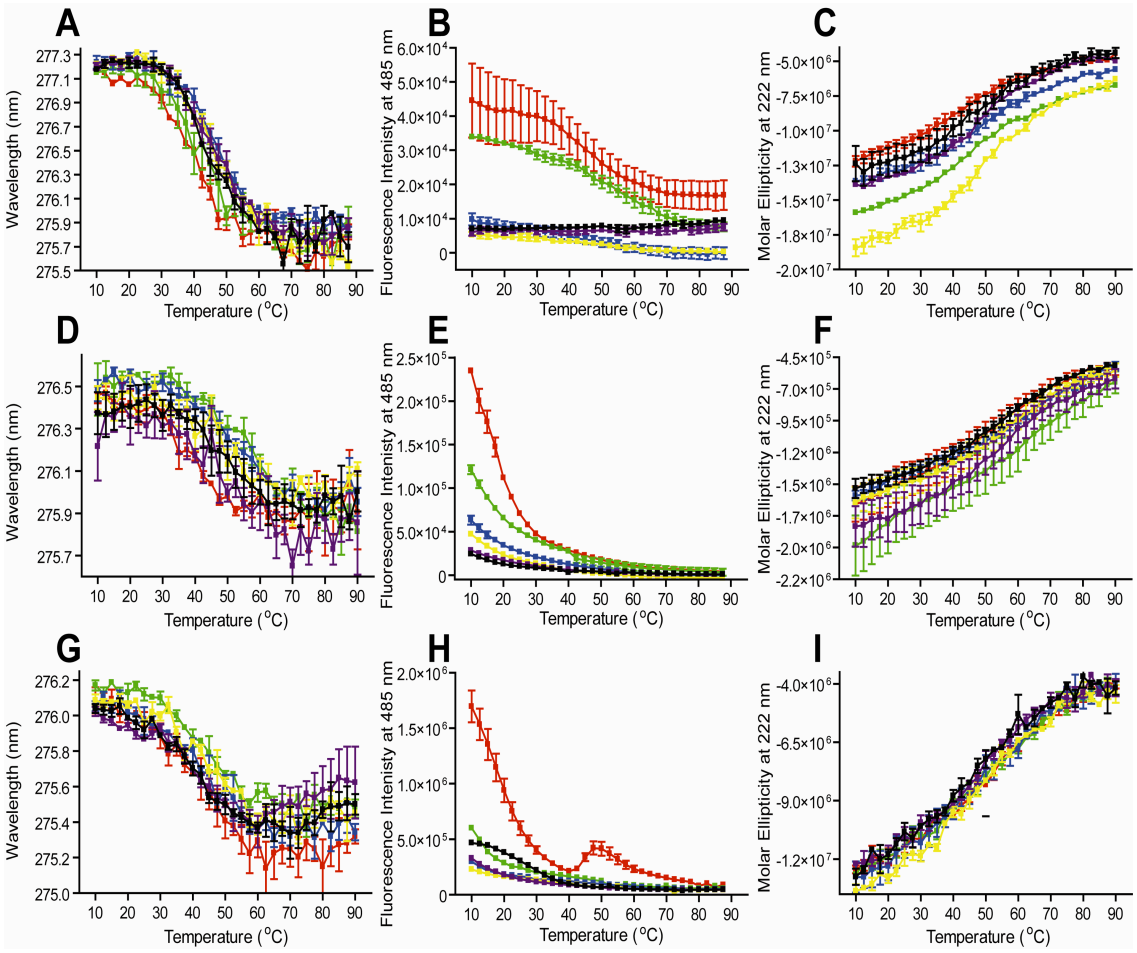

Figure 2.4 Effect of temperature on MxiH$^{\Delta 5}$ (A-C), BsaL$^{\Delta 5}$ (D-F) and PrgI$^{\Delta 5}$ (G-I) as observed by multiple spectroscopic techniques at pH 3.0 (red), 4.0 (green), 5.0 (blue), 6.0 (yellow), 7.0 (purple), and 8.0 (black). (A, D, G) Shift in second derivative near-UV absorbance peak position representing the contribution made by the three Tyr residues as a function of temperature. (B, E, H) ANS fluorescence intensity as a function of temperature. (C, F, I) Molar ellipticity at 222 nm as a function of temperature.

midpoints of roughly 40 ^{o}C (data not shown). Based on the previously described data of the individual contributions of each type of aromatic residue, the changes seen in the combination peaks presumably reflect a dominating contribution of the Tyr residues.

The optical density at 350 nm was concurrently monitored to evaluate the propensity of the proteins to associate upon thermal stress. In the case of all three proteins, no significant change was seen as the temperature was increased (data not shown). This suggests that the observed thermal transitions do not result in the formation of large insoluble aggregates, and is consistent with previous findings regarding the reversible nature of MxiH$^{\Delta 5}$ and PrgI$^{\Delta 5}$ thermal transitions [28].

2.3.2 Intrinsic Trp Fluorescence Spectroscopy

The single Trp residue in each of the three proteins was used as an intrinsic fluorescent probe to monitor changes in protein tertiary structure under varying pH and temperature conditions. Each of the three monomeric proteins exhibited a maximum emission wavelength between 345 and 350 nm at 10 ^{o}C at all six pH values which remained unchanged with increasing temperature (data not shown). This observation suggests that the indole ring of the Trp sidechain is extensively exposed to the solvent at 10 ^{o}C, and upon thermal perturbation does not experience a change in polarity in its local environment. Furthermore, the intensity of the fluorescence at the maximum emission wavelength decreases in a curvi-linear manner for all three proteins at all six pH values suggestive of intrinsic temperature effects (data not shown). The fluorescence intensity at 295 nm was also monitored during the thermal perturbation of the samples and used to

monitor potential changes in oligomerization state. Similar to the results observed while monitoring optical density upon thermal stress, no apparent increase was observed (data not shown). This observation indicates that at the protein concentration studied here, association and/or aggregation of the monomeric proteins upon thermal stress over the pH range of 3-8 is not detectable.

2.3.3 ANS Fluorescence Spectroscopy

ANS was used as an extrinsic fluorescent probe to monitor changes in protein apolar binding sites upon increasing temperature and varying pH. In general, the quantum yield of ANS increases upon binding to apolar regions. As proteins partially unfold, the internally buried apolar groups become more exposed to the solvent, and consequently interaction with ANS often increases with subsequent enhancement of ANS emission. For each of the three proteins, similar trends in intensity changes of ANS at each pH were observed. Slight differences, however, were evident. All three proteins appear to have the greatest apolar character at pH 3 and 10 ^{o}C, suggesting that they are somewhat structurally disrupted at low pH even at reduced temperatures.

At 485 nm, the intensity of ANS fluorescence in the presence of MxiH$^{\Delta 5}$ at pH 3 and 4 exhibits a melting curve with a transition midpoint of approximately 50 ^{o}C (Figure 2.3b). A slight decrease in intensity with temperature probably due to intrinsic temperature effects is seen at pH 5 and 6, which both initiate at notably lower intensity at 10 ^{o}C relative to the results at pH 3 and 4. ANS spectra at pH 7 and 8 also exhibit similar

intensities, but do not display any significant alteration over the temperature range examined.

In the case of $BsaL^{\Delta 5}$, the ANS intensity at pH 3 decreases in a nearly linear manner until approximately 30 ^{o}C, at which point it continues to decrease but with a more positive slope (Figure 2.3e). When the pH is increased to 4, a similar trend is again observed but with significantly lower intensity. Subsequent increases in pH produce the same trend for each pH, differing only in the decreasing intensity with increasing pH.

The fluorescence intensity at 485 nm of ANS in the presence of $PrgI^{\Delta 5}$ at pH 3 exhibits more commonly observed ANS behavior with a distinct transition onset temperature of approximately 40 ^{o}C, and midpoint at 50 ^{o}C (Figure 2.3h). The same decreasing intensity with increasing temperature seen for $BsaL^{\Delta 5}$, however, is exhibited by PrgI for the remaining pH conditions (4-7), since significantly less fluorescence intensity is observed with increasing pH and temperature. At pH 8 and low temperatures, a slight increase in ANS fluoresce intensity is observed, which suggests an increase in ANS binding. It should be emphasized that ANS binding may also be influenced by an electrostatic component. The pI of each of the three proteins is 4.5, 4.8 and 4.8 for MxiH, PrgI and BsaL respectively, which suggests that the results seen at low pH could, in fact, be complicated by electrostatic interactions with the negatively charged dye.

2.3.4 Far-UV Circular Dichroism Spectroscopy

At each of the six pH values, all three proteins produced spectra displaying double minima at 208 and 222 nm consistent with a α-helical structure [28]. The thermal

stability of the secondary structure at varying pH values was evaluated by monitoring the molar ellipticity at 222 nm as a function of temperature. All three proteins exhibited evidence of a major loss of secondary structure as implied by the large decrease in negative molar ellipticity with increasing temperature (Figure 2.3c, f, i). The transition representing a change in secondary structure with temperature was broad but sigmoidal in all cases, and appeared to begin at temperatures as low as 10 ^{o}C. The midpoint of the thermal transition (T_m) for each of the three proteins over the pH range studied varied from 35 +/- 0.5 to 50 +/- 1.1 ^{o}C, and at the concentrations examined, thermal transitions were >90 % reversible [30]. Data were not available below 200 nm due to interference from buffer components; therefore, no attempt was made to analyze the spectra further for secondary structure content.

With respect to MxiH$^{\Delta 5}$, pH 5 and 6 produced the greatest thermal stability (T_m values of 42.9 and 42.1 ^{o}C respectively). In the case of BsaL$^{\Delta 5}$, pH 4 and 5 resulted in the greatest thermal stability with T_m values of 50.8 and 50.1 ^{o}C, with a subsequent increase or decrease in pH again resulting in a notable decrease in the T_m. PrgI$^{\Delta 5}$ displayed the greatest thermal stability at pH 3 and 4 (42.7 and 42.5 ^{o}C), with an increase in pH characterized by a significant decrease in thermal stability.

2.3.5 Thermodynamics

Given the reversible nature of the transitions observed using circular dichroism (Figure 2.5a), the thermodynamics of thermal unfolding of the three proteins were analyzed to obtain a more quantitative description of the conformational changes induced

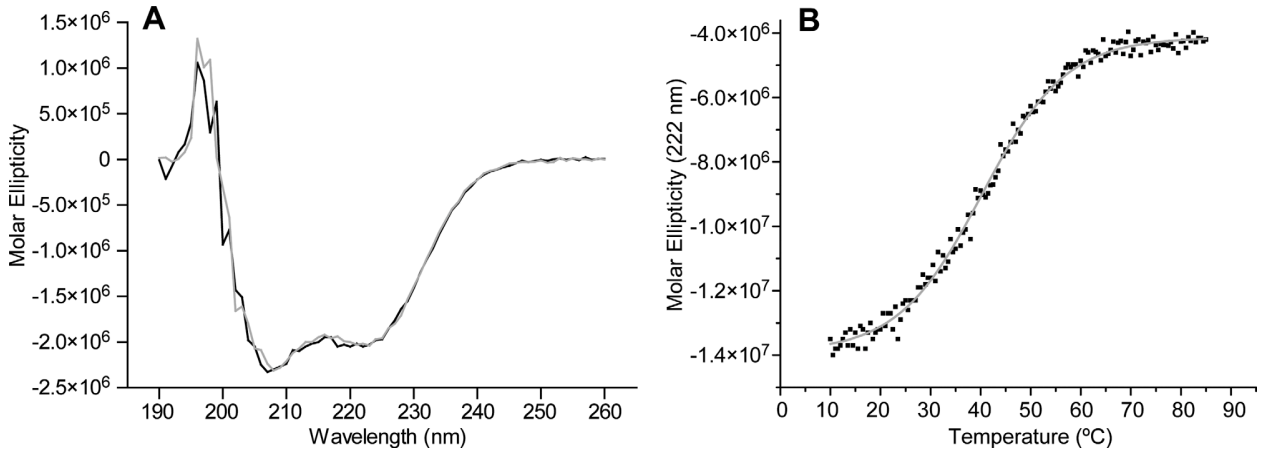

Figure 2.5 (A) A circular dichroism spectrum prior to thermal unfolding is shown in black, while the grey line indicates the same sample following the thermal melt and re-cooling to 10 ^{o}C. (B) Thermal melting curves acquired using circular dichroism are well fit by a two state transition model as shown by the solid grey line. Plots shown in both (A) and (B) represent data acquired for MxiH$^{\Delta 5}$ at pH 7, and are representative of trends observed for all three proteins at all pH values.

by both temperature and pH. Despite the lack of highly cooperative character observed in the surprisingly gradual transitions (probably due to the flexible nature of the C and N termini observed by NMR and crystallography), the data were well fit by a 2-state model with r^2 values exceeding 0.98 in all cases (Figure 2.5b). The apparent Gibbs free energy of unfolding (ΔG_u) obtained at 37 ^oC is found to vary in magnitude with respect to pH, but is, as expected, unfavorable (positive) for all three proteins across the pH range of interest (Figure 2.6b). $MxiH^{\Delta 5}$ displayed the lowest intrinsic stability at pH 3 (0.27 +/- 0.02 KJ/mol) and the greatest at pH 6 (1.75 +/- 0.09 KJ/mol). Similarly, $PrgI^{\Delta 5}$ demonstrated the greatest intrinsic stability at pH 5 (1.77 +/- 0.22 KJ/mol), and significantly decreased with both increases and decreases in pH. $BsaL^{\Delta 5}$ produced the most consistent values across the pH gradient, experiencing the least intrinsic stability at pH 4 (1.08 +/- 0.12 KJ/mol), and the greatest at pH 6 (1.59 +/- 0.07 KJ/mol). As temperature increases above the physiological range, however, and approaches the various melting temperatures for each of the proteins, ΔG_u decreases and becomes negative indicating thermal unfolding is a spontaneous process at higher temperatures. Further analysis of the thermodynamic parameters conducted at 37 ^oC reveals that the thermal unfolding of all three proteins over the pH range of 3-8 is enthalpically driven, with enthalpy (Figure 2.6c) and entropy (Figure 2.6d) contributions displaying significant pH dependence across the range of interest. We emphasize caution in the use of these parameters, however, due to the unusual shape of the transition.

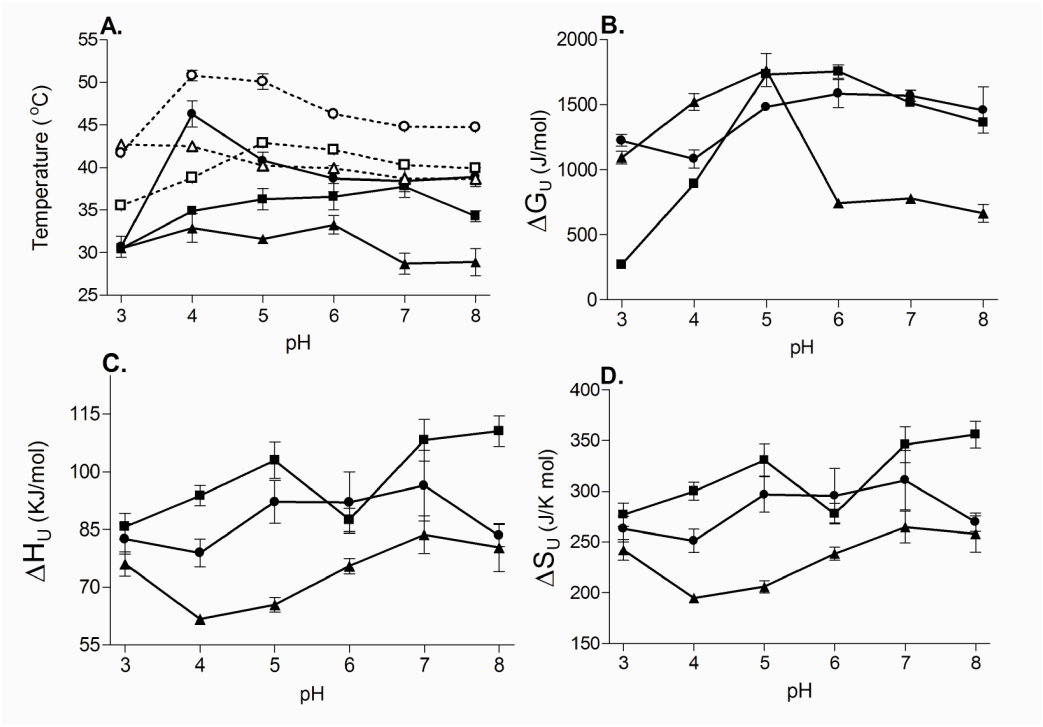

Figure 2.6 Summary of the midpoint of thermal unfolding (T_m) and thermodynamic parameter values for MxiH$^{\Delta5}$, BsaL$^{\Delta5}$ and PrgI$^{\Delta5}$. (A) T_m values as monitored by molar ellipticity at 222 nm for MxiH$^{\Delta5}$ (□ dashed line), BsaL$^{\Delta5}$ (○ dashed line) and PrgI$^{\Delta5}$ (Δ dashed line), as well as by uv-absorbance at 277nm (Tyr) for MxiH$^{\Delta5}$ (■ solid line), BsaL$^{\Delta5}$ (● solid line) and PrgI$^{\Delta5}$ (▲ solid line). (B) Values of $\Delta G_{unfolding}$ at 37 °C for MxiH$^{\Delta5}$ (■), BsaL$^{\Delta5}$ (●) and PrgI$^{\Delta5}$ (▲). (C) Values of $\Delta H_{unfolding}$ at 37 °C for MxiH$^{\Delta5}$ (■), BsaL$^{\Delta5}$ (●) and PrgI$^{\Delta5}$ (▲). (D) Values of $\Delta S_{unfolding}$ at 37 °C for MxiH$^{\Delta5}$ (■), BsaL$^{\Delta5}$ (●) and PrgI$^{\Delta5}$ (▲).

2.3.6 Empirical Phase Diagrams

To summarize the effect of pH and temperature on the truncated monomeric needle proteins, an empirical phase diagram (EPD) was constructed (Figures 2.7A-C). The components of the vectors that comprise each T, pH point are based on the far-UV circular dichroism, extrinsic (ANS) fluorescence and the high resolution UV absorbance spectroscopy data described above. We emphasize that these are not necessarily equilibrium (thermodynamic) phase diagrams (the reversibility of all pH induced changes has not been established), but are an empirical representation of changes in structure as a function of environmental variables. In this case, regions of similar color indicate physically similar conformational states of the protein. Thus, EPDs incorporate data sensitive to multiple aspects of protein secondary and tertiary structure. Note that the assignment of color is arbitrary. Therefore, similar colors between the three individual EPDs are not meant to imply similar conformational states. One marked similarity among the EPDs for each of the three proteins is the presence of a structurally altered state at low pH (3) and low temperatures. While the temperatures at which abrupt color changes for each protein at each pH vary, it appears that a major change in physical state occurs in the temperature range of 35-40 ^{o}C for all three proteins. With the exception of the molar ellipticity temperature data, thermal transitions appear relatively minor for all three proteins. The gradations in color seen over a fairly wide temperature range for all proteins suggests the presence of transient intermediate states despite the fact that the thermal unfolding data is well fit by a two state model.

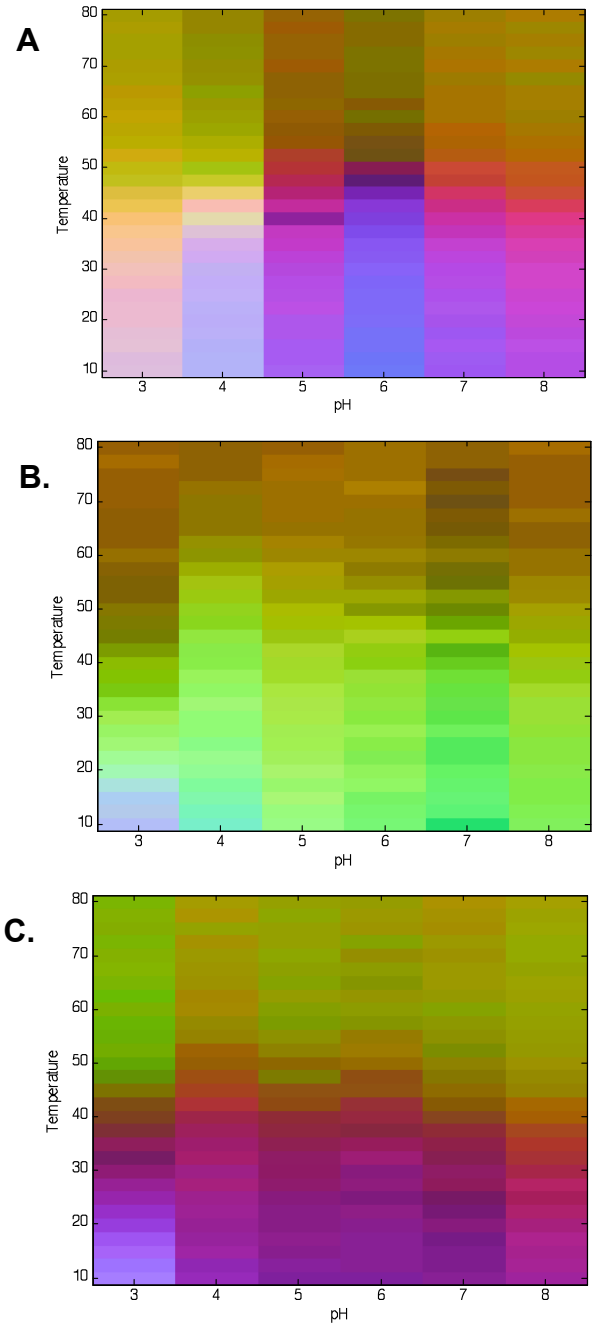

Figure 2.7 Empirical phase diagrams (EPDs) for (A) MxiH$^{\Delta 5}$, (B) BsaL$^{\Delta 5}$ and (C) PrgI$^{\Delta 5}$ generated using Tyr second derivative near-UV absorbance peak positions, ANS fluorescence intensity, and CD molar ellipticity at 222 nm data all as a function of temperature and pH.

2.4 Discussion

The results presented here describe a comprehensive set of thermal and pH perturbation studies of the $MxiH^{\Delta5}$, $BsaL^{\Delta5}$ and $PrgI^{\Delta5}$ monomeric TTSS needle proteins. The truncated versions of interest contained a His_6 tag for purification purposes, but previous results indicate the tag does not inhibit the formation of functional needles. Thus it is not expected to interfere with the conformational and thermal perturbation studies presented here [35]. It must be acknowledged, however, that it is possible that the presence of the His_6 tag may induce a degree of instability in the monomeric variants.

Circular dichroism spectroscopy data is consistent with the NMR solution and crystal structure data recently obtained for $BsaL^{\Delta5}$, $PrgI^{\Delta5}$ and $MxiH^{\Delta5}$ which demonstrated that these proteins' secondary structures consist of two anti-parallel alpha helices flanked by unstructured N and C termini [8, 11, 34]. Thus, the CD spectra indicate that the secondary structure of all three proteins is largely alpha helical, but additionally, remarkably thermally unstable. Thermal transitions indicating a major loss in secondary structure appear to begin at temperatures as low as 10 ^{o}C, with midpoints of thermal unfolding in the range of 35 +/- 0.5 to 50 +/- 1.1 ^{o}C for all three proteins over the pH range of 3-8. At low temperatures, $PrgI^{\Delta5}$ does not appear to exhibit variations in secondary structure with respect to pH, while $BsaL^{\Delta5}$ and $MxiH^{\Delta5}$ display small differences in molar ellipticity from one pH to another. Circular dichroism experiments were also conducted at a constant salt concentration (ionic strength) of 0.15 where it was observed that transitions seen in the temperature and pH studies described here were

shifted to lower temperatures, but displayed very similar pH dependence (data not shown). Furthermore, fluorescence data obtained at constant salt concentration also revealed trends analogous to those presented here.

Observations using both fluorescence and absorbance spectroscopy concerning the tertiary structure of the proteins confirm that the local environment surrounding the single Trp residue found in the N terminal region of each protein is relatively polar at low temperatures as well as across the entire pH region examined. This is consistent with the N terminus being unstructured as observed in the previously mentioned NMR and X-Ray based structures for $BsaL^{\Delta 5}$ and $MxiH^{\Delta 5}$ [8, 11, 34]. Phe absorbance measurements as a function of temperature and pH also provide little evidence for major conformational changes, although a careful inspection of the data for all three proteins does find a subtle deviation from the curvilinear wavelength maximum versus temperature behavior above 40 ^{o}C at higher pH (>6). Thus, some subtle disruption of the protein's tertiary structure does appear to be occurring. Additionally, the effect of temperature on the multiple Tyr residues dispersed throughout the structure of each of the proteins show clear transitions indicating the occurrence of a thermal event.

A global presentation of the spectroscopic data for each truncated protein was presented in the form of EPDs to better illustrate the combined effects of temperature and pH on both the secondary and tertiary structure of the proteins. The most striking observation for each of the three proteins is their low thermal stability over the entire pH range examined. For all three proteins, pH 3 appears to induce a thermally altered conformational state at temperatures as low as 10 ^{o}C, which correlates with the increased

ANS fluorescence observed under those conditions, and is indicative of solvent accessibility within the apolar protein core. Based on the EPDs, it appears that $MxiH^{\Delta 5}$ displays the greatest thermal stability at pH 6, $BsaL^{\Delta 5}$ at pH 5 and $PrgI^{\Delta 5}$ at pH 4.

Evaluation of the intrinsic conformational stability of $MxiH^{\Delta 5}$, $BsaL^{\Delta 5}$ and $PrgI^{\Delta 5}$ with respect to thermal unfolding as monitored by circular dichroism provides information concerning the driving force behind the formation of each protein's native structure. At physiological temperatures (37 ^{o}C), the free energy difference between the folded and unfolded state of each protein varies with pH, but is positive in all cases and ranges from approximately 0.3 to 1.8 KJ/mol. It has been reported that for a globular protein of this size, a more common ΔG_U value under physiological conditions would be 20 to 60 KJ/mol [36]. It is possible that this very low free energy difference may be a reflection of the biological significance of the unfolded or molten globule like states displayed by the needle proteins under physiological like conditions. A lack of favorable changes in free energies is also observed, and together with the low free energy change suggests that the proteins lack a substantial apolar interior.

Comparison of the transition midpoint temperatures obtained using CD and Tyr UV-absorbance spectroscopy indicates that upon thermal stress, all three proteins may exist in one or more intermediate conformational states in which their tertiary structure has been compromised, but secondary structure elements remain (Figure 2.6a). This partially structured or molten globule like state persists in some cases over as wide a range as 12 ^{o}C, but varies in duration across the pH range for each protein. It is interesting to note that for each protein, the bulk of the transition temperatures acquired

from the CD and UV absorbance thermal melting curves follow similar trends across the pH range of interest. For example, BsaL$^{\Delta 5}$ displays the lowest thermal stability at pH 3 with respect to both secondary and tertiary structure relative to the higher pH values. As the pH is increased to 4, however, the midpoints representing the corresponding transitions both significantly increase. Further increases in pH (5-8) are characterized by a continuing decrease in transition midpoints as detected by both methods. Thus, while the absolute transition temperatures representing the thermal stability of the secondary and tertiary structural elements of BsaL$^{\Delta 5}$ at each pH differ significantly, their trend across the pH range investigated here appears to be the same. The same is seen for PrgI$^{\Delta 5}$ and MxiH$^{\Delta 5}$. A transient nature for the unfolding intermediates is suggested by the fact that the data are still well fit by a two state model.

A role for partially unfolded states of proteins in their transport across cellular barriers has frequently been suggested. Such studies have argued that these nonnative states can be induced by membrane surfaces, with the induction of structural disruption attributable to two phenomena [37]. The first involves the presence of the negative electrostatic potential found on most membrane surfaces [38]. This attracts protons to exterior negative charges, and consequently the pH near the surface may drop by up to two pH units [38]. Such an effect is thought to lower the pH in a region up to 15 Å from the membrane surface [39, 40]. A second phenomenon involves increased electrostatic repulsion of negative charges resulting from a reduced dielectric constant near the membrane surface [39]. This could also lead to protein structure alterations. Although this model has been more commonly applied to eukaryotic cell surfaces, it appears

reasonable in this case given the presence of phosphatidylglycerol, a negatively charged lipid, on the cytoplasmic surface of the inner bacterial membrane of gram negative bacteria [41].

The pH at which each protein experiences its greatest thermal stability with respect to both secondary and tertiary structure differs despite their structural and functional similarities. The dependence of pH has been previously noted in the *S. typhimurium* system where needles dissociated upon an increase in pH from 8.0 to 10.5 [42]. It is possible that this variation in stability may reflect a functional aspect of the monomeric proteins' behavior. Due to the size difference between the inner pore of the needle and fully folded proteins, it seems clear that the needle subunits must be secreted in a partially or completely unfolded state to reach the distal tip of the needle for assembly. Additionally, while both *Salmonella* and *Shigella* access host epithelium via specialized M cells, *Salmonella* gains access to a host through the small intestine, while *Shigella* uses a structurally and functionally conserved TTSS to invade in the large intestine [43]. The variation in pH within different segments of the intestinal tract in coordination with the low thermal stability of the needle subunits at critical pH values could thus be involved in dictating the formation of the external needle structures.

Table 2.1 Summary of the midpoint of thermal unfolding (T_m) and thermodynamic parameter values for MxiH$^{\Delta 5}$, BsaL$^{\Delta 5}$ and PrgI$^{\Delta 5}$. Thermal data in ^{o}C and thermodynamic data in J/mol, J/mol and J/K*mol for $\Delta G_{unfolding}$, $\Delta H_{unfolding}$ and $\Delta S_{unfolding}$ respectively.

		T_m for 2^o (CD)		T_m for 3^o (Tyr)		$\Delta G_{unfolding}$		$\Delta H_{unfolding}$		$\Delta S_{unfolding}$	
	pH	*Average*	*St.Dev.*	*Average*	*St.Dev.*	*Average*	*St.Dev.*	*Average*	*St.Dev.*	*Average*	*St.Dev.*
MxiH	3	35.5	0.5	30.5	0.6	271	15	8.58E+04	5.99E+03	277.0	20
	4	38.8	0.8	34.9	0.6	893	43	9.38E+04	3.62E+03	300.1	12
	5	42.9	0.3	36.3	2.2	1732	24	1.03E+05	8.12E+03	330.7	27
	6	42.1	0.3	36.6	2.7	1755	89	8.75E+04	5.29E+03	277.9	18
	7	40.3	0.2	37.8	1.1	1515	37	1.08E+05	9.36E+03	346.1	31
	8	39.9	0.3	34.3	1.1	1363	57	1.11E+05	5.60E+03	355.9	19
BsaL	3	41.7	0.3	30.7	2.2	1225	76	8.25E+04	6.75E+03	263.0	22
	4	50.8	1.1	46.3	2.7	1082	121	7.89E+04	6.24E+03	251.2	20
	5	50.1	1.6	40.8	1.7	1481	42	9.21E+04	9.64E+03	296.8	30
	6	46.3	0.5	38.7	2.6	1584	184	9.20E+04	1.39E+04	295.6	46
	7	44.8	0.1	38.4	3.3	1569	71	9.64E+04	1.59E+04	310.8	51
	8	44.7	0.1	38.9	1.9	1457	306	8.34E+04	4.97E+03	269.7	16
PrgI	3	42.7	0.6	30.5	0.9	1093	88	7.60E+04	5.47E+03	242.5	18
	4	42.5	0.6	32.9	2.9	1522	114	6.17E+04	2.05E+03	194.9	6
	5	40.2	0.8	31.6	0.5	1766	221	6.54E+04	3.32E+03	206.1	11
	6	39.9	0.2	33.3	1.9	745	51	7.55E+04	3.35E+03	238.7	11
	7	38.7	0.6	28.7	2.1	780	59	8.37E+04	8.49E+03	264.9	27
	8	38.7	0.4	28.9	2.7	667	120	8.03E+04	1.07E+04	258.0	31

2.5 Bibliography

[1] Torok TJ, Tauxe RV, Wise RP, Livengood JR, Sokolow R, Mauvais S. A large community outbreak of salmonellosis caused by intentional contamination of restaurant salad bars. JAMA 1997;278:389-95.

[2] Blocker A, Komoriya K, Aizawa S-I. Type III secretion systems and bacterial flagella: Insights into their function from structural similarities. Proc Natl Acad Sci USA 2003 March 18, 2003;100(6):3027-30.

[3] Hueck CJ. Type III Protein Secretion Systems in Bacterial Pathogens of Animals and Plants. Microbiol Mol Biol Rev 1998 June 1, 1998;62(2):379-433.

[4] Blocker A, Jouihri N, Larquet E, Gounon P, Ebel F, Parsot C, et al. Structure and composition of the *Shigella flexneri* 'needle complex', a part of its type III secreton. Molec Microbiol 2001;39(3):652-63.

[5] Tamano K, Aizawa S, Katayama E, Nonaka T, Imajoh-Ohmi S, Kuwae A, Nagai, et al. Supramolecular structure of the *Shigella* type III secretion machinery: The needle part is changeable in length and essential for delivery of effectors. . EMBO J 2000;19(15):3876-87.

[6] Deane JE, Roversi P, Cordes FS, Johnson S, Kenjale R, Daniell S, et al. Molecular model of a type III secretion system needle: Implications for host-cell sensing. Proc Natl Acad Sci USA 2006 August 15, 2006;103(33):12529-33.

[7] Kubori T, Matsushima Y, Nakamura D, Uralil J, Lara-Tejero M, Sukhan A, et al. Supramolecular Structure of the *Salmonella typhimurium* Type III Protein Secretion System. Science 1998 April 24, 1998;280(5363):602-5.

[8] Zhang L, Wang Y, Picking WL, Picking WD, De Guzman RN. Solution Structure of Monomeric BsaL, the Type III Secretion Needle Protein of *Burkholderia pseudomallei*. J Molec Biol 2006;359(2):322-30.

[9] Espina M, Olive AJ, Kenjale R, Moore DS, Ausar SF, Kaminski RW, et al. IpaD Localizes to the Tip of the Type III Secretion System Needle of *Shigella flexneri*. Infect Immun 2006 August 1, 2006;74(8):4391-400.

[10] Olive AJ, Kenjale R, Espina M, Moore DS, Picking WL, Picking WD. Bile Salts Stimulate Recruitment of IpaB to the Shigella flexneri Surface, Where It Colocalizes with IpaD at the Tip of the Type III Secretion Needle. Infect Immun 2007 May 1, 2007;75(5):2626-9.

[11] Wang Y, Ouellette AN, Egan CW, Rathinavelan T, Im W, De Guzman RN. Differences in the Electrostatic Surfaces of the Type III Secretion Needle Proteins PrgI, BsaL, and MxiH. Journal of Molecular Biology 2007;371(5):1304-14.

[12] Cornelis GR. The type III secretion injectisome. Nat Rev Micro 2006;4(11):811-25.

[13] Cordes FS, Komoriya K, Larquet E, Yang S, Egelman EH, Blocker A, et al. Helical Structure of the Needle of the Type III Secretion System of *Shigella flexneri*. J Biol Chem 2003 May 2, 2003;278(19):17103-7.

[14] Cleland JL, Powell MF, Shire SJ. The development of stable protein formulations: a close look at protein aggregation, deamidation, and oxidation. Crit Rev Ther Drug Carrier Syst 1993;10(4):307-77.

[15] Gamble CN. The role of soluble aggregates in the primary immune response of mice to human gamma globulin. Int Arch Allergy Appl Immunol 1966 446-455;30:1966.

[16] Dintzis RZ, Okajima M, Middleton MH, Greene G, Dintzis HM. The immunogenicity of soluble haptenated polymers is determined by molecular mass and hapten valence. J Immunol 1989 August 15, 1989;143(4):1239-44.

[17] Rosenberg AS. Effects of Protein Aggregates: An Immunologic Perspective. AAPS J 2006;8(3):E501-7.

[18] Pastor A, Chabert J, Louwagie M, Garin J, Attree I. PscF is a major component of the *Pseudomonas aeruginosa* type III secretion needle. FEMS Microbiol Lett 2005;253(1):95-101.

[19] Kenjale R, Wilson J, Zenk SF, Saurya S, Picking WL, Picking WD, et al. The Needle Component of the Type III Secreton of *Shigella* Regulates the Activity of the Secretion Apparatus. J Biol Chem 2005 December 30, 2005;280(52):42929-37.

[20] Fan H, Kashi RS, Middaugh CR. Conformational lability of two molecular chaperones Hsc70 and gp96: Effects of pH and temperature. Arch Biochem Biophys 2006;447(1):34-45.

[21] Fan H, Li H, Zhang M, Middaugh CR. Effects of solutes on empirical phase diagrams of human fibroblast growth factor 1. J Pharm Sci 2006;9999(9999):n/a.

[22] Fan H, Ralston J, Dibiase M, Faulkner E, Middaugh CR. Solution behavior of IFN-γ-1a: an empirical phase diagram based approach. J Pharm Sci 2005;94(9):1893-911.

[23] Harn NR, Jeng YN, Kostelc JG, Middaugh CR. Spectroscopic analysis of highly concentrated suspensions of bovine somatotropin in sesame oil. J Pharm Sci 2005;94(11):2487-95.

[24] Kueltzo L, Ersoy B, Ralston JP, Middaugh CR. Derivative absorbance spectroscopy and protein phase diagrams as tools for comprehensive protein characterization: A bGCSF case study. J Pharm Sci 2003;92(9):1805-20.

[25] Kueltzo LA, Middaugh CR. Structural characterization of bovine granulocyte colony stimulating factor: Effect of temperature and pH. J Pharm Sci 2003;92(9):1793-804.

[26] Peek LJ, Brey RN, Middaugh C. A rapid, three-step process for the preformulation of a recombinant ricin toxin A-chain vaccine. J Pharm Sci 2007;96(1):44-60.

[27] Ruponen M, Braun CS, Middaugh CR. Biophysical characterization of polymeric and liposomal gene delivery systems using empirical phase diagrams. J Pharm Sci 2006;95(10):2101-14.

[28] Harrington A, Darboe N, Kenjale R, Picking WL, Middaugh CR, Birket S, et al. Characterization of the Interaction of Single Tryptophan Containing Mutants of IpaC from *Shigella flexneri* with Phospholipid Membranes. Biochemistry 2006;45(2):626-36.

[29] Picking WL, Mertz JA, Marquart ME, Picking WD. Cloning, Expression, and Affinity Purification of Recombinant *Shigella flexneri* Invasion Plasmid Antigens IpaB and IpaC. Prot Expr Purif 1996;8(4):401-8.

[30] Darboe N, Kenjale R, Picking WL, Picking WD, Middaugh CR. Physical characterization of MxiH and PrgI, the needle component of the type III secretion apparatus from *Shigella* and *Salmonella*. Protein Sci 2005 2005;15(3):543-52.

[31] Kueltzo LA, Osiecki J, Barker J, Picking WL, Ersoy B, Picking WD, et al. Structure-Function Analysis of Invasion Plasmid Antigen C (IpaC) from *Shigella flexneri*. J Biol Chem 2003 January 24, 2003;278(5):2792-8.

[32] Matulis D, Lovrien R. 1-Anilo-8-naphthalene sulfonate anion-protein binding depends primarily on ion pair formation. Biophys J 1998;74:422-9.

[33] Peek LJ, Brandau DT, Jones LS, Joshi SB, Middaugh CR. A systematic approach to stabilizing EBA-175 RII-NG for use as a malaria vaccine. Vaccine 2006;24(31-32):5839-51.

[34] Deane JE, Cordes FS, Roversi P, Johnson S, Kenjale R, Picking WD, et al. Expression, purification, crystallization and preliminary crystallographic analysis of MxiH, a subunit of the *Shigella flexneri* type III secretion system needle. Acta Crystallogr Sect F: Struct Biol Cryst Commun 2006;62:302-5.

[35] Jouihri N, Sory MP, Page AL, Gounon P, Parsot C, Allaoui A. MxiK and MxiN interact with the Spa47 ATPase and are required for transit of the needle components MxiH and MxiI, but not of Ipa proteins, through the type III secretion apparatus of *Shigella flexneri*. Molec Microbiol 2003;49:755-67.

[36] Cooper A. Thermodynamics of Protein Folding and Stability: JAI Press Inc., 1999.

[37] Mach H, Ryan JA, Burke CJ, Volkin DB, Middaugh CR. Partially structured self-associating states of acidic fibroblast growth factor. Biochemistry 1993;32(30):7703-11.

[38] Endo T, Schatz G. Latent membrane perturbation activity of a mitochondrial precursor protein is exposed by unfolding. EMBO J 1988;7(4):1153-8.

[39] Bychkova VE, Ptitsyn OB. The molten globule *in vitro* and *in vivo*. Chemtracts Biochem Mol Biol 1993;4:133-63.

[40] Ptitsyn OB, Bychkova VE, Uversky VN. Kinetic and equilibrium folding intermediates. Philos Trans R Soc Lond 1995;348(B):35-41.

[41] Raetz CRH, Reynolds MC, Trent SM, Bishop RE. Lipid A Modification Systems in Gram-Negative Bacteria. The Annual Review of Biochemistry 2007 July;76:295-329.

[42] Marlovits TC, Kubori T, Sukhan A, Thomas DR, Galan JE, Unger VM. Structural Insights into the Assembly of the Type III Secretion Needle Complex. Science 2004 November 5, 2004;306(5698):1040-2.

[43] Mecsas J, Strauss E. Molecular Mechanisms of Bacterial Virulence: Type III Secretion and Pathogenicity Islands. Emerg Infect Dis 1996;2(4):271-88.

[44] Baker NA, Sept D, Joseph S, Holst MJ, McCammon JA. Electrostatics of nanosystems: Application to microtubules and the ribosome. Proc Natl Acad Sci USA 2001 August 28, 2001;98(18):10037-41.

Chapter 3

Pre-formulation studies of TTSS needle antigens

3.1 Introduction

Shigella flexneri, *Salmonella typhimurium* and *Burkholderia pseudomallei* are three pathogens responsible for an extensive number of potentially preventable disease cases. For example, *Shigella* is one of the leading causes of infant mortality in developing countries, and is responsible for endemic infection levels worldwide which involve more than 165 million people each year [1]. *Salmonella* is best known for its high-profile outbreaks in the developed world and is associated worldwide with more than 200 million cases every year [2-4]. *Burkholderia* is endemic to tropical regions, and is listed as a Category B Bioterrorism Agent by the CDC due to its severe course of action, potential for aerosol delivery and worldwide availability [5]. Perhaps the most disturbing fact is the lack of licensed vaccines for prevention of infection by all three of these opportunistic pathogens and their increasing resistance to antibiotic treatment [6-9]. The need for further vaccine development in this area is widely recognized and work shown here is intended to support that effort.

These extremely virulent, opportunistic pathogens are most dangerous to young, elderly and otherwise immuno-compromised individuals. *Shigella* and *Salmonella* are most commonly transmitted through contaminated food or water via the fecal oral route, thus countries with limited sanitation systems are often the most affected. Symptoms of Shigellosis and Salmonellosis include fever, vomiting and dysentery. *Burkholderia* differs in that infection is typically acquired from bacteria found in the soil and water through open sores or lesions [10]. Person-to-person spreading, however, has been documented [5]. Symptoms of mellioidosis vary widely depending on the severity of the

infection. In some cases the bacteria will lie dormant for years, while in more extreme cases, acute localized, pulmonary, bloodstream and chronic infections are possible [10].

Each of these pathogens relies upon a Type Three Secretion System (TTSS) for virulence. This system, commonly referred to as a molecular 'injectisome', is composed of more than 20 proteins which assemble to form basal and extracellular components [11]. This macromolecular conduit allows the bacteria direct physical contact with a host cell and is responsible for the transport of effector proteins from the bacterial cytoplasm directly into the host cell where they subvert normal cell function [12, 13]. The surface exposed 'needle' portion of the structure is composed of approximately 120 copies of a monomeric subunit arranged in a hollow helical array with an inner diameter of approximately 2.0-3.0 nm [12-17]. This appendage is required for virulence and is intimately involved in the initial stages of an infection. Therefore we have explored the use of these surface exposed proteins as potential vaccine antigens [18, 19].

The vaccine antigens studied here are the monomeric subunits of the oligomerized needle appendage from each bacterial system. These small (~10 kDa), acidic (pI <5) proteins are characterized by distinct patches of both positive and negative surface charge, which likely contribute to their intrinsic polymerization [20]. When recombinantly expressed, their propensity to oligomerize results in a viscous solution of highly associated products; however, it is possible to attain soluble monomer protein if 5 residues from the C terminus are deleted [21]. The resultant recombinant mutant proteins MxiH $^{\Delta 5}$, PrgI $^{\Delta 5}$ and BsaL $^{\Delta 5}$ from the gram-negative bacteria *Shigella flexneri*,

Salmonella typhimurium and *Burkholderia pseudomallei* respectively have been shown to retain native structure [22].

Previously, we characterized the solution stability of the mutant monomeric needle antigens, and found them to be pH sensitive, thermally labile proteins with reversible transitions and molten globule-like behavior in the physiological temperature range [23]. Additionally, initial immunogenicity studies have shown MxiH $^{\Delta 5}$ and PrgI $^{\Delta 5}$ to be antigenic in a murine model (submitted). Here we describe pre-formulation studies of these vaccine candidates. It should be emphasized that the intention of this work is not to propose clinical formulations, but rather to examine aspects of potential future formulations which may be useful for further development of these and other related vaccines based on the needle proteins.

3.2 Materials and Methods

3.2.1 Materials

C terminal truncated proteins were expressed in *E. coli* with a C terminal His_6 tag as described previously [17, 21, 22]. Affinity purification was performed using nickel chelation chemistry, and the samples were dialyzed against isotonic pH 6 citrate phosphate buffer and stored at -80 ^{o}C until use. Alhydrogel® (2%) and Adjuphos® were acquired from E.M. Sergeant Pulp and Co., Inc. (Clifton, NJ).

3.2.2 Screening for Excipients

Potential excipients were screened for stabilizing effects using far-UV circular dichroism spectroscopy. Secondary structure was used as the stability indicating parameter in this case because of the lack of other temperature sensitive signals (ie: Trp fluorescence, static light scattering) exhibited by these proteins [23]. Thermal melts were conducted using a Jasco J-720 spectropolarimeter equipped with a six position sample holder and a Peltier temperature control device (Easton, MD). Initially, individual far-UV CD spectra were recorded for each of 6 samples at 10 ^{o}C from 260 to 190 nm in a 0.1 cm path length cell. The cell holder temperature was then increased from 10 to 85 ^{o}C in increments of 0.5 ^{o}C, and at each temperature step the cell holder was incubated for 5 min to ensure thermal equilibration of the samples before a scan was obtained. For each thermal melt, a control protein sample containing 0.25 mg/mL protein in isotonic citrate phosphate buffer at pH 6.0 was run simultaneously with 5 samples containing test compounds at the indicated concentrations. Spectra of the compounds alone were also collected and subtracted from the protein spectra when necessary. Using the instrument software, the resulting data were converted to molar ellipticity as a function of temperature. Midpoints of thermal transition (T_m) were determined using Microcal Origin® sigmoidal fit graphing tools.

3.2.3 Adsorption Isotherms

Protein was dialyzed into isotonic 10 mM Histidine buffer at pH 6 overnight at 4 ^{o}C using 3,500 MWCO Slide-A-Lyzer Dialysis Cassettes (Thermo Scientific, Rockford,

IL). Upon completion, the protein concentration was determined by UV absorbance spectroscopy using an Agilent 8453 UV/Vis spectrophotometer equipped with diode array detector (Agilent Technologies, Santa Clara, CA). Extinction coefficients of 9,970, 11,460, and 12,950 M^{-1} cm^{-1} at 280 nm were used for MxiH $^{\Delta 5}$, PrgI $^{\Delta 5}$ and BsaL $^{\Delta 5}$ respectively [23]. Protein was then adsorbed to aluminum hydroxide by combining a pre-determined volume of aluminum hydroxide stock, protein stock and histidine buffer to produce a range of protein concentrations (0-1.25 mg/mL) and a constant aluminum concentration (0.5 mg/mL), and allowing it to rotate end-over-end at 4 ^{o}C for 1 hour. Samples were then centrifuged at 14,000 g for 30 sec, and the resulting supernatant was removed and assayed for protein content by UV absorbance spectroscopy. The amount of protein adsorbed was determined by subtracting the amount found in the supernatant from the original amount added.

3.2.4 Adsorption Mechanism

'Elution' solutions were prepared in isotonic pH 6 histidine buffer using ACS grade reagents and were not pH adjusted. The adsorption protocol described above was used to prepare several 1.5 mL samples containing 0.2 mg/mL protein per 0.5 mg/mL aluminum, a ratio at which > 95% of the protein is adsorbed. The samples were then centrifuged for 2 min at 3,000 g to pellet the aluminum-protein complex, and the resulting supernatant was removed. A control sample was prepared by adding 1 mL of isotonic 10 mM Histidine buffer at pH 6 to an aluminum-protein pellet. In the same way, 1 mL of a previously prepared 'elution' solution was added to each aluminum-protein

pellet containing vial. All vials were then rotated end-over-end at 4 ^{o}C for 48 hours. The samples were then once again centrifuged, and the supernatant of each evaluated for protein content.

3.2.5 ELISA

A standard Enzyme Linked Immunosorbent Assay (ELISA) was used to evaluate the stability of the adsorbed PrgI $^{\Delta 5}$ vaccine. Solution PrgI$^{\Delta 5}$ and incubated aluminum adsorbed samples were plated (100 µL) onto Nunc-Immuno™ MediSorp™ (Nalge Nunc International, Wiesbaden, Germany) 96-well plates at 10 µg/mL in carbonate buffer (pH 9.6) overnight at 4 ^{o}C. Plates were blocked with Superblock per product instructions. A 1:10,000 dilution of Anti-PrgI$^{\Delta 5}$ IgG was prepared in Superblock and allowed to incubate on the plate for 2 hours at RT. The plates were then washed 4 times using a 0.85% Sodium Chloride solution. HRP-conjugated Goat anti Mouse Monoclonal Antibody (Sigma, St. Louis, MO) was diluted 1:500 in blocking buffer, plated (100 µL) and incubated for 1 hour at RT. The plates were then washed as above, and 3,3'5,5'-TetraMethylBenzidine (TMB) substrate (100 µL) (Sigma, St. Louis, MO) was added. After 30 minutes at RT, 2 M HCl (100 µL) was added to quench the reaction and plates were read using a SpectraMax M5 plate reader (Molecular Devices, Sunnyvale, CA) at 450 nm. Statistical significance ($p \leq 0.05$) was evaluated using a Student's t-test in Microsoft Excel.

3.2.6 Capillary liquid chromatography-mass spectrometry analysis and protein mapping

A 0.1 mg/mL trypsin solution was prepared by dissolving 5.2 mg of trypsin in 52 mL of 0.05 M Ammonium Bicarbonate buffer at pH 6.6. Protein was exposed to the trypsin solution at a 1:200 concentration ratio, and incubated at 37 ^{o}C for > 1 hour to permit adequate digestion. Samples were introduced into an LTQ-FT Ultra Hybrid Mass Spectrometer (ThermoFinnigan) via capillary liquid chromatography as described [110]. A data-dependant acquisition method was used for setting up the experiments. The five most intensive precursor ions in a survey MS1 mass spectrum acquired in the Fourier transform-ion cyclotron resonance over a mass range of 300–2000 *m*/*z* were selected and sequentially fragmented for MS2 analysis in the linear ion trap by collision-induced dissociation. Experimental raw files were processed by TurboSequest batch search using BioWorks 3.2 software. All text files generated by BioWorks 3.2 for every MS2 fragmentation spectrum were combined within each experiment using an in-house written Perl script. The resulted files were submitted for peptide/protein identification to Mascot (v2.2, Matrix Science) database-searching program. Parameters set during the searches were as follows: custom protein database, a peptide mass tolerance of 2.2 u to account for higher isotopes of large peptides and MS/MS tolerance of 0.6 Da, semi-trypsin specificity with up to two missed cleavages. Variable modification was set to consider oxidation on methionine residues. Sequest and Mascot results were imported into Scaffold 2.2.03 software (Proteome Software Inc.) for analyzing with X!Tandem search algorithm and statistical validation of peptide/protein identities. Peptides validated by Scaffold at a confidence level of 50% and greater were taken to calculate protein coverage.

Identification of peptides at a confidence level of less than 50% was considered positive if their corresponding m/z value from the survey MS1 scans were found to be within 10 ppm mass tolerance.

3.3 Results

3.3.1 Screening for Excipients

A panel of Generally Regarded as Safe (GRAS) compounds was screened for potential stabilizing effects on the secondary structure of all three recombinant proteins using temperature dependent circular dichroism spectroscopy. As shown in Figure 3.1, MxiH $^{\Delta 5}$ and PrgI $^{\Delta 5}$ displayed broad yet distinctly sigmoidal transitions with midpoints of thermal melting (T_m) of 40.6 +/- 0.2 and 34.8 +/- 0.5 ^{o}C respectively. The melting curve for BsaL $^{\Delta 5}$ did not display sigmoidal behavior and as a result no thermal midpoint could be assigned. The difference observed in the melting curves may be attributed to the absence of a critical salt bridge in BsaL $^{\Delta 5}$ which is present in both MxiH $^{\Delta 5}$ and PrgI $^{\Delta 5}$ [20]. For the purposes of excipient selection, we used changes in T_m as a quantitative measure of potential excipient effects.

For both MxiH $^{\Delta 5}$ and PrgI $^{\Delta 5}$, stabilization, as represented by an increase in T_m, was observed in the presence of polyols and carbohydrates including glycerol, sorbitol, dextrose, trehalose, and sucrose. As shown in Figure 3.2, greater stabilization was, for the most part, a function of increased excipient concentration. Although it was not

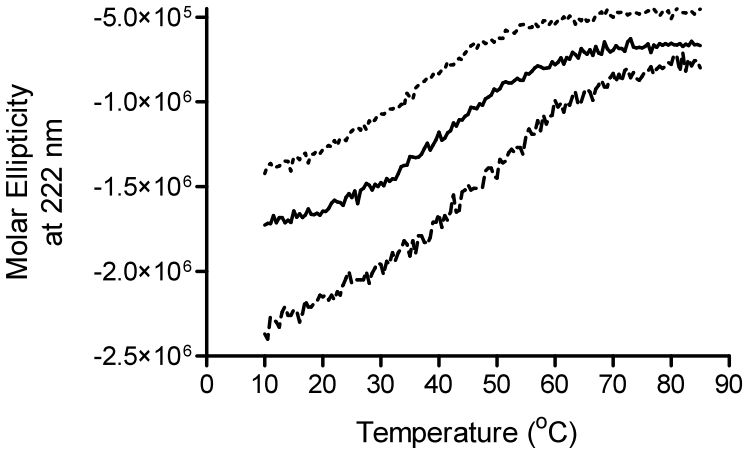

Figure 3.1 Circular dichroism thermal melting curves for each MxiH $^{\Delta 5}$ (——), PrgI $^{\Delta 5}$ (·····) and BsaL $^{\Delta 5}$ (---) at 0.2 mg/mL in isotonic 10 mM Histidine buffer at pH 6.0.

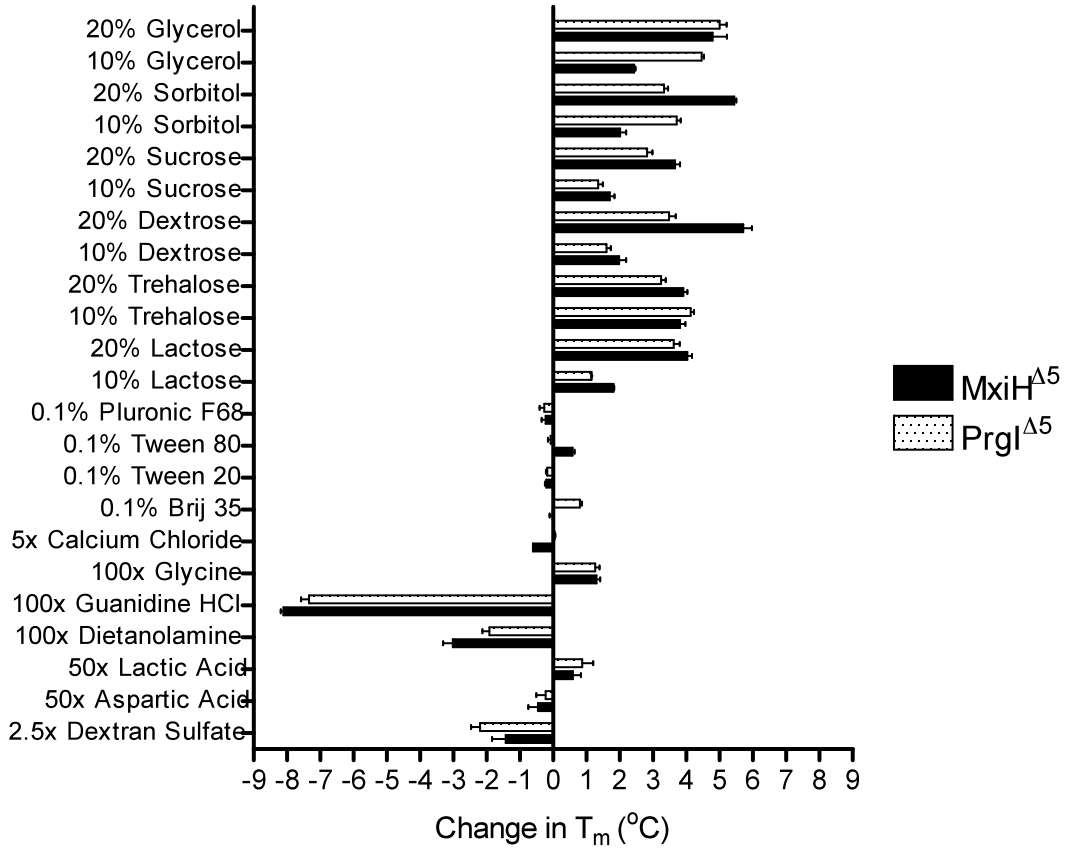

Figure 3.2 Changes in T_m (^oC) as measured by circular dichroism spectroscopy for MxiH$^{\Delta5}$ (▒) and PrgI$^{\Delta5}$ (▒).

possible to confirm with T_m values, visual comparison of the BsaL$^{\Delta 5}$ melting curves showed similar stabilization trends (data not shown). Combinations of excipients were also screened using circular dichroism spectroscopy (data not shown). Shown in Figure 3.3 are the thermal melting curves for both MxiH$^{\Delta 5}$ and PrgI$^{\Delta 5}$ in the presence and absence of 10% Sucrose and 5% Dextrose, an excipient combination which was identified as optimal for all three proteins. In both cases, approximately 4 ^{o}C of additional thermal stabilization was gained in the presence of 10% Sucrose and 5% Dextrose (MxiH$^{\Delta 5}$, 40.4 to 44.4 ^{o}C and PrgI$^{\Delta 5}$, 35.7 to 39.3 ^{o}C).

3.3.2 Adsorption Isotherms

The three proteins studied in this work are all quite acidic, with iso-electric points in the region of 4.5-5.0. The two most commonly used FDA approved aluminum salt adjuvants are aluminum hydroxide, which is positively charged at neutral pH and has a point of zero charge (PZC) of 11, and aluminum phosphate, which is negatively charged at neutral pH and has a PZC of approximately 5-7 [25]. As one would expect, minimal adsorption of the needle proteins occurs in the presence of aluminum phosphate (data not shown), while substantial interaction was observed with aluminum hydroxide. This phenomenon is presumably due to the electrostatic repulsive forces present between the aluminum phosphate and the protein at neutral pH, and the electrostatic attractive forces present on aluminum hydroxide and the proteins. As shown in Figure 3.4, the three proteins display similar adsorption isotherms with high levels of protein loading. When

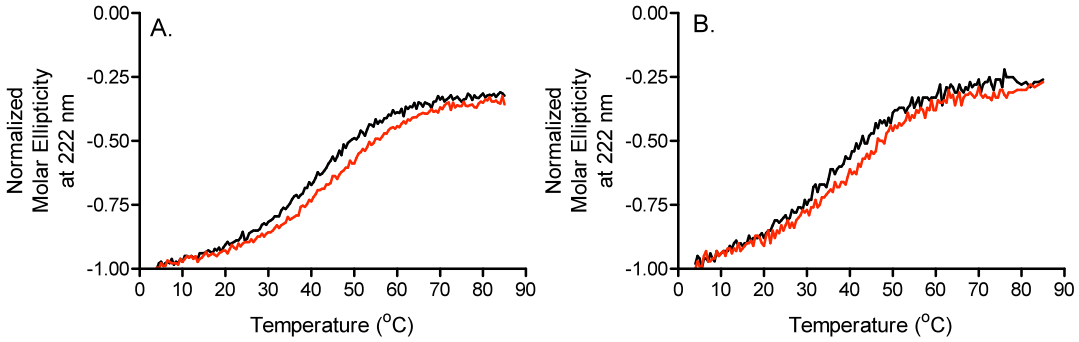

Figure 3.3 Circular dichroism thermal melting curves for (A) MxiH$^{\Delta 5}$ and (B) PrgI$^{\Delta 5}$ at 222 nm in the presence (-) and absence (-) of 10% Sucrose and 5% Dextrose.

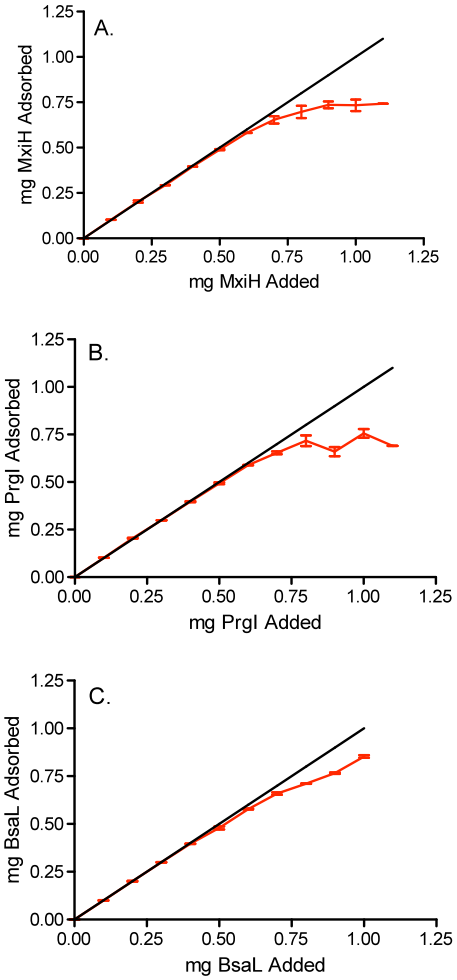

Figure 3.4 Adsorption isotherms for MxiH $^{\Delta 5}$ (A), PrgI $^{\Delta 5}$ (B) and BsaL $^{\Delta 5}$ (C) with 0.5 mg/mL aluminum in isotonic 10 mM histidine buffer at pH 6.

the data were plotted according to the Langmuir equation [26], straight lines with R^2 values in the range of 0.984 to 0.999 were obtained. The adsorptive capacities were calculated to be 1.56, 1.72 and 1.62 mg/mg aluminum for PrgI $^{\Delta 5}$, BsaL $^{\Delta 5}$ and MxiH $^{\Delta 5}$ respectively.

3.3.3 Adsorption Mechanism

To investigate the forces responsible for adsorption of the needle proteins to aluminum hydroxide, a series of 'elution' solutions were prepared and adsorbed samples exposed to them. Each solution is expected to primarily inhibit a specific type of protein-adjuvant interaction. Adsorbed samples were prepared as described above and supernatants were assayed for protein content prior to treatment. In all cases, < 2% residual protein was observed indicating that approximately 98% of the protein was adsorbed prior to 'elution' treatment. As shown in Table 3.1, when freshly adsorbed samples (< 24 h incubation) were treated nearly all the protein was desorbed from the surface in the presence of 1.0 M Guanidine Hydrochloride, 1.0 M Sodium Citrate, 1.0 M Monobasic Sodium Phosphate or 1.0 M Dibasic Sodium Phosphate. Although the proteins have highly charged surfaces [20], they do not appear to interact with the adjuvant directly through electrostatic interactions since they are not eluted in the presence of up to 3.0 M Sodium Chloride. If the adsorbed formulations were aged prior to analysis, the results differed significantly. After 2 weeks of incubation at 4 ^{o}C, only the Sodium Phosphate and Sodium Citrate solutions were able to desorb the protein, and

Table 3.1 Protein (mg/mL) present in sample supernatant as assayed by UV absorbance spectroscopy following 'elution' treatment. All samples originally contained 0.2 mg/mL protein in the presence of 0.5 mg/mL aluminum. Where a dash is present no sample was analyzed. Error was estimated at approximately 0.05 mg/mL.

MxiH $^{\Delta 5}$	**Freshly Prepared**	**2 wks, 4 °C**	**2 wks, 40 °C**
Prior to Elution	0.001	0.001	0.000
10 mM Histidine	0.003	0.002	0.014
0.5 M NaCl	0.001	-	-
0.75 M NaCl	0.002	-	-
1.0 M NaCl	0.002	-	-
2.0 NaCl	0.005	-	-
3.0 M NaCl	0.001	0.000	-
1.0 M Gdn HCl	0.003	0.003	0.001
1.0 M NaCit	0.143	0.091	0.039
1.0 M NaPhos	0.201	0.160	0.078
70 mM SDS	0.088	-	-
PrgI $^{\Delta 5}$			
Prior to Elution	0.001	0.002	0.002
10 mM Histidine	0.003	0.003	0.000
0.5 M NaCl	0.001	-	-
0.75 M NaCl	0.002	-	-
1.0 M NaCl	0.004	-	-
2.0 NaCl	0.003	-	-
3.0 M NaCl	0.000	0.006	-
1.0 M Gdn HCl	0.005	0.006	0.004
1.0 M NaCit	0.137	0.081	0.036
1.0 M NaPhos	0.197	0.151	0.092
70 mM SDS	0.056	-	-
BsaL $^{\Delta 5}$			
Prior to Elution	0.001	0.002	0.002
10 mM Histidine	0.004	0.003	0.003
0.5 M NaCl	0.000	-	-
0.75 M NaCl	0.001	-	-
1.0 M NaCl	0.006	-	-
2.0 NaCl	0.003	-	-
3.0 M NaCl	0.000	0.000	-
1.0 M Gdn HCl	0.002	0.005	0.002
1.0 M NaCit	0.171	0.105	0.036
1.0 M NaPhos	0.196	0.154	0.082
70 mM SDS	0.100	-	-

in both cases, the quantity eluted represented only approximately 75% of the total protein. At an increased incubation temperature of 40 ^{o}C, the results were similar, but the quantity eluted was further reduced to less than half of the original amount. These observations suggest that interactions occurring upon initial adsorption change with time as the protein establishes new contacts with the surface [30]. Given the lack of elution in the presence of high salt concentrations and the strongly hydrophilic nature of the proteins and the surface, we hypothesize that adsorption probably involves Van der Waals interactions and/or hydrogen bonding.

3.3.4 ELISA

To examine the stability of the adsorbed product, we employed a standard ELISA method. Unfortunately, only Anti-PrgI $^{\Delta 5}$ antibodies were available and therefore only the PrgI formulation was studied in this manner. We were particularly interested in evaluating the effect of decreased protein desorption over time in terms of changes in the protein as detected by interaction with a specific antibody. We therefore compared the antibody binding of solution protein to that of adsorbed protein which had either been stored at 4 or 40 ^{o}C for > 6 months. As shown in Figure 5, no significant difference ($p<0.0001$) in interaction with antibody was observed for PrgI $^{\Delta 5}$ in solution and an adsorbed sample stored for 6 months at 4 ^{o}C. A second sample which had been stored at 40 ^{o}C, however, did display a significantly lower response than both the solution material and the adsorbed material stored at 4 ^{o}C. This result suggests loss of at least one epitope upon long-term storage at elevated temperatures.

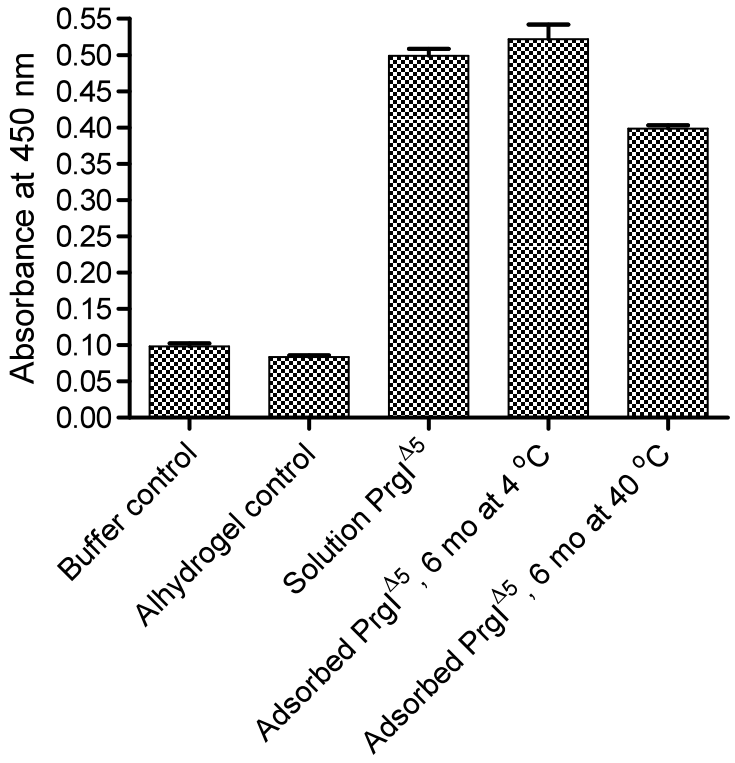

Figure 3.5 Absorbance values observed at 450 nm when each sample was plated and analyzed by a standard ELISA protocol.

3.3.5 Capillary liquid chromatography-mass spectrometry analysis and protein mapping

To further examine the difference observed by ELISA between the adsorbed PrgI $^{\Delta 5}$ formulations stored at 4 vs. 40 ^{o}C, we eluted protein from the adjuvant surface using 1.0 M Sodium Phosphate and obtained a peptide map for both samples. We also acquired a map of the solution protein which had been frozen since production. Although the coverage was not optimal due to the presence of several small peptides, all residues commonly associated with chemical degradation reactions were covered and no changes were observed in either of the adsorbed samples (Figure 3.6). This suggests that the decrease in antibody binding observed in the ELISA assay was due to a change in protein conformation as opposed to an alteration in primary structure.

3.4 Discussion

As described above, previous work has thoroughly defined the solution stability of each of the three proteins over a range of pH 3-8 and under thermal stress. We found that these mutant proteins, which are composed of helix-turn-helix structural elements, are sensitive to pH, thermally labile and have reversible thermal transitions. Additionally, they display molten globule-like behavior in the physiological temperature range which may be critical to their transport through the growing needle structure given its limited diameter of 2.0-3.0 nm.

Here we have further characterized the proposed vaccine antigens for the purposes of formulation development. Excipient screening indicates that their thermal stability is increased by the presence of polyols and carbohydrates probably by the well

A.

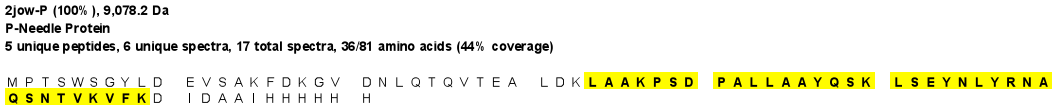

B.

C.

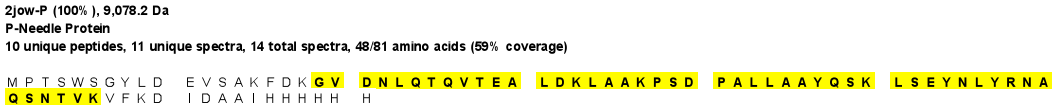

Figure 3.6 Peptide maps for (A) untreated PrgI$^{\Delta 5}$ (B) PrgI $^{\Delta 5}$ eluted from aluminum hydroxide surface following 6 mos of incubation at 4 ^{o}C and (C) PrgI $^{\Delta 5}$ eluted from aluminum hydroxide surface following 6 mos of incubation at 40 ^{o}C.

described mechanism of preferential hydration [27]. Binding isotherms for each antigen to aluminum hydroxide were also presented. In all three cases, data was well described by the Langmuir equation with adsorptive capacities in the range of 1.56-1.72 mg/mg aluminum. The proteins do not appear to interact with aluminum hydroxide through electrostatic interactions despite their highly charged surfaces, but rather that hydrogen bonds, Van der Waals or apolar forces are involved. Additionally, a time-dependent change was observed in the desorption profile of adsorbed proteins. These changes in adsorption behavior were characterized over time using both an ELISA method and peptide mapping for one of the proteins. ELISA results indicated a difference in the antibody binding ability of the adsorbed protein stored for ~ 6 mos at 40 ^{o}C while no change was observed at 4 ^{o}C. Peptide maps of the adsorbed protein indicate that relative to the protein primary structure prior to adsorption; no chemical changes in amino acids were observed.

Concurrent with this work, a second protein integral to the TTSS has also been developed as a potential vaccine candidate. This protein, often referred to as the 'tip' protein, has been shown in *Shigella* to transverse the needle and reside at the distal tip during the initial stages of infection [28]. Many groups have shown this protein from the *Shigella* system, IpaD, to be highly immunogenic [29]. Additionally, antibodies specific to this protein have been shown to neutralize host-cell infection by *Shigella* suggesting protective behavior [28]. It is interesting to note that the excipients which provided the greatest degree of thermal stabilization for the needle proteins were similar to those which stabilized the tip proteins (Markham *et al*, unpublished results), and that both

groups of proteins strongly adsorb to aluminum hydroxide. We have hypothesized that a bivalent vaccine would be superior to a monovalent one and to that end have conducted initial immunogenicity studies of the two types of vaccines. We were able to show that administration of a bivalent vaccine to mice containing both the needle and tip proteins from the *Shigella* system resulted in a synergistic increase in immune response relative to monovalent doses (submitted).

3.5 Bibliography

[1] *Shigella*. 2009 [cited 2009 February 19]; Available from: http://www.who.int/vaccine_research/diseases/shigella/en/

[2] World Health Organization Drug-Resistant *Salmonella.* 2005 [cited 2009 February 19]; Available from: http://www.who.int/mediacentre/factsheets/fs139/en/print.html

[3] *Salmonella Saintpaul* Outbreak. 2008 [cited 2009 February 19]; Available from: http://www.fda.gov/oc/opacom/hottopics/tomatoes.html

[4] Peanut Product Recalls: *Salmonella Typhimurium*. 2008 [cited 2009 February 19]; Available from: http://www.fda.gov/oc/opacom/hottopics/Salmonellatyph.html

[5] National Center for Zoonotic V-B, and Enteric Diseases (ZVED). Melioidosis. 2008 March 27 2008 [cited 2009 February 20]; Available from: http://www.cdc.gov/nczved/dfbmd/disease_listing/melioidosis_gi.html

[6] Ashkenazi S, Levy I, Kazaronovski V, Samra Z. Growing antimicrobial resistance of *Shigella* isolates. J Antimicrob Chemother 2003 February 1, 2003;51(2):427-9.

[7] Avgeri SG, Matthaiou DK, Dimopoulos G, Grammatikos AP, Falagas ME. Therapeutic options for Burkholderia cepacia infections beyond co-trimoxazole: a systematic review of the clinical evidence. International Journal of Antimicrobial Agents;In Press, Corrected Proof.

[8] Ergönül Ö, Imre A, Çelikbas A, Dokuzoguz B. Drug resistance of *Shigella* species: changes over 20 years in Turkey. International Journal of Antimicrobial Agents 2004;23(5):527-8.

[9] Melloul AA, Hassani L. Antibiotic resistance of *Salmonella* strains isolated from children living in the wastewater-spreading field of Marrakesh city (Morocco) World Journal of Microbiology and Biotechnology 1999 February;15(1):81-5.

[10] Dance DA. Melioidosis: the tip of the iceberg? Clin Microbiol Rev 1991 January 1, 1991;4(1):52-60.

[11] Blocker A, Komoriya K, Aizawa S-I. Type III secretion systems and bacterial flagella: Insights into their function from structural similarities. Proc Natl Acad Sci USA 2003 March 18, 2003;100(6):3027-30.

[12] Blocker A, Jouihri N, Larquet E, Gounon P, Ebel F, Parsot C, *et al.* Structure and composition of the *Shigella flexneri* 'needle complex', a part of its type III secreton. Molec Microbiol 2001;39(3):652-63.

[13] Tamano K, Aizawa S, Katayama E, Nonaka T, Imajoh-Ohmi S, Kuwae A, Nagai, *et al.* Supramolecular structure of the *Shigella* type III secretion machinery: The needle part is changeable in length and essential for delivery of effectors. . EMBO J 2000;19(15):3876-87.

[14] Cordes FS, Komoriya K, Larquet E, Yang S, Egelman EH, Blocker A, *et al.* Helical Structure of the Needle of the Type III Secretion System of *Shigella flexneri*. J Biol Chem 2003 May 2, 2003;278(19):17103-7.

[15] Deane JE, Roversi P, Cordes FS, Johnson S, Kenjale R, Daniell S, *et al.* Molecular model of a type III secretion system needle: Implications for host-cell sensing. Proc Natl Acad Sci USA 2006 August 15, 2006;103(33):12529-33.

[16] Kubori T, Matsushima Y, Nakamura D, Uralil J, Lara-Tejero M, Sukhan A, et al. Supramolecular Structure of the *Salmonella typhimurium* Type III Protein Secretion System. Science 1998 April 24, 1998;280(5363):602-5.

[17] Zhang L, Wang Y, Picking WL, Picking WD, De Guzman RN. Solution Structure of Monomeric BsaL, the Type III Secretion Needle Protein of *Burkholderia pseudomallei*. J Molec Biol 2006;359(2):322-30.

[18] Galan JE, Wolf-Watz H. Protein delivery into eukaryotic cells by type III secretion machines. Nature 2006;444(7119):567-73.

[19] He SY, Nomura K, Whittam TS. Type III protein secretion mechanism in mammalian and plant pathogens. Biochimica et Biophysica Acta (BBA) - Molecular Cell Research 2004;1694(1-3):181-206.

[20] Wang Y, Ouellette AN, Egan CW, Rathinavelan T, Im W, De Guzman RN. Differences in the Electrostatic Surfaces of the Type III Secretion Needle Proteins PrgI, BsaL, and MxiH. Journal of Molecular Biology 2007;371(5):1304-14.

[21] Kenjale R, Wilson J, Zenk SF, Saurya S, Picking WL, Picking WD, *et al.* The Needle Component of the Type III Secreton of *Shigella* Regulates the Activity of the Secretion Apparatus. J Biol Chem 2005 December 30, 2005;280(52):42929-37.

[22] Darboe N, Kenjale R, Picking WL, Picking WD, Middaugh CR. Physical characterization of MxiH and PrgI, the needle component of the type III secretion apparatus from *Shigella* and *Salmonella*. Protein Sci 2005 2005;15(3):543-52.

[23] Barrett BS, Picking WD, Picking WL, Middaugh CR. The response of type three secretion system needle proteins $MxiH^{\Delta 5}$, $BsaL^{\Delta 5}$, and $PrgI^{\Delta 5}$ to temperature and pH. Proteins 2008;73(3):632-43.

[24] Ikehata K, Duzhak TG, Galeva NA, Ji T, Koen YM, Hanzlik RP. Protein Targets of Reactive Metabolites of Thiobenzamide in Rat Liver in Vivo. Chemical Research in Toxicology 2008;21(7):1432-42.

[25] Hem SL, White JL. Structure and properties of aluminum containing adjuvants. In: Powell MF, Newman MJ, editors. Vaccine Design: The Subunit and Adjuvant Approach. New York: Plenum Press, 1995: 249-76.

[26] Martin A. Interfacial Phenomena. Physical Pharmacy. Philadelphia: Lippincott Williams and Wilkins, 1993: 380-1.

[27] Lee JC, Timasheff SN. The stabilization of proteins by sucrose. J Biol Chem 1981 July 25, 1981;256(14):7193-201.

[28] Espina M, Olive AJ, Kenjale R, Moore DS, Ausar SF, Kaminski RW, *et al.* IpaD Localizes to the Tip of the Type III Secretion System Needle of *Shigella flexneri*. Infect Immun 2006 August 1, 2006;74(8):4391-400.

[29] Turbyfill KR, Mertz JA, Mallett CP, Oaks EV. Identification of Epitope and Surface-Exposed Domains of *Shigella flexneri* Invasion Plasmid Antigen D (IpaD). Infect Immun 1998 May 1, 1998;66(5):1999-2006.

[30] Norde W. Adsorption of proteins from solution at the solid-liquid interface. Adv Colloid Interface Sci 1986;25(4):267-340.

Chapter 4

Immunogenicity of Recombinant TTSS Proteins

4.1 Introduction

Gram-negative bacterial pathogens are responsible for millions of debilitating infections each year. For example, *Shigella flexneri* and *Salmonella* spp., account for upwards of 165 and 200 million cases annually, respectively [1,2].

The *Shigella* species primarily use fecal-oral transmission to invade human hosts, most commonly via contaminated food or water. Host-to-host spreading, however, has also been observed. As a result, densely populated regions lacking proper sanitation are among the most heavily impacted. Symptoms of infection include fever, vomiting, severe abdominal cramping and/or bleeding, diarrhea and dysentery. Immuno-compromised populations, including the young and elderly, are more susceptible to serious complications arising from infection, which may ultimately result in death. *Salmonella* spp. also infects via the fecal-oral route with symptoms similar to those of Shigella; however, select serotypes are also known to induce bacteremia [3]. While Shigella infections are more common in developing nations, high profile food-borne Salmonella outbreaks are increasingly frequent in the U.S. [4, 5].

Due to the frequency and severity of disorders caused by gram-negative bacteria, and their prevalence in the developing world, an inexpensive efficacious vaccine is a leading priority. This need is further emphasized by the emergence of antibiotic resistant strains over the last twenty years. For instance, in separate studies of *Shigella* outbreaks in Kenya and Chile, resistance to Ampicillan was more than 80% percent [6,7]. Also observed in Kenya, 47% of isolated *Salmonella* species were resistant to at least 3 commonly used antibiotics [8]. In the developed world, drug resistance is also on the

rise. In the United States, the number of drug-resistant strains has risen from 0.6% to 34% in a sixteen year period [9].

These two pathogens have in common Type Three Secretion Systems (TTSS) which facilitate host cell invasion. TTSS complexes are composed of more than 20 proteins organized in basal and extracellular regions which span the inner and outer bacterial membranes. They protrude approximately 60 nm from the bacterial surface [10, 11]. The extracellular portion is commonly referred to as the 'needle' for its tubular geometry and involvement in transporting effector proteins directly from the bacterial interior to the host cell cytoplasm. The needle is primarily composed of approximately 120 copies of a repeating polymeric unit arranged in a helical array [10, 11]. The subunit (MxiH, *Shigella flexneri* and PrgI, *Salmonella* spp.) is a small (9-10 kDa) protein composed largely of alpha helical structure. On the distal needle tip lies a multimer which regulates secretion of the effector proteins [12]. The monomer (IpaD, *Shigella flexneri* and SipD, *Salmonella* spp.) is a slightly acidic dumbbell shaped protein (35-37 kDa) with a coiled coil at its center [13, 14].

Here we focus on the needle (MxiH and PrgI) and tip (IpaD and SipD) proteins as potential vaccine antigens due to their surface exposure and essential function during infection. It is thought that antigens with repeating epitopes are more immunogenic than those possessing only a single recognition site [15]. Additionally, increased antigen size has been shown to increase immunogenicity. For this reason we chose to formulate a recombinant polymeric needle construct which mimics the TTSS structure. This would

be combined with tip proteins to create a vaccine with multi-valency and multi-epitope specificity.

Vaccine research directed toward these two pathogens has primarily focused on employing lipopolysaccharide (LPS) and attenuated bacteria, with limited success [16, 17]. In general, vaccines for Salmonella have focused on prevention of enteric fevers such as typhoid, but little work has been done to combat non-typhoidal indications [16, 18, 19]. In the case of *Shigella*, both an attenuated form of the bacteria as well as a formulation containing an O-polysaccharide linked to a carrier protein have reached Phase III clinical trials, but have not yet attained approval [17]. Significant work has also been done on IpaD, the tip protein from the *Shigella* system. Several groups have shown IpaD to be immunogenic [20], and most recently that antibodies raised against IpaD neutralize host-cell invasion of Shigella in-vitro [12]. Furthermore, epitope mapping has been completed for IpaD, which indicates that immune responses are greater in the amino-terminal region [20]. In the same study, it was noted that the *Salmonella* analog, SipD, shares significant sequence homology with the C-terminal region of IpaD. Thus, it is possible that the epitopic response in these regions may provide a degree of cross-protection [20].

Another bacterium for which vaccine efforts have focused on TTSS components is *Yersenia pestis*. In this case, work has focused on subunit forms of the F1 capsular antigen and LcrV, the TTSS needle tip protein. Both have been proven immunogenic and protective, although development has been slowed by several factors including a demonstrated immuno-suppressive effect of LcrV on innate immunity [21-24].

Regardless, it has been established that LcrV activates dendritic cells (DCs) [25]. Similar to the work indicated here, the needle component, YscF, has also been considered as a vaccine antigen for this species. The wild type needle protein was shown to elicit a strong antibody response, and provide a degree of protection (60%) upon challenge [26, 27]. In contrast to the protective effect of antibodies to IpaD, anti-YscF does not inhibit translocation of effector proteins suggesting that its protective effect is probably due to opsinization and/or enhanced complement binding [26].

The work presented represents an initial attempt to develop human vaccines for two of these pathogens. To this end, we have selected an approved adjuvant, aluminum hydroxide, to include in our proposed recombinant subunit formulations.

4.2 Materials and Methods

4.2.1 Vaccine

Recombinant proteins were expressed in *E. coli* as described previously [28-31]. The needle proteins (MxiH and PrgI) were expressed with a five residue C-terminal truncation to prevent inherent polymerization and ensure monomeric behavior. Additionally, MxiH was expressed in its full length form, resulting in largely polymerized material referred to as 'needle' hereafter (data not shown). All proteins were purified by means of a C-terminal His_6 tag, and dialyzed to 10 mM Histidine, 144 mM NaCl buffer at pH 6.0. Proteins were adsorbed to aluminum hydroxide, a positively charged aluminum salt adjuvant, at a concentration of 0.5 mg/mL aluminum by stirring at

4 ^{o}C. In bivalent formulations, the solution materials were mixed, and the adsorption step was performed subsequent to mixing. Characterization and analysis of each formulation are documented elsewhere (in preparation). In all cases complete adsorption (>95%) of the antigens was observed.

4.2.2 Animals and Immunization

Animal studies were performed at the University of Kansas in accordance with regulations set forth by the Institutional Animal Care and Use Committee and guidelines of the Association for Assessment and Accreditation of Laboratory Animal Care. For all experiments, BALB/c mice were acquired from Charles River Breeding Laboratory (Wilmington, MA) and quarantined for 7 days prior to study start. Inoculations (100 μL) were administered intramuscularly on study days 1, 14 and 28 and mice were bled via the submandibular vein on days 0, 7, 21, 35 and 49. Weights were recorded at each time-point and monitored for indications of adverse effects due to dosing, however none were observed. Mice were euthanized following the final bleed on day 49.

In the first study, each group contained 10 mice (5 female and 5 male) with the exception of the histidine buffer control group which contained only 7 mice. No significant differences were observed in end-point titers between male and female mice. Formulations containing only one antigen (MxiH or IpaD) were dosed at 1 (M1, D1), 10 (M10, D10) and 50 (M50, D50) μg/dose, while formulations containing both antigens (MD1, MD10 and MD50) were administered at the same total protein concentration (1, 10 and 50 μg protein/dose); containing one-half the amount of each. The two control

groups were dosed with either formulation buffer or 0.5 mg/mL aluminum in formulation buffer.

Study 2 contained groups of 7 mice (female), and a single control group containing 5 mice (0.5 mg/mL aluminum in isotonic His buffer). MxiH, MxiH Needle and IpaD were all dosed separately at 10 µg, both in the formulation buffer as well as adsorbed to aluminum hydroxide (M-Soln, M-His, N-Soln, N-His, D-Soln and D-His respectively). Bivalent formulations containing IpaD and either MxiH or Needle were administered adsorbed to aluminum hydroxide at total protein concentrations of 20 µg/mL (10 µg of each).

The third study, conducted concurrently with study 2, involved groups of 8 mice, and a control group of 5 mice (0.5 mg/mL aluminum in isotonic His buffer). Monovalent formulations of both PrgI and SipD were administered at 1, 10 and 50 µg/dose (P1, P10, P50, S1, S10 and S50), while bivalent formulations were dosed at total protein concentrations of 2, 20 and 100 µg/dose (PS1, PS10 and PS50). Non-adsorbed formulations were also administered at 50 µg for PrgI, SipD and the bivalent combination (P50-Soln, S50-Soln and PS50-Soln).

4.2.3 IgG Detection in Serum Samples

Antigen specific IgG titers were determined for individual sera samples using a standard Enzyme Linked Immunosorbent Assay (ELISA). The optimal protocol differed for the needle (MxiH and PrgI) and tip (IpaD and SipD) proteins. Needle proteins were adsorbed (100 µL) onto Nunc-Immuno™ MediSorp™ (Nalge Nunc International,

Wiesbaden, Germany) 96-well plates at 10 μg/mL in carbonate buffer (pH 9.6) overnight at 4 ^{o}C. Plates were blocked with Superblock per product instructions. Sera dilutions (100 μL) were made using the blocking buffer and allowed to incubate on the plate for 2 hours at RT. The plates were then washed 3 times using PBS buffer containing 0.05% Tween 20, and a final time with PBS buffer alone. HRP-conjugated Goat anti-Mouse Monoclonal Antibody (Sigma, St. Louis, MO) was diluted 1:500 in blocking buffer, plated (100 μL) and incubated for 1 hour at RT. The plates were then washed as above, and 3,3'5,5'-TetraMethylBenzidine (TMB) substrate (100 μL) (Sigma, St. Louis, MO) was added. After 30 minutes at RT, 2 M HCl (100 uL) was added to quench the reaction and plates were read using a SpectraMax M5 plate reader (Molecular Devices, Sunnyvale, CA) at 450 nm.

Tip proteins were adsorbed (100 μL) onto Costar® non-treated black with clear bottom plates (Corning Life Sciences, Lowell, MA) at 10 μg/ml in carbonate buffer overnight at 4 ^{o}C. Plates were blocked with casein buffer (pH 7.5) for 30 min. Subsequent steps were the same as those for the needle ELISA protocol with the exception that the casein buffer was used in place of the Superblock. In all cases, endpoint titers were determined as the inverse of the dilution with optical density at 450 nm greater than 3 times the negative control.

4.2.4 Statistical Analysis

The geometric mean was used to represent group responses, and error was determined as the standard deviation. Statistical significance was determined with Student's t-test using Microsoft Excel. Significance was determined as $p \leq 0.05$.

4.3 Results

4.3.1 Generation of Humoral Response

Mice were intramuscularly immunized three times at two week intervals (study days 1, 14 and 28), and blood samples were collected via the submandibular vein on days 0, 7, 21, 35, and 49. For all cases, in which significant increases in IgG were observed, all mice had endpoint titers within two dilutions of the geometric mean. Figures displaying individual titers for each experiment can be found in Supplemental Data. On day 0 of the first experiment, all mice had Anti-MxiH IgG titers near 128 (Figure 4.1A). Mice in the control group maintained a similar value throughout the study. Animals dosed with 1 μg of MxiH (M1) showed only a slight increase in antibody response throughout the study ($p<0.02$, day 49 compared to day 0), while those administered a 10 μg dose (M10) showed some response after the second booster compared to the control groups ($p<0.0015$). Mice who received the highest dose of 50 μg (M50) displayed an increase in serum IgG following the initial dose ($p=0.0002$), and continued to increase following the two booster injections. Those animals who received bivalent doses of 1 μg (MD1) did

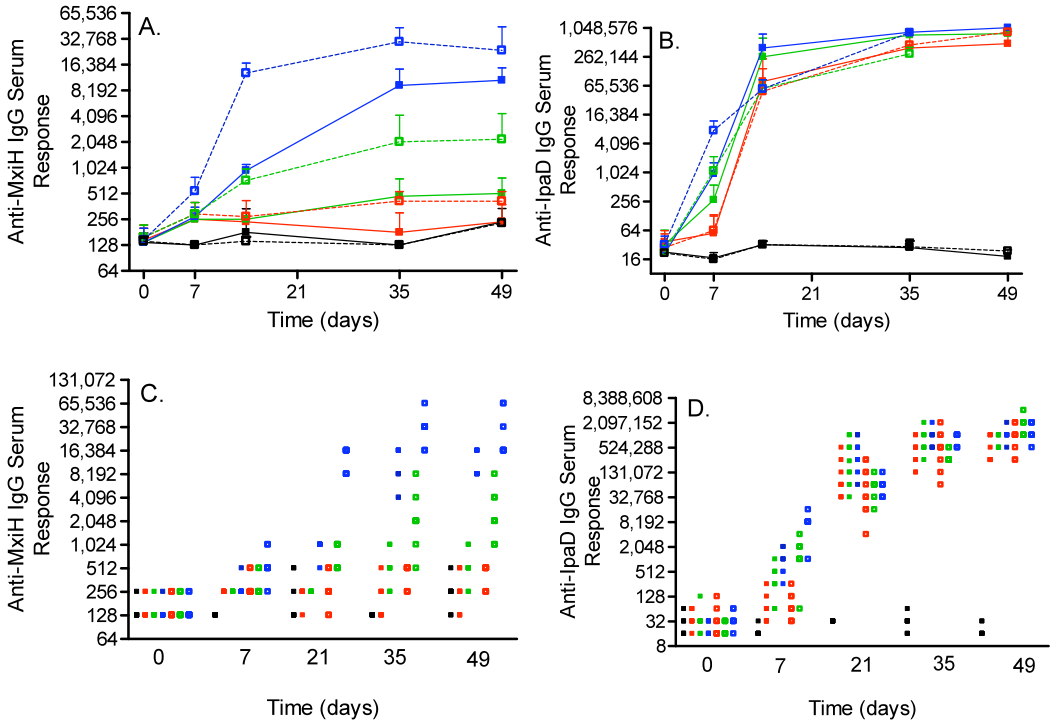

Figure 4.1 Geometric mean anti-MxiH$^{\Delta 5}$ (A) and IpaD (B) IgG serum responses following intramuscular injections on study days 1, 14, 28 of Control (■), M1/D1 (■), M10/D10 (■), M50/D50 (■),MD1 (□), MD10 (□), MD50 (□). Endpoint titer values for anti-MxiH$^{\Delta 5}$ (C) and IpaD (D) IgG.

not show a significant increase in Anti-MxiH IgG during the experiment ($p<0.0001$); however, when the dose was increased to 10 μg (MD10) an increased response relative to the control groups was observed after the initial dose and rose again following the first and second boosters. The largest bivalent dose of 50 μg (MD50) resulted in a dramatically increased response relative to the lower bivalent and all monovalent groups. In all cases, the responses observed following the second booster were sustained for three weeks after the last injection.

When assayed for Anti-IpaD antibodies at day 0, all mice had endpoint titers of approximately 32, and those mice in the control groups continued at a similar low level throughout the remainder of the experiment (Figure 4.1B). Mice which were injected with 1 μg of IpaD (D1) showed a slight increase in IpaD IgG following the first injection ($p<0.05$) followed by an increase of greater than 10 dilutions after the first booster. The 10 μg dose (D10) showed a larger increase in antibody titer compared to the 1 μg dose following the initial injection, and a similar increase following the first booster. The 50 μg dose (D50) followed the same trend with higher endpoints following the first two doses relative to the two lower dose groups. IgG titers for IpaD when administered in the presence of MxiH (MD 1, 10, 50) are analogous to those observed when IpaD was dosed alone. The only significant difference occurs following the initial injection, where the bivalent dosed mice have higher IgG titers than those who received IpaD alone. As seen with the MxiH IgG responses, those observed for IpaD following the second booster remained at a comparable level for all groups when sampled on study day 49.

The second and third studies followed the same immunization and blood collection schedule as the initial experiment. In the second study, all monovalent doses were 10 μg while those containing both antigens had 10 μg of each included. Similar to the initial experiment, all mice had Anti-MxiH IgG endpoint titers of approximately 256 on day 0, and the control group maintained similar values throughout the study (Figure 4.2 A). Those animals who received a 10 μg dose of MxiH in formulation buffer (M-Soln) did not show a significant response throughout the entire study. When the same dose was administered adsorbed to aluminum hydroxide (M-Al), again no response was observed. In the presence of IpaD, however, an increase in Anti-MxiH IgG was observed following the second booster ($p<0.0001$). A significant Anti-MxiH IgG response was observed following the initial injection and further increased following the first booster when mice were inoculated with the polymerized form of MxiH in solution (N-Soln.). The responses observed following the second booster increased only slightly ($p<0.05$). When the same dose was administered adsorbed to the adjuvant (N-Al), a similar trend was observed with increased magnitude. In the presence of IpaD, the response was identical to that in its absence with the exception of the response following the initial injection which was slightly higher in the presence of IpaD.

The anti-IpaD endpoint dilution for all mice prior to the first injection of study 2 as well as mice in the control group throughout was 32 (Figure 4.2B). Mice inoculated with a 10 μg dose of IpaD in solution (D-Soln) displayed a significant response following the first and second injections and maintained the IgG titer thereafter. When adsorbed to aluminum hydroxide (D-Al), the same response trend was observed but with a higher

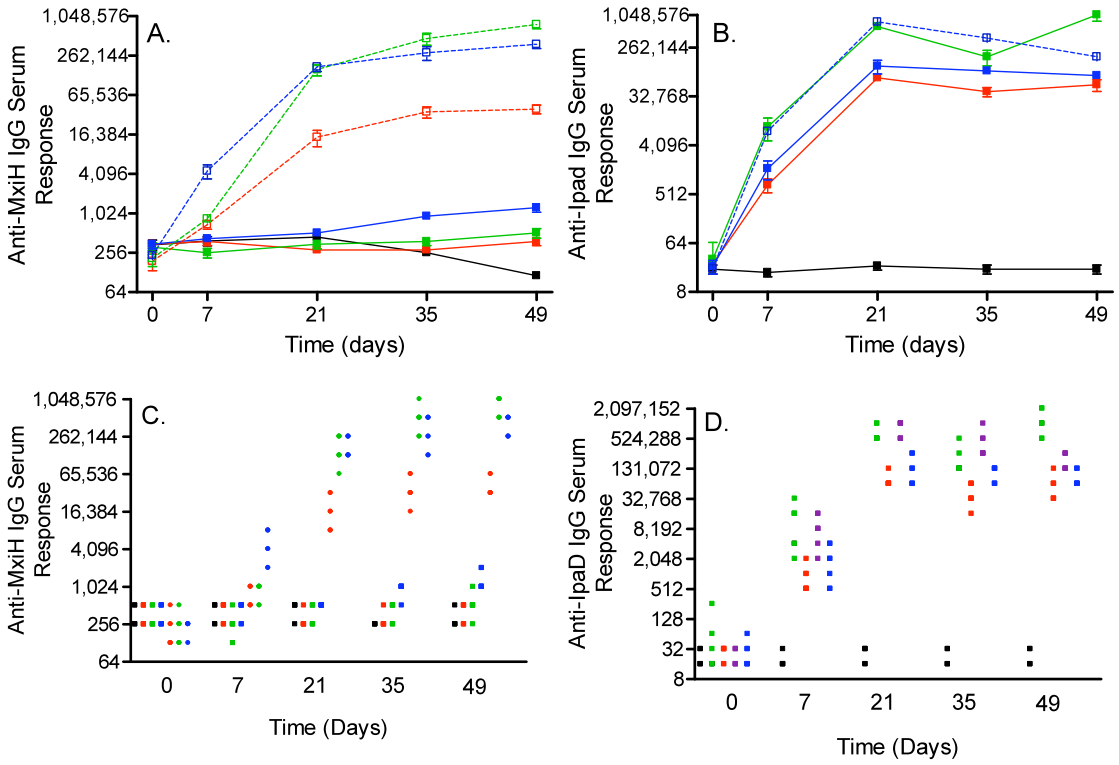

Figure 4.2 Geometric mean anti-MxiH $^{\Delta 5}$ (A) and IpaD (B) IgG serum responses following intramuscular injections on study days 1, 14, 28 Control (■), M-Soln/D-Soln (■), M-Al/D-Al (■), MD-Al (■), N-Soln (□), N-Al (□), and ND-Al (□). Endpoint titer values for anti-MxiH$^{\Delta 5}$ (C) and IpaD (D) IgG.

titer ($p<0.004$, day 49). In the presence of monomeric MxiH (MD-Al), the initial dose elicited a slightly lower response than that of adsorbed IpaD alone ($p<0.01$), and the bivalent formulation did not reach the same endpoint titer following the boost injections. Mice given the bivalent formulation containing the polymerized MxiH displayed an identical profile to that of D-Al with the exception of the final time-point where the response was slightly lower ($p<0.01$).

The final study involved analogous needle and tip proteins from *Salmonella spp.* At the study start, all mice displayed PrgI specific IgG endpoint titers of approximately 64 (Figure 4.3A). The control group displayed a similar value throughout the study. Mice given the 1 μg dose of PrgI (P1) demonstrated an increase in titer over the course of the experiment ($p<0.005$, day 49 compared to day 0). The mice inoculated with 10 μg (P10) displayed an increase following the first dose, and levels rose somewhat during the remainder of the experiment. The mice in the highest aluminum hydroxide adsorbed dose group (P50), had increasing titers following each injection, while in the absence of aluminum hydroxide (P50-Soln), the response was comparable to that of P1 and P10. When dosed in the presence of SipD, the response to 1 μg (PS1) is slightly higher at day 21 ($p<0.05$), but similar thereafter to P1. At 10 μg (PS10), the PrgI IgG endpoints mirrored that of the antigen in the absence of SipD. At the highest dose level (PS50), the response followed a similar trend to that of the P50 treated mice, although the level was not as great following the second boost injection. The bivalent 50 μg solution dose (PS50-Soln) had similar values to that of the monovalent solution dose (P50-Soln) with

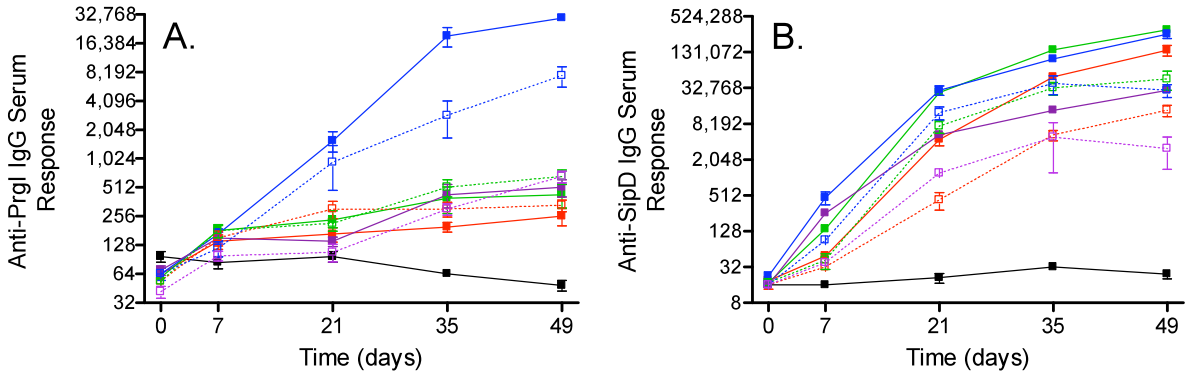

Figure 4.3 Anti PrgI (A) and SipD (B) IgG serum responses following intramuscular injections on study days 1, 14, 28 of Control (■), P1/S1 (■), P10/S10 (■), P50/S50 (■), P50-Soln/S50-Soln (■), PS1 (□), PS10 (□), PS50 (□) and PS50-Soln (□).

the exception of day 7 where P50-Soln mice were slightly higher than PS50-Soln ($p<0.05$).

The endpoint titers in the SipD groups of Study 3 were roughly 16 prior to injections (Figure 4.3B). Mice given 1 μg doses of SipD (S1) demonstrated a slightly elevated endpoint after the first injection, but experienced a boost of more than 5 dilutions following the second dose. Mice in the 10 μg dose (S10) group followed a similar trend with increased endpoint titers at each time-point. The 50 μg (S50) dose did not elicit a significant difference in antibody response compared to that of S10 treated mice with the exception of day 7 where S50 was greater ($p<0.01$). When no aluminum hydroxide was present (S50-Soln), the response to the initial injection was comparable to that observed for S10 and S50. Following the booster doses, however, the increase in antibody levels was not as great. The 1 μg bivalent formulation (PS1) followed the trend observed for the monovalent (S1) formulation, but with lower antibody values. The 10 and 50 μg combination doses (PS10 and PS50) also behaved similarly to their monovalent analogues, S10 and S50, but with lower titers at all time-points. When the bivalent formulation was injected in the absence of aluminum hydroxide (PS50-Soln), the observed response was lower than that of the S50-Soln group throughout the study.

4.4 Discussion

In the present study we have demonstrated the immunogenicity of TTSS needle and tip proteins both in monovalent and bivalent formulations. Additionally, no adverse effects were observed throughout the dosing regimen as indicated by normal weight gain

patterns (data not shown). In all studies where increases in specific antibody titers were observed, there were no non-responders suggesting that the formulations may be efficacious if IgG levels are predictive of protection.

MxiH monomer has shown to be weakly immunogenic and dose dependent, requiring fairly high doses of antigen, multiple boosts and the presence of an adjuvant to elicit a strong response. When administered in the presence of IpaD, however, the Anti-MxiH specific IgG was significantly boosted. This enhanced response does not appear to be the result of physical interaction between the two proteins when combined in solution (data not shown.) It is possible however that the presence of aluminum hydroxide provides a platform for interaction between the two. It is also possible that IpaD has inherent adjuvant-like properties as evidenced by its sizeable immunogenicity when dosed alone in the absence of an adjuvant.

The polymerized form of the needle protein, expressed without the C-terminal truncation, is drastically more immunogenic than the monomeric version. There exists a well established correlation between antigen size and immune response [15]. Thus, it is possible that the increase observed here is a result of the increased size of the polymeric version of the needle monomer. Another possibility is the existence of repeating epitopes in the polymeric unit which has also been shown to greatly increase immunogenicity. Finally, it is also possible that the 5 residue C-terminal region which is absent in the monomeric form constitutes a potent epitope. Similar to the monomeric version, the response of the polymerized form is further boosted by adsorption to an adjuvant.

The tip protein from the *Shigella* system is shown here to be highly immunogenic in agreement with previous work [20]. In contrast to the needle monomer MxiH, IpaD does not show significant dose-dependent behavior when administered in a multi-dose regimen; however there does appear to be an indication of dose-dependency following the first inoculation. As stated above, it is possible that due to its potent immunogenicity, IpaD may act as an adjuvant in multivalent formulations. While IpaD is strongly immunogenic alone, it does benefit from adsorption to aluminum hydroxide.

Antigens from the *Salmonella* system also appear to elicit substantial immune responses. Similar to the results observed for the *Shigella* system, the monomeric needle protein PrgI is less immunogenic than the tip protein SipD. PrgI displays dose dependent behavior, and titers increase markedly when booster doses are administered. As one would expect, IgG responses to PrgI are enhanced when the antigen is adsorbed to aluminum hydroxide. Contrary to the immune response to MxiH seen in the presence of the analogous tip protein, however; PrgI does not produce higher antibody levels in the presence of SipD.

Mice injected with SipD had high antibody titers following the first dose and were relatively dose independent after the first booster injection. This trend is similar to that observed for IpaD, but in all cases, responses to SipD were lower in magnitude. Additionally, where IpaD was boosted slightly by the presence of MxiH, SipD titers appear to be reduced when administered in the presence of PrgI. Despite differences in primary sequence, this observation is strikingly similar to the documented immuno-suppressing activity associated with LcrV, the tip protein of *Yersinia pestis* [24].

While the studies presented here support further vaccine development utilizing TTSS needle and tip proteins, further work is clearly necessary. Additional studies will focus on tailoring the formulation to elicit an appropriate response based on the pathogenesis of each species to ensure protection. *Salmonella* spp. bacterial infections often result in systemic invasion, which are responsible for some of the most severe symptoms [3]. Preventing a systemic infection may be possible using versions of the formulation studied here which was dosed intramuscularly. While no data is currently available to definitively associate the presence of PrgI/SipD specific IgG with protection, needle proteins have been shown to enhance well-established opsinization phenomenon and *in-vitro* studies suggest that tip protein antibodies prevent host-cell invasion [12].

In contrast, *Shigella* infections generally involve the epithelial cells of the intestines and do not commonly result in septicemia. This suggests that a vaccine will need to protect the mucosal surfaces to be effective. It is not yet certain whether the current formulation will meet this requirement. To explore this question, it will be necessary to conduct additional immunogenicity experiments focusing on IgA levels. Other tests which may be necessary include evaluation of cellular responses and associated adjuvants and the effect of the route of administration. In this study, an aluminum salt adjuvant was chosen because it is currently the only FDA approved vaccine adjuvant. Novel adjuvants are now becoming available, however, and they will need to be examined in this system [32-35].

As previously stated, the main purpose of the work presented here is to establish the antigenic potential of TTSS needle and tip proteins. We have shown here that

administration of these proteins results in robust humoral immune responses. Based on previous work, this may be sufficient for protection. While some bivalent formulations did not have a synergistic effect, we propose that the multivalent approach may be advantageous for several reasons including increased likelihood of protection across populations and potential cross-protection among similar species. In summary, work shown here supports the development of TTSS proteins as antigens in multivalent subunit vaccines.

4.5 Bibliography

[1] World Health Organization Drug-Resistant *Salmonella.* 2005 [cited 2009 February 19]; Available from: http://www.who.int/mediacentre/factsheets/fs139/en/print.html

[2] *Shigella*. 2009 [cited 2009 February 19]; Available from: http://www.who.int/vaccine_research/diseases/shigella/en/

[3] S.M. G. Salmonellosis in children in developing and developed countries and populations. Curr Opin Infect Dis 2002 October;15(5):507-12.

[4] *Salmonella Saintpaul* Outbreak. 2008 [cited 2009 February 19]; Available from: http://www.fda.gov/oc/opacom/hottopics/tomatoes.html

[5] Peanut Product Recalls: *Salmonella Typhimurium*. 2008 [cited 2009 February 19]; Available from: http://www.fda.gov/oc/opacom/hottopics/Salmonellatyph.html

[6] Brooks JT, Shapiro RL, Kumar L, Wells JG, Phillips-Howard PA, Shi Y-P, et al. Epidemiology of Sporadic Bloody Diarrhea in Rural Western Kenya. Am J Trop Med Hyg 2003 June 1, 2003;68(6):671-7.

[7] Fulla N, Prado V, Duran C, Lagos R, Levine M. Surveillance for Antimicrobial Resistance Profiles Among *Shigella* Species Isolated from a Semirural

Community in the Northern Administrative Area of Santiago, Chile. Am J Trop Med Hyg 2005;72(6):851-4.

[8] Kariaki S, Gilks C, Corkill J, Kimari J, Benea A, Waiyaki P, et al. Multi-drug resistant non-typhi salmonellae in Kenya. J Antimicrob Chemother 1996 September 1, 1996;38(3):425-34.

[9] Glynn MK, Bopp C, Dewitt W, Dabney P, Mokhtar M, Angulo FJ. Emergence of Multidrug-Resistant Salmonella enterica SerotypeTyphimurium DT104 Infections in the United States. N Engl J Med 1998 May 7, 1998;338(19):1333-9.

[10] Deane JE, Roversi P, Cordes FS, Johnson S, Kenjale R, Daniell S, et al. Molecular model of a type III secretion system needle: Implications for host-cell sensing. Proc Natl Acad Sci USA 2006 August 15, 2006;103(33):12529-33.

[11] Kubori T, Matsushima Y, Nakamura D, Uralil J, Lara-Tejero M, Sukhan A, et al. Supramolecular Structure of the *Salmonella typhimurium* Type III Protein Secretion System. Science 1998 April 24, 1998;280(5363):602-5.

[12] Espina M, Olive AJ, Kenjale R, Moore DS, Ausar SF, Kaminski RW, *et al.* IpaD Localizes to the Tip of the Type III Secretion System Needle of *Shigella flexneri*. Infect Immun 2006 August 1, 2006;74(8):4391-400.

[13] Espina M, Ausar SF, Middaugh CR, Picking WD, Picking WL. Spectroscopic and Calorimetric Analyses of Invasion Plasmid Antigen D (IpaD) from *Shigella flexneri* Reveal the Presence of Two Structural Domains. Biochemistry 2006;45(30):9219-27.

[14] Johnson S, Roversi P, Espina M, Olive A, Deane JE, Birket S, *et al.* Self-chaperoning of the type III secretion system needle tip proteins IpaD and BipD. J Biol Chem 2006 October 31, 2006:M607945200.

[15] Dintzis RZ, Okajima M, Middleton MH, Greene G, Dintzis HM. The immunogenicity of soluble haptenated polymers is determined by molecular mass and hapten valence. J Immunol 1989 August 15, 1989;143(4):1239-44.

[16] Guzman CA, Borsutzky S, Griot-Wenk M, Metcalfe IC, Pearman J, Collioud A, et al. Vaccines against typhoid fever. Vaccine 2006;24(18):3804-11.

[17] Levine MM, Kotloff KL, Barry EM, Pasetti MF, Sztein MB. Clinical trials of *Shigella* vaccines: two steps forward and one step back on a long, hard road. Nat Rev Micro 2007;5(7):540-53.

[18] Boyle EC, Bishop JL, Grassl GA, Finlay BB. Salmonella: from Pathogenesis to Therapeutics. J Bacteriol 2007 March 1, 2007;189(5):1489-95.

[19] Plotkin SA, Orenstein WA. Typhoid Fever Vaccines. In: Levine MM, editor. Vaccines. 4 ed. Philadelphia: Elsevier, Inc., 2004: 1057-93.

[20] Turbyfill KR, Mertz JA, Mallett CP, Oaks EV. Identification of Epitope and Surface-Exposed Domains of *Shigella flexneri* Invasion Plasmid Antigen D (IpaD). Infect Immun 1998 May 1, 1998;66(5):1999-2006.

[21] Hill J, Leary SE, Griffin KF, Williamson ED, Titball RW. Regions of *Yersinia pestis* V antigen that contribute to protection against plague identified by passive and active immunization. Infect Immun 1997 November 1, 1997;65(11):4476-82.

[22] Williamson ED, Eley SM, Stagg AJ, Green M, Russell P, Titball RW. A single dose sub-unit vaccine protects against pneumonic plague. Vaccine 2000;19(4-5):566-71.

[23] Williamson ED, Vesey PM, Gillhespy KJ, Eley SM, Green M, Titball RW. An IgG1 titre to the F1 and V antigens correlates with protection against plague in the mouse model. Clin Exp Immunol 1999;116(1):107 - 14.

[24] Brubaker RR. Interleukin-10 and Inhibition of Innate Immunity to *Yersiniae*: Roles of Yops and LcrV (V Antigen). Infect Immun 2003 July 1, 2003;71(7):3673-81.

[25] Kingston R, Burke F, Robinson JH, Bedford PA, Jones SM, Knight SC, et al. The fraction 1 and V protein antigens of *Yersinia pestis* activate dendritic cells to induce primary T cell responses. Clinical and Experimental Immunology 2007;149(3):561-9.

[26] Matson J, Durick K, Bradley D, Nilles M. Immunization of mice with YscF provides protection from *Yersinia pestis* infections. BMC Microbiology 2005;5(1):38.

[27] Swietnicki W, Powell BS, Goodin J. *Yersinia pestis* Yop secretion protein F: Purification, characterization, and protective efficacy against bubonic plague. Protein Expression and Purification 2005;42(1):166-72.

[28] Darboe N, Kenjale R, Picking WL, Picking WD, Middaugh CR. Physical characterization of MxiH and PrgI, the needle component of the type III secretion apparatus from *Shigella* and *Salmonella*. Protein Sci 2005 2005;15(3):543-52.

[29] Espina M, Ausar SF, Middaugh CR, Baxter MA, Picking WD, Picking WL. Conformational stability and differential structural analysis of LcrV, PcrV, BipD, and SipD from type III secretion systems. Protein Sci 2007;16(4):704-14.

[30] Kenjale R, Wilson J, Zenk SF, Saurya S, Picking WL, Picking WD, et al. The Needle Component of the Type III Secreton of *Shigella* Regulates the Activity of the Secretion Apparatus. J Biol Chem 2005 December 30, 2005;280(52):42929-37.

[31] Marquart ME, Picking WL, Picking WD. Structural Analysis of Invasion Plasmid Antigen D (Ipad) from *Shigella flexneri*. Biochemical and Biophysical Research Communications 1995;214(3):963-70.

[32] Aguilar JC, Rodríguez EG. Vaccine adjuvants revisited. Vaccine 2007;25(19):3752-62.

[33] Ott G, Radhakrishnan R, Fang JH, Hora M. The adjuvant MF59: a ten year perspective Vaccine Adjuvants: Preparation Methods and Research Protocols. Totowa, N.J.: Humana Press, 2001: 211-28.

[34] Skene CD, Sutton P. Saponin-adjuvanted particulate vaccines for clinical use. Methods 2006;40(1):53-9.

[35] Wikman M, Friedman M, Pinitkiatisakul S, Andersson C, Lovgren-Bengtsson K, Lunden A, et al. Achieving directed immunostimulating complexes incorporation. Expert Review of Vaccines 2006;5(3):395-403.

Chapter 5

Physical Measurements as Stability Indicating Assays in Protein Formulations: RiVax® Stability and Immunogenicity

5.1 Introduction

Ricin toxin is widely recognized as a potential bioterrorism agent due to its ease of acquisition and distribution as well as its stability and potent toxicity. Perhaps the most disturbing aspect of a possible ricin attack is human vulnerability given the non-existence of both preventative and therapeutic treatment. Several ricin vaccine candidates have been identified and investigated, however, all have been hindered by concerns of antigen toxicity and none have reached the commercial market [1-5].

Ricin, an exotoxin found in the seeds of the castor bean plant (*Ricinus communis*), is a 64 kDa heterodimer composed of a ribotoxic A (RTA) and a lectin binding B chain linked by a single disulfide bond [6]. The protein dimer belongs to the family of ribosome inactivating proteins (RIPs) and is synthesized as a single polypeptide chain which is enzymatically cleaved inside the seed to produce the toxic dimer form. During exposure, the B chain binds galactose residues of the cell surface glycolipids and glycoproteins, facilitating endocytosis of the holotoxin. Once inside the cell, the disulfide bond maintaining the dimer is reduced and the enzymatic A chain escapes the Golgi to the cytosol. There it disrupts cellular protein synthesis by depurinating a specific adenine of the 28s ribosomal RNA subunit [7-11]. Due to its catalytic activity, a single molecule of ricin can significantly inhibit cellular protein synthesis and ultimately induce cell death. A lethal human dose is in the range of 1-10 μg/kg for aerosol delivery and slightly higher for oral delivery. Within 4 hours of lethal exposure, the condition is irreversible and death ensues within 4-5 days [8, 9, 12].

The A chain (RTA) is an attractive vaccine candidate given its ability to induce a protective immune response against ricin challenge and its intimate involvement during infection [1, 12, 13]. It is however, associated with dose limiting toxicity due to its ribotoxic activity and ability to induce Vascular Leak Syndrome (VLS) in humans [14]. The toxic nature of RTA can be eliminated by mutating two specific residues (V76M and Y80A), one in each of the enzymatic sites [13, 15, 16]. The resulting recombinant mutant, RiVax®, has no associated toxic activity as evaluated by toxicology studies in rabbits, retains all immunodominant epitopes, and maintains the protein's native structure as well as its ability to induce protection against a ricin challenge [13, 16-18].

As expected for a recombinant protein antigen, it has been shown that the presence of an adjuvant greatly increases the immunogenicity of rRTA over soluble material [1]. Additionally, previous work has shown that RiVax® efficiently adsorbs to aluminum hydroxide. Here we present optimization of an aluminum hydroxide adsorbed RiVax® product [19]. It is widely accepted that the stability profiles of biological molecules are complex and often understood only to a limited degree. In the specific case of aluminum adsorbed vaccine formulations, the comprehensive characterization of adjuvant-antigen interactions is essential for understanding product stability, yet can be difficult to achieve given the opaque nature of the suspensions. In solution, a wide range of physicochemical assays can be used to determine product stability, consistency, and potency. In the presence of an aluminum salt such as aluminum hydroxide, however, many of the more commonly used methods are not applicable and only a limited number of specialized techniques are available to directly probe the stability of such vaccines.

Examples of such stability relevant techniques include, but are not necessarily limited to immune correlates (ICs), Enzyme-Linked Immunosorbent Assay (ELISA), Front-face Fluorescence emission (ff-Fluorescence), Fourier Transform Infrared Spectroscopy (FTIR) and Differential Scanning Calorimetry (DSC). Here we employ ff-Fluorescence as a stability indicating assay for aluminum hydroxide adsorbed RiVax® and present associated stability studies.

5.2 Materials and Methods

5.2.1 Materials

Isotonic histidine buffer (10 mM) was prepared using L-histidine monohydrochloride monohydrate (Sigma) and Sodium Chloride (144 mM) (Sigma) and adjusted to pH 6.0 with 6 N Sodium Hydroxide. Aluminum hydroxide (2%) was obtained from E.M. Sergeant Pulp and Co., Inc. (Clifton, NJ), and RiVax® was received from Cambrex BioScience (Baltimore, MD) in a highly purified form (>95% pure) [19]. All other chemicals used were of scientific grade.

5.2.2 Preparation of solution RiVax®

RiVax® was extensively dialyzed at 4 ^{o}C into isotonic Histidine buffer at pH 6.0 using SpectraPor Dialysis Membrane (Spectrum Labs, MWCO 10 kDa). It was then concentrated using an Amicon Ultra Centrifugal Filter Device (Millipore, MWCO 30 kDa) and protein concentration was determined using UV absorbance spectroscopy with

an Agilent 8453 UV-Visible diode array spectrophotometer (Palo Alto, CA). Protein concentration was determined using the absorbance value at 280 nm and an extinction coefficient of 0.77 $(cm*mg/mL)^{-1}$.

5.2.3 Preparation of adsorbed RiVax®

The concentrated RiVax® solution prepared above was combined with stock aluminum hydroxide (10.1 mg/mL) in volumes calculated to deliver 0.2 mg/mL RiVax® in 0.85 mg/mL aluminum. The solution was stirred gently on a stir plate at 4 ºC for > 1 hour, and subsequently aliquoted into microcentrifuge tubes (1 mL). A corresponding blank solution was prepared in the same manner and aliquoted in the same manner.

5.2.4 Stability Studies

Samples and blanks prepared as described above were placed in incubators set at 40, 25, or 4 ^{o}C (Isotemp Fisher Scientific, Kendo Laboratory Products, Asheville, EchoTherm Chilling Incubator, Torey Pines Scientific, San Marcos, Laboratory Cold Room, Environmental Inc., Fenton respectively). Samples were pulled from incubation at designated time intervals and transferred to front-face fluorescence cuvettes for analysis. Cuvettes were capped and placed back in the respective incubator overnight (>12 hours) in order that the adsorbed protein settled to the bottom to minimize variability due to settling of the adjuvant during the course of fluorescence measurements. The following day, without disturbing the settled sample, the cuvette was placed in a PTI QuantaMaster™ spectrofluorometer with a Peltier-controlled cell holder

(Photon Technology International, Lawrenceville, NJ). An excitation wavelength of 295 nm (>95% Trp emission) was used, and intrinsic tryptophan fluorescence emission spectra were collected from 300-400 nm while maintaining the temperature of the cell at the respective incubation temperatures. The front-face cuvettes have a triangular geometry which allows the collection of emission spectra despite the opaque nature of the samples. The cuvettes are positioned such that the excitation beam falls fully on the settled slurry. The excitation slit widths were adjusted to 4 nm, and the emission slit widths to 2 nm for all measurements. Spectra were obtained in duplicate and averaged, although only one sample was pulled per time-point due to sample quantity limitations. As shown in Figure 5.1, a spectrum was also collected for the blank material and was subtracted from the sample spectrum to eliminate the scattering contributed by the presence of the aluminum hydroxide. The subtracted data was exported into Microcal Origin 6.0 TM where they were processed by obtaining the wavelength at which the first derivative spectrum crossed the x-axis. This emission maximum peak position was plotted for each sample as a function of incubation time. In addition to the intrinsic Trp fluorescence, each sample was also assayed for free protein. This was done by centrifuging the sample for 30 sec at 14,000 g, removing the supernatant and obtaining an absorbance spectrum of the supernatant to quantify the antigen remaining unbound in solution. Blanks were once again used as a reference for the absorbance measurements.

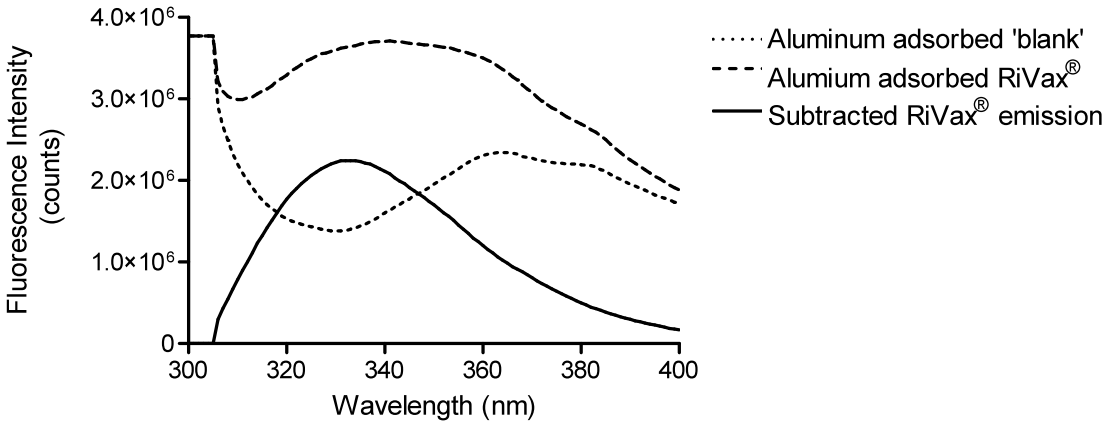

Figure 5.1 Fluorescence emission spectra (obtained using front face cuvettes) of an adsorbed 'blank' sample, an adsorbed RiVax® sample and the resulting subtracted peak representing fluorescence emission of the sole Trp residue.

5.2.5 Elution

Solutions were prepared in isotonic histidine buffer and were not pH adjusted. Adsorbed samples were centrifuged at 3,000 g for 30 sec and the resulting supernatant was removed and assayed for protein content by absorbance spectroscopy. In all cases, the supernatant was found to contain <10% (0.02 mg/mL) of the adsorbed protein. For each of the elution solutions prepared, 1 mL was added to a vial containing the centrifuged aluminum hydroxide-RiVax® complex. The resulting suspension was rotated end-over-end at 4 ^{o}C for 48 hours. Samples were then centrifuged at 14,000 g for 30 sec, and the supernatant was assayed for protein content by UV absorbance spectroscopy.

5.2.6 Adsorption Isotherms

Adsorbed samples were prepared by adding concentrated RiVax® in isotonic 10 mM Histidine buffer at pH 6.0 and aluminum hydroxide (stock 10.1 mg/mL) to deliver a known protein concentration to a known aluminum concentration (0.5-1.25 mg/mL). The samples were tumbled end-over-end at 4 ^{o}C for 1 hour, centrifuged at 14,000 g for 30 sec and an absorbance spectrum of the supernatant was obtained. The amount of protein bound was determined by subtracting the concentration in the supernatant from the concentration initially added. A blank sample containing only buffer and 0.85 mg/mL aluminum was also prepared and used as a reference. In some experiments, adsorption isotherms were generated in the presence of an added excipient or buffer component. In these instances, the order of addition was RiVax®, buffer (if required), excipient,

aluminum hydroxide. In all cases the solutions were stirred prior to the addition of the aluminum hydroxide.

5.2.7 Animal Studies

Animal studies conducted at SRI International (SRI) were performed in accordance with the National Research Council (NRC) *Guide for the Care and Use of Laboratory Animals* (1996) and the Animal Welfare Standards incorporated in 9 CFR Part 3, 1991. Swiss Webster mice (20-30 grams) were acquired from Charles River Laboratories and quarantined for 3 days. Subcutaneous inoculations were completed on days 0 and 21 and mice were bled via retro orbital sinus while under isoflurane anesthesia before study initiation and at day 21 and 28.

Animal studies were also performed at The University of Texas Southwestern Medical Center (UTSW) and were conducted in accordance with regulations set forth by the Institutional Animal Care and Use Committee (IACUC) and guidelines of the Association for Assessment and Accreditation of Laboratory Animal Care. Swiss Webster mice (weight) were intramuscularly inoculated on study days 0, 28 and 56 and bled retroorbitally on study days 0 and 70. Mice in the challenge study were administered a 10x LD50 intra-peritoneal dose (100ng/kg) 14 days following the last vaccination, and subsequently weighed and monitored for indications of morbidity for 14 days. Mice were sacrificed when moribund or < 75% of the pre-challenge weight.

5.2.8 Sera Analysis

Sera samples collected at SRI were analyzed according to the following ELISA method. Polystyrene 384 well plates (Greiner Bio-One, Germany) were coated with a 10 ug/mL RiVax® in 10 mM phosphate buffer at pH 7.8 and stored for less than one week at 4 ^{o}C. Plates were washed and subsequently blocked using PBS buffer containing 1% Caesin and 1% BSA for 2 h at room temperature. Plates were then washed three times and treated with sample or standard in a dilution buffer consisting of 1% caesin, 1% BSA and 0.05% Tween 20 in PBS and again incubated for 2 hours at room temperature. Plates were once again washed three times before the addition of HRP-Goat Anti Mouse IgG (Invitrogen) prepared at 1:32,000 in the dilution buffer. After a 2 hour incubation period, 3, 3', 5, 5'-tetramethylbenzidine (Sigma) was added and allowed to react for 30 minutes before 2 N Sulfuric Acid was added and the plate was read using a Tecan GENios Plate Reader (Tecan Group Ltd., Switzerland).

Sera collected at UTSW were analyzed by RIA as previously described [151, 155]. A 20 µg/mL RiVax® solution in PBS was administered (100 µL) to 96 well plates (Costar, Corning, NY) and incubated overnight at 4 ^{o}C. The plates were then washed and subsequently blocked with 5% fetal calf serum. Standard dilutions and samples were then added and the plates were once again incubated overnight at 4 ^{o}C. The following day, the plates were washed and [^{125}I]-labeled rabbit anti-mouse Ig was added and incubated for 2 hours at room temperature. The plates were then washed and read using a Gamma Counter (Pharmacia).

5.3 Results

It has been shown previously that RiVax® strongly adsorbs appreciably to aluminum hydroxide while not interacting significantly with aluminum phosphate [55]. It has also been shown that the antigenicity of the recombinant protein is greatly increased in the presence of an adjuvant [1]. Thus, we identified conditions under which >95% of the protein was adsorbed to aluminum hydroxide, which for the target dose of 0.2 mg/mL required the use of 0.85 mg/mL aluminum in isotonic 10 mM Histidine buffer at pH 6.0. RiVax® contains only one Tryptophan (Trp) residue which is buried in the protein's interior. Therefore, its intrinsic fluorescence emission represents a sensitive probe of the protein's tertiary structure.

Upon excitation at 295 nm, the fluorescence emission maximum for the native protein in solution is approximately 330 nm. Upon adsorption, the emission maximum red shifts to approximately 333 nm suggesting that the Trp residue is in an environment of increased polarity presumably due to a slight conformational alteration of the protein on the surface (Figure 5.2). To evaluate the stability of adsorbed RiVax®, samples were formulated and stored under various conditions to evaluate both real time (4 ^{o}C) and accelerated degradation stability (25 and 40 ^{o}C). Samples were monitored using the front face fluorescence method as well as by assaying the sample supernatant for protein content using UV absorbance spectroscopy. In all cases in which the sample supernatant is not mentioned, no significant protein presence (< 0.03 AU) was observed. As shown in Figure 3, the peak position of maximum emission of the Trp residue red shifted

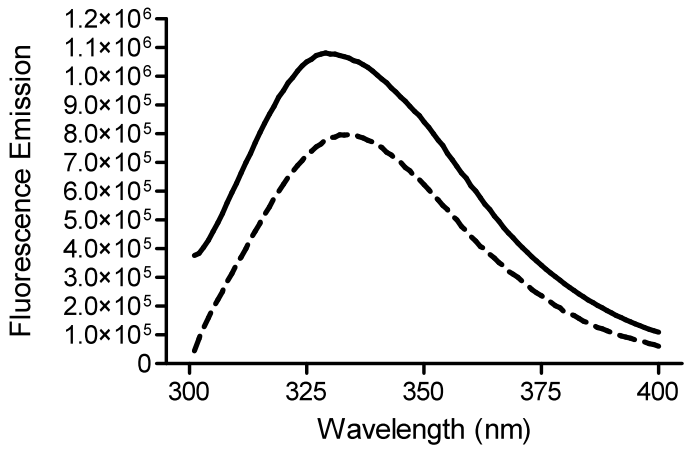

Figure 5.2 Fluorescence emission spectra for solution (—) and adsorbed (----) RiVax®. Both spectra were obtained using front face fluorescence and represent a protein concentration of 0.2 mg/mL. The adsorbed RiVax® spectrum was taken approximately 12 hours following adsorption. The emission maximum for solution RiVax® is 330.0 nm while that of adsorbed RiVax® is 333.6 nm.

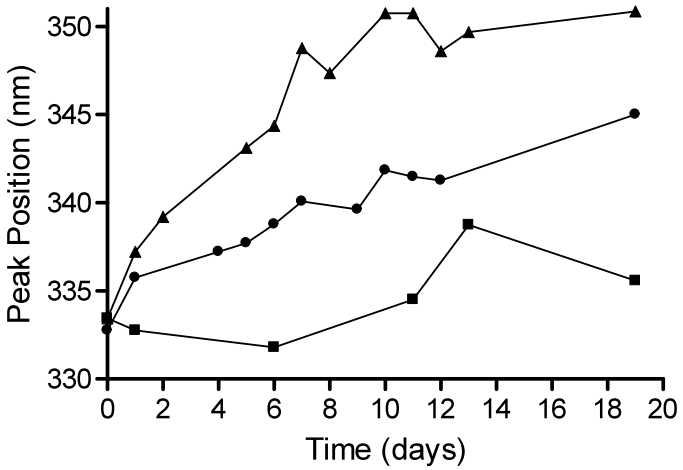

Figure 5.3 Fluorescence peak position of adsorbed Rivax® with respect to storage time at 4 (■), 25 (●) and 40 (▲) °C. Samples contained 0.2 mg/mL protein and 0.85 mg/mL aluminum in isotonic 10 mM Histidine buffer at pH 6.0. The uncertainty in wavelength position is estimated to be +/-0.5 nm.

significantly over the course of the 20 day study for formulations stored at all 3 temperatures. This indicates that the residue was exposed to an increasingly polar environment due to conformational perturbation. To further investigate this change, a longer term study was established under the same formulation and storage conditions.

The long term study revealed that the protein Trp emission continued to red shift over extended periods of time (Figure 5.4). This observation is not unexpected for protein-solid interfaces and probably depicts changes which occur as the protein optimizes its interaction with the surface through subtle step-wise structural changes [20]. The effect of the observed conformational changes on the immunogenicity of the product was unknown from these studies. Accordingly, animal studies were organized to further investigate this relationship.

Mice were challenged with a 10x LD50 intra-peritoneal dose (100ng/kg) of active ricin toxin 14 days following the final administration of 3 doses ranging from 0.1-1.0 ug RiVax® adsorbed to 0.85 mg/mL aluminum. The latter material was stored for 60 days at either 4 or 40 ^{o}C. As shown in Figure 5.5, the total IgG responses for the samples stored at 4 ^{o}C correlated well with dose and protection. The samples stored at 40 ^{o}C, however, did not induce the same level of antibody protection as the 4 ^{o}C samples. Furthermore, they did not confer protection upon challenge. By comparing the IgG responses and protection rates for the 0.1 ug (4 ^{o}C) and 1.0 ug (40 ^{o}C) samples, we see that despite similar IgG levels, the 4 ^{o}C samples protected the mice while the 40 ^{o}C samples did not. This observation suggests the loss of protective epitopes in samples

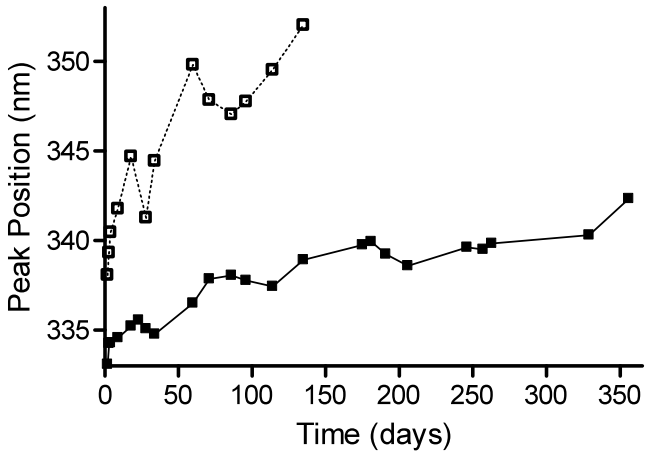

Figure 5.4 Fluorescence peak position with respect to storage time at 4 (■) or 40 (□) ^{o}C. Samples contained 0.2 mg/mL RiVax® and 0.85 mg/mL in isotonic 10 mM Histidine buffer at pH 6.0. The uncertainty in wavelength position is estimated to be +/-0.5 nm.

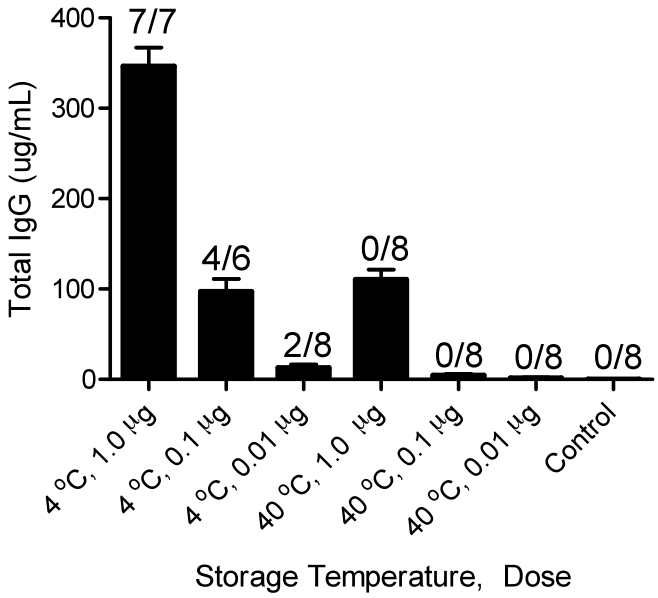

Figure 5.5 IgG and protection rates 28 days following 3/3 monthly injections with adsorbed RiVax® stored for 60 days at 4 or 40 °C.

stored at 40 ^{o}C. The differences observed in immune response in combination with the observed spectral changes suggest that the altered conformational structure of RiVax® as monitored by intrinsic fluorescence changes may be directly implicated in the loss of antigenicity.

It was unclear whether the spectral shifts induced at each temperature were distinct from one another or intermediates along a similar unfolding pathway. Thus, a second animal study was performed to investigate the antigenicity of formulations stored at 4 ^{o}C for differing lengths of time (7 or 120 days). Shown in Figure 5.6 is the response of the groups one week following the second of two injections. It appears visually that a difference is observed in the lower dose groups. Upon statistical analysis, however, it was found that the two data sets are not statistically different. Thus, we conclude that upon storage at 4 ^{o}C, the vaccine does not decrease in potency.

If the spectral shifts are either directly or indirectly related to the antigenicity of the product, this result would suggest that the conformational change occurring upon storage of the formulation at 4 ^{o}C is not severe enough to alter antigenicity, but has the potential to do so if, for example, a cold chain is broken. To better understand the significance of the changing RiVax® conformation, we attempted to desorb the protein and inspect it for any chemical modifications. We were most interested in the samples which had been stored for extended periods at elevated temperatures, and hoped to track the changes by sampling several points along the stability profile. Samples were treated with one of several elution solutions and rotated end-over-end for 48 hours at 4 ^{o}C. Higher temperatures were not used for fear that additional chemical changes might occur

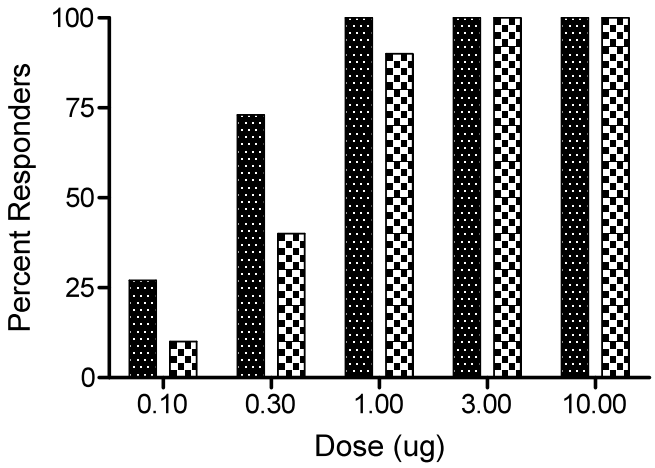

Figure 5.6 Endpoint titer >1/4096 28 days post vaccination for RiVax® formulations stored at 4 °C for 7 (▓) or 120 (▒) days.

Desorption Solution	Fresh	4 ºC, 30 days	40 ºC, 30 days
None (Control)	1%	1%	1%
2.0 M NaCl	0%	0%	1%
3.0 M NaCl	2%	1%	0%
1.0 M NaPhos (Mono)	34%	12%	2%
2.0 M NaPhos (Mono)	5%	1%	1%
1.0 M NaPhos (Di)	41%	17%	2%
2.0 M NaPhos (Di)	27%	12%	0%
1.0 M NaCit	0%	0%	0%
70 mM SDS	0%	0%	0%
1.0 M Gdn HCl	1%	0%	0%

Table 5.1 Percent RiVax® desorbed following 48 hour exposure to each condition. Samples contained 0.2 mg/mL RiVax® and 0.85 mg/mL aluminum in 10 mM Histidine buffer at pH 6.0

and be indistinguishable from those which occurred while the protein was on the surface. As shown in Table 1 as well as in previous work, [19], high concentrations of Sodium Chloride do not desorb RiVax® suggesting that the primary interactions responsible for adsorption are not electrostatic in nature. The use of SDS and Sodium Citrate was also unsuccessful at releasing the protein, an observation which is relatively common for aluminum hydroxide adjuvants [21]. Sodium Phosphate, which can compete with the protein for sites on the adjuvant, was the only eluent capable of releasing a portion of the adsorbed material. It is interesting to note that if samples are treated approximately 24 hours post-adsorption, approximately 40% can be desorbed by 1.0 M Sodium Phosphate. If, however, the samples are aged, and/or the incubation temperature is increased, the amount decreases significantly. This observation is supported by the observed spectroscopic shifts as the product ages and confirms that RiVax® optimizes its contacts with the aluminum salt by slightly altering its conformation over time. It may be that the exposed hydrophobic loop of RiVax® [1] is responsible for the bulk of the interaction with the adjuvant. When the protein was treated with an organic solvent to investigate the proposed hydrophobic interactions however gross aggregation was observed [22].

Given the loss in antigenicity associated with the conformational change, we attempted to prevent the shift from occurring. To that end, we considered the use of various GRAS excipients and examined each for their ability to stabilize RiVax® structure on the surface of the adjuvant based on their capacity to inhibit a red shift in fluorescence emission upon storage at 40 ^{o}C. As shown in Table 5.2, the presence of 30% glycerol induces a greater degree of unfolding than the protein experiences in the

Excipient	Red Shift (nm)
NONE	2.7
30% Glycerol	8.2
1.0 mg/mL Phystic Acid	0.7
0.3 M L-Arginine	1.8
0.01% Brij 35	1.9
Recombinant Human Gelatin	1.7
Trimethylamine Oxide	-0.3

Table 5.2 Fluorescence peak position for adsorbed RiVax® samples stored at 40 ^{o}C for 2 days in the presence of various excipients.

absence of an excipient. This is a surprising observation considering previous work on solution stability which predicted glycerol increased the stability of the protein [23]. With the exception of glycerol, the remaining excipients which previously were shown to increase solution stability appeared to have somewhat small effects over the first two days of incubation. Thus, longer duration studies were performed, but each excipient was found to have unfavorable effects on long term stability (data not shown).

It has been established that due to its positive charge, aluminum hydroxide attracts anions from solution resulting in the formation of a double layer at its surface [24]. As a result, the surface microenvironment is characterized by an elevated pH relative to the bulk solution. Thus, adsorbed proteins are susceptible to the potential physical and chemical changes (e.g. deamidation) induced by an increase in pH. The magnitude of this pH change has been estimated to be approximately 2 units. Therefore, RiVax® which is formulated in isotonic Histidine buffer at pH 6, may actually experience pH 8 conditions upon adsorption [24]. Previous work on the solution stability of RiVax® has shown that relative to pH 6, the protein is less thermally stable at pH 8 [19]. Perhaps more importantly, however, is the increased incidence of chemical degradation in the form of deamidation reactions at pH 8. The surface microenvironment can, however, be adjusted by treating aluminum hydroxide with phosphate anion [24]. As a result of its higher valency, phosphate has a higher affinity for interaction with aluminum than does a hydroxyl ion. Thus, if phosphate anion is added to aluminum hydroxide, it will displace hydroxyl anions and alter double layer formation. This creates an aluminum hydroxide-phosphate hybrid adjuvant with a reduced surface pH.

It is possible that the continuous time and temperature induced fluorescence red shift observed for adsorbed RiVax® is a result of the increased pH on the surface which produces physical and/or chemical changes. Thus, we examined the effect of phosphate anion on the stability of RiVax® when adsorbed to aluminum hydroxide. Order of addition studies were conducted to elucidate any differences induced by pre-treatment of the aluminum hydroxide versus addition of phosphate to the bulk buffer, and none were observed. As shown in figure 5.7, the presence of 5 mM phosphate anion dramatically altered the stability profile of the formulation resulting in a consistent peak position of approximately 334 nm when stored at 4 ^{o}C and 337 nm when stored at 40 ^{o}C for approximately 4 months.

Although the presence of phosphate seems to prevent the gradual unfolding of RiVax® on the surface of aluminum hydroxide, it has a significant drawback associated with its use. As mentioned above, the presence of phosphate anion on the aluminum hydroxide surface reduces its positive charge and modifies its surface chemistry. Therefore, depending on the nature of the interaction between the antigen and adjuvant, adsorption of the antigen may be affected. Unfortunately, adsorption of RiVax® is reduced to approximately 50% in the presence of 5 mM phosphate anion relative to 95-100% in its absence (data not shown). As previously mentioned, the increased antigenicity of adsorbed rRTA relative to solution rRTA has been repeatedly demonstrated, and illustrates the requirement that a successful vaccine be >95% adsorbed. Additionally, stability studies of the solution based material indicate that the product is not sufficiently stable when stored in solution for extended periods [19] (data

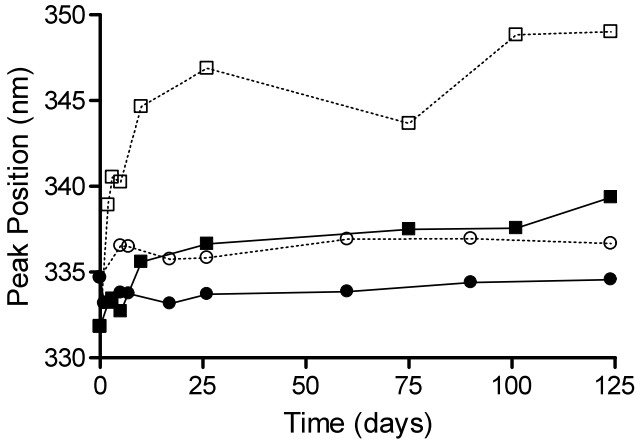

Figure 5.7 Fluorescence peak position with respect to storage time for 0.2 mg/mL RiVax® samples formulated on 0.85 mg/mL aluminum in isotonic 10 mM Histidine buffer at pH 6 in the absence of an excipient at 4 (■) vs. 40 (□) ^{o}C and in the presence of 5 mM phosphate anion at 4 (●) vs. 40 (○) ^{o}C. The uncertainty in wavelength position is estimated to be +/-0.5 nm.

not shown), suggesting that the adjuvant may not only be essential its immunogenicity, but also necessary for the long term stability of the vaccine.

In an attempt to increase the adsorption of RiVax® to aluminum hydroxide in the presence of phosphate anion, the salt concentration of the buffer was modulated. As expected, adsorption of RiVax® decreased in the presence of increasing salt concentration due to charge shielding (Figure 5.8). By decreasing the salt concentration from 150 mM NaCl to 50 mM NaCl, adsorption was increased significantly, but >95% adsorption was not achieved. Additionally, if the final formulation contained a reduced salt concentration, an additional excipient would be required to supplement isotonicity.

Therefore, we considered the possibility that a lower concentration of phosphate might provide the same degree of stabilization while perturbing rRTA adsorption to a lesser degree. To evaluate this, we formulated samples containing 0.2 mg/mL RiVax® adsorbed to 0.85 mg/mL aluminum in the presence of increasing phosphate anion concentration. As shown in Figure 5.9, adsorption decreases from 95% to approximately 50% as the phosphate concentration increases from 0 to 2 mM, but appears to saturate at concentrations above 2 mM. Prior to evaluating the stabilizing potential of the varying phosphate anion concentrations, a second experiment was conducted. Although most vaccines contain 0.5 - 0.85 mg/dose aluminum, it is acceptable to employ up to 1.25 mg [25]. Thus, we evaluated the adsorption of RiVax® to increasing aluminum concentrations in both the presence and absence of 0.5 and 2.0 mM phosphate anion. As shown in Figure 5.10, RiVax® is >95% adsorbed in the absence of phosphate anion in the range of 0.5-1.25 mg/mL aluminum. In the presence of 0.5 mM phosphate anion, the

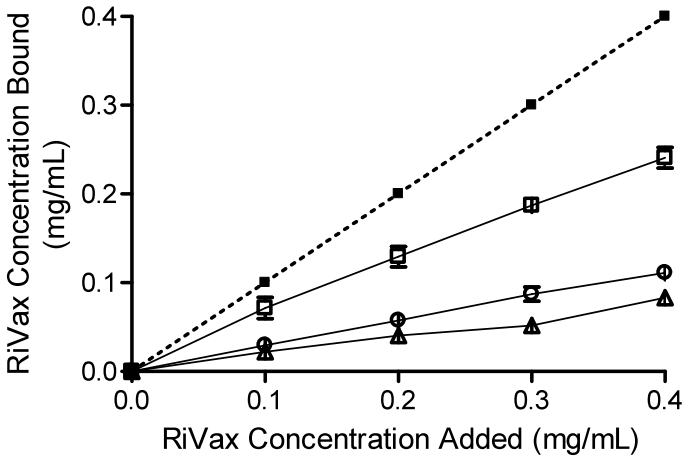

Figure 5.8 Adsorption isotherm of RiVax® to 0.85 mg/mL aluminum in the presence of 5 mM phosphate anion and 50 mM NaCl (□), 150 mM NaCl (○) or 500 mM NaCl (Δ) where 100% adsorption is designated with the dotted line (---).

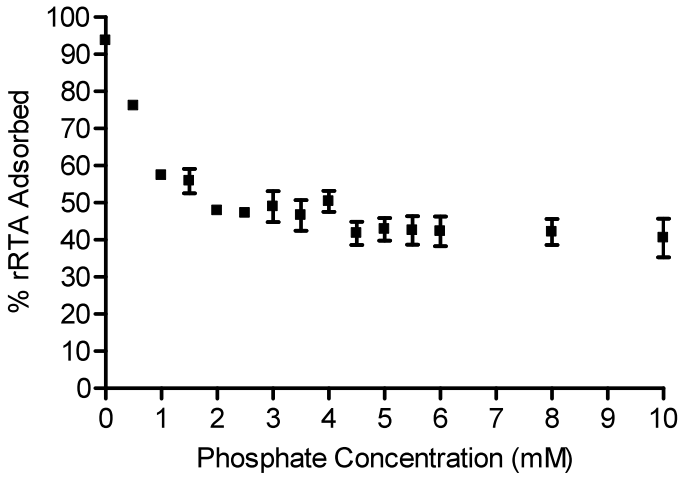

Figure 5.9 Effect of phosphate concentration of RiVax® adsorption. Samples contained 0.2 mg/mL RiVax® and 0.85 mg/mL aluminum and the designated phosphate anion concentration.

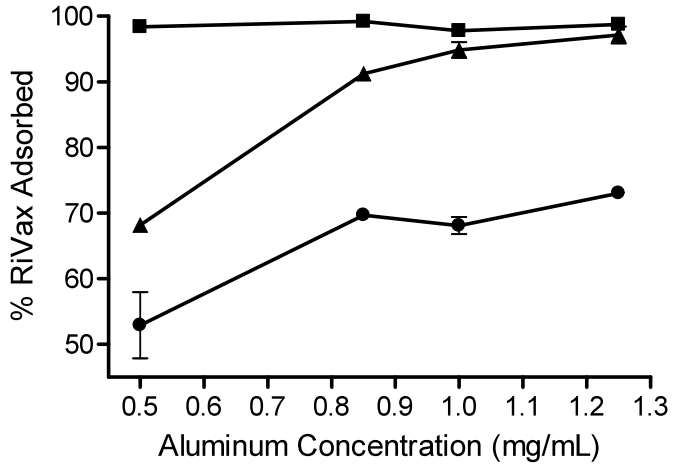

Figure 5.10 Adsorption of 0.2 mg/mL RiVax® in the presence of 0 (■), 0.5 (▲), or 2.0 (●) mM phosphate anion to increasing concentrations of aluminum.

adsorption is less than 70% to 0.5 mg/mL aluminum, but at 1.25 mg/mL aluminum adsorption increases to approximately 95%. In the presence of 2.0 mM phosphate anion, RiVax® is reduced to approximately 70% adsorbed at the highest aluminum concentration. Thus, we chose to pursue an increased aluminum concentration of 1.25 mg/mL. A stability study was initiated to evaluate the ability of these phosphate concentrations to prevent the gradual unfolding observed in its absence.

Results from this stability study indicate a relationship between phosphate concentration and preservation of protein structure upon storage on the adjuvant surface. As shown in Figure 5.11, protein in each of the phosphate containing formulations manifests a difference in the level of structural change observed relative to protein in its absence. It appears that 0.5 mM phosphate anion prevents only a limited degree of change, but that 2.0 mM protects the protein at a similar level to that of 5.0 mM phosphate in the previous study. At all time-points, however, approximately 25-30% of the protein was detected in the supernatant of samples containing 2.0 mM phosphate anion.

5.4 Discussion

In addition to the stability of adsorbed RiVax®, the use of phosphate anion may also enhance its immunogenicity. Recently, several groups have investigated the effect of the strength of interaction between antigens and adjuvant on immunogenicity and have established an inverse relationship between the two [26, 27. This suggests that our initial formulation, which contained no additional excipient, and persisted in adsorption upon

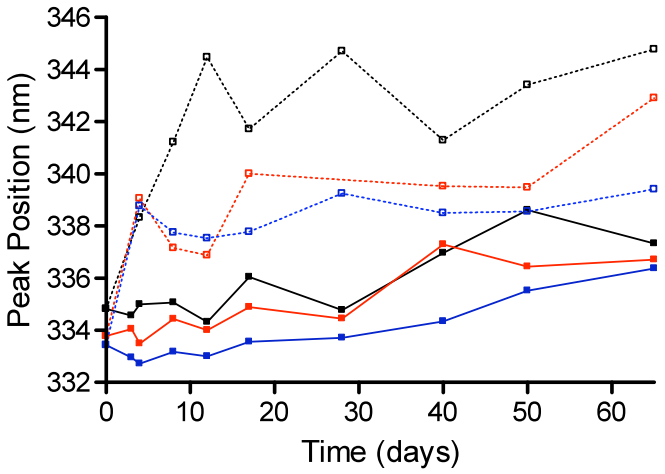

Figure 5.11 Fluorescence peak position with respect to storage time for 0.2 mg/mL RiVax® samples formulated on 1.25 mg/mL aluminum in isotonic 10 mM Histidine buffer at pH 6 in the absence of an excipient at 4 (■) vs. 40 (□) °C, in the presence of 0.5 mM phosphate anion at 4 (■) vs. 40 (□) °C and 2 mM phosphate anion at 4 (■) vs. 40 (□) °C. The uncertainty in wavelength position is estimated to be +/-0.5 nm.

elution treatment (after 30 days of storage), would offer a decreased response relative to a phosphate containing formulation.

The use of ricin toxin as a biological weapon is a valid threat considering the absence of both protective and therapeutic countermeasures. Previous work has described the production, solution characterization and stabilization of RiVax®, a double mutant recombinant A-chain antigen which provides protection against both aerosol and oral challenge without inducing toxicity [13, 17-19]. Here we have investigated the stability of the adsorbed protein and found that in the absence of phosphate anion, the protein conformation slowly changes over time to enhance its interaction with the adjuvant. As the storage temperature is increased, the structural differences are greater and a loss of immunological protection is observed. GRAS excipients were screened for stabilizing activity, but only phosphate anion was found to significantly inhibit the structural changes. Reduced adsorption of the antigen associated with the presence of phosphate anion was overcome by reducing the phosphate concentration and increasing the amount of aluminum hydroxide present. Thus, we have identified formulation conditions under which RiVax® is adsorbed to an aluminum salt adjuvant and remains structurally stable as indicated by the front face fluorescence assay. Future work involves testing the efficacy of the aged phosphate containing formulations in mice.

5.5 Bibliography

[1] Carra JH, Wannemacher RW, Tammariello RF, Lindsey CY, Dinterman RE, Schokman RD, et al. Improved formulation of a recombinant ricin A-chain vaccine increases its stability and effective antigenicity. Vaccine 2007;25(21):4149-58.

[2] Hewetson J. A Formalized Toxoid For Proection Of Mice From Inhaled Ricin. Vaccine Res 1995;4:179-87.

[3] Hewetson J, Assaad A, Teters D, Kotes J, Washington E, Tamaiello R. Immune response and protection of rats and mice from ricin aerosol exposure after vaccination with a deglycolsylated ricin A chain (Abstract). Fundam Appl Toxicol 1996;30:59.

[4] Olson MA, Carra JH, Roxas-Duncan V, Wannemacher RW, Smith LA, Millard CB. Finding a new vaccine in the ricin protein fold. Protein Engineering, Design and Selection 2004 April 1, 2004;17(4):391-7.

[5] McHugh CA, Tammariello RF, Millard CB, Carra JH. Improved stability of a protein vaccine through elimination of a partially unfolded state. Protein Sci 2004 October 1, 2004;13(10):2736-43.

[6] Montfort W, Villafranca JE, Monzingo AF, Ernst S, Katzin B, Rutenber E, et al. The three-dimensional strucutre of ricin at 2.8A. J Biol Chem 1987;262:5398-403.

[7] Doan LG. Ricin: Mechanism of Toxicity, Clinical Manifestations, and Vaccine Development. A Review. Journal of Toxicology -- Clinical Toxicology 2004 03;42(2):201-8.

[8] Franz DR, Jaax NK. Medical Aspects of Chemical and Biological Warfare, Chapter: 32 Ricin Toxin. Falls Church, VA: Office of the Surgeon General 1997:631-42.

[9] Lord MJ, Jolliffe NA, Marsden CJ, Pateman C, S.C., Smith DC, Spooner RA, et al. Ricin. Mechanisms of Cytotoxicity. Toxicol Rev 2003;22(1):53-64.

[10] Olsnes S, Kozlov JV. Ricin. Toxicon 2001;39(11):1723-8.

[11] Endo Y, Tsurugi K. The RNA N-glycosidase activity of ricin A-chain. The characteristics of the enzymatic activity of ricin A-chain with ribosomes and with rRNA. J Biol Chem 1988 June 25, 1988;263(18):8735-9.

[12] Maddaloni M, Cooke C, Wilkinson R, Stout AV, Eng L, Pincus SH. Immunological Characteristics Associated with the Protective Efficacy of Antibodies to Ricin. J Immunol 2004 May 15, 2004;172(10):6221-8.

[13] Smallshaw JE, Firan A, Fulmer JR, Ruback SL, Ghetie V, Vitetta ES. A novel recombinant vaccine which protects mice against ricin intoxication. Vaccine 2002;20(27-28):3422-7.

[14] Amlot PL, Stone MJ, Cunningham D, Fay J, Newman J, Collins R, et al. A phase I study of an anti-CD22-deglycosylated ricin A chain immunotoxin in the treatment of B-cell lymphomas resistant to conventional therapy. Blood 1993 November 1, 1993;82(9):2624-33.

[15] Ready MP, Kim Y, Robertus JD. Site-Directed Mutagenesis of Ricin A-Chain and Implications for the Mechansim of Action. Proteins 1991;10:270-8.

[16] Smallshaw JE, Ghetie V, Rizo J, Fulmer JR, Trahan LL, Ghetie M-A, et al. Genetic engineering of an immunotoxin to eliminate pulmonary vascular leak in mice. Nat Biotech 2003;21(4):387-91.

[17] Smallshaw JE, Richardson JA, Pincus S, Schindler J, Vitetta ES. Preclinical toxicity and efficacy testing of RiVax®, a recombinant protein vaccine against ricin. Vaccine 2005;23(39):4775-84.

[18] Vitetta ES, Smallshaw JE, Coleman E, Jafri H, Foster C, Munford R, et al. A pilot clinical trial of a recombinant ricin vaccine in normal humans. Proc Natl Acad Sci USA 2006 February 14, 2006;103(7):2268-73.

[19] Peek LJ, Brey RN, Middaugh C. A rapid, three-step process for the preformulation of a recombinant ricin toxin A-chain vaccine. J Pharm Sci 2007;96(1):44-60.

[20] Norde W. Adsorption of proteins from solution at the solid-liquid interface. Adv Colloid Interface Sci 1986;25(4):267-340.

[21] Gupta RK, Rost BE. Aluminum Compounds as Vaccine Adjuvants. Methods in Molecular Medicine Vaccine Adjuvants: Preparation Methods and Research Protocols 2000;42(4).

[22] Al-Shakhshir RH, Regnier FE, White JL, Hem SL. Contribution of electrostatic and hydrophobic interactions to the adsorption of proteins by aluminum-containing adjuvants. Vaccine 1995;13(1):41-4.

[23] Jones LS, Peek LJ, Power J, Markham A, Yazzie B, Middaugh CR. Effects of Adsorption to Aluminum Salt Adjuvants on the Structure and Stability of Model Protein Antigens. J Biol Chem 2005 April 8, 2005;280(14):13406-14.

[24] Wittayanukulluk A, Jiang D, Regnier FE, Hem SL. Effect of microenvironment pH of aluminum hydroxide adjuvant on the chemical stability of adsorbed antigen. Vaccine 2004;22(9-10):1172-6.

[25] Gupta RK. Aluminum compounds as vaccine adjuvants. Advanced Drug Delivery Reviews 1998;32(3):155-72.

[26] Hansen B, Belfast M, Soung G, Song L, Egan PM, Capen R, et al. Effect of the strength of adsorption of hepatitis B surface antigen to aluminum hydroxide adjuvant on the immune response. Vaccine 2009;27(6):888-92.

[27] Hansen B, Sokolovska A, HogenEsch H, Hem SL. Relationship between the strength of antigen adsorption to an aluminum-containing adjuvant and the immune response. Vaccine 2007;25(36):6618-24.

Chapter 6

Conclusions

6.1 Summary and Conclusions

Recent trends in vaccine development are moving away from the historical attenuated and inactivated vaccine forms because of growing public safety concerns. Instead, the industry is focusing on new approaches which involve synthetically constructed materials such as recombinant subunit vaccines to reproducibly manufacture large quantities of high purity vaccine products. Despite the decreased antigenicity of subunit vaccines relative to their whole cell counterparts, several FDA approved examples of recombinant vaccines exist and many more are currently in development. Presented here are data from each of several stages involved in the development of a recombinant subunit vaccine from the time of antigen identification to clinical studies.

In chapter 2, we began by taking an in depth look at the applications of biophysical chemistry to vaccine development. Using a multitude of spectroscopic techniques, we identified thermal stability boundaries over a range of pH (3-8) for a series of three structurally and functionally related mutated protein antigens, $MxiH^{\Delta 5}$, $PrgI^{\Delta 5}$ and $BsaL^{\Delta 5}$, each from different gram-negative bacterial pathogens. Using circular dichroism spectroscopy, we confirmed NMR structural results indicating that the proteins are largely alpha-helical in character. We also found that the mutant proteins are all extremely thermally labile with changes in secondary and tertiary structural elements beginning at temperatures below 25 ^{o}C in many cases. Furthermore, we discovered that the proteins displayed molten globule-like behavior in the physiological temperature range. This observation was significant not only for formulation development, but also relevant to studies of the biological function of these proteins in their respective systems.

At a concentration of approximately 0.2 mg/mL, all observed thermal transitions were reversible and no indications of insoluble aggregation were observed using static light scattering techniques. This knowledge aided us in the development of excipient screening assays discussed in Chapter 3.

Using knowledge acquired during the comprehensive structural studies of each of the three antigens, we conducted a pre-formulation survey of several key formulation aspects. We first evaluated the effect of a series of 'generally regarded as safe' (GRAS) compounds on the thermal stability of the antigens. This type of assay is often commonly done by monitoring inhibition of protein aggregation through the use of static light scattering techniques. As mentioned above, however, no insoluble aggregation was observed for any of the three antigens during the biophysical characterization studies. Therefore, we used circular dichroism spectroscopy and evaluated excipients based on their ability to increase the midpoint of the thermal melting (T_m). An increase in thermal stability was observed for $MxiH^{\Delta 5}$ and $PrgI^{\Delta 5}$ in the presence of certain carbohydrates and polyols, and an optimal concentration of 10% Sucrose and 5% Dextrose established. $BsaL^{\Delta 5}$ displayed non-sigmoidal thermal melting curves preventing the calculation of T_m values. Visual analysis of the data, however, suggested that this protein was also stabilized by the presence of the same excipients identified for $MxiH^{\Delta 5}$ and $PrgI^{\Delta 5}$. We next examined the adsorption behavior of each of the antigens to both aluminum hydroxide and aluminum phosphate adjuvants. Given the overall acidic nature of the antigens (pI<5), it was not surprising to find that their interactions with aluminum hydroxide (PZC 11) were far greater than those with aluminum phosphate (PZC 5). We

found that the nature of the interaction between the antigens and adjuvant, however, was not primarily electrostatic in nature, but rather appeared to be a result of hydrogen bonding and Van der Waals interactions among other potential interactions. Furthermore, it was observed that the nature of the interactions between the antigen and adjuvant changed over time ultimately resulting in a degree of irreversible binding. This phenomenon has been observed previously [1], and is attributed to adjustments in protein structure resulting in the establishment of new and stronger contacts with the adjuvant surface. It was unclear what effect the change in adsorption properties over time had on the availability of the antigen, thus we studied the interactions of the adsorbed antigens with specific antibodies. We found that a decrease in interaction was observed for the adsorbed samples which had been stored at an accelerated temperature (40 ^{o}C), but not those stored at 4 ^{o}C. In our final study, we used elution treatment and peptide mapping and concluded that the difference was probably structural in nature because no detectable changes were observed in the protein primary sequence.

Chapter 4 presented immunogenicity data for two of the three antigens, MxiH$^{\Delta 5}$ and PrgI$^{\Delta 5}$. The experiments were performed in a murine model in which animals were intramuscularly inoculated 3 times at two week intervals. Blood was collected via the submandibular vein and assayed for antigen-specific IgG using a standard ELISA assay. We found that MxiH$^{\Delta 5}$ and PrgI$^{\Delta 5}$ are immunogenic, and display significant dose dependency. Additionally, we found that as expected, the co-administration of aluminum hydroxide resulted in an increased antibody response relative to inoculation with soluble protein. We had previously proposed that administration of an oligomerized version of

the needle antigens would elicit a superior immune response relative to monomer antigen. We were able to confirm this hypothesis for MxiH from the *Shigella* system. We also hypothesized that co-administration of one of the needle antigens with a second surface exposed protein from the bacterial system would result in a greater response than each of the antigens elicited alone. We were interested to find that this hypothesis was true for antigens from *Shigella*, but not necessarily for those from *Salmonella*.

The final chapter pertains to accelerated and real time studies of an adsorbed recombinant subunit vaccine (rRTA) for ricin toxin. Work similar to that presented for the bacterial antigens in chapters 2-4 has been previously documented for this antigen by this laboratory [2]. Here we further investigated the effect of adjuvant surface adsorption, similar to the approach briefly discussed in chapter 3 for the pathogenic subunit antigens, for rRTA stability. We used a fluorescence emission method which was not helpful in initial studies of the adsorbed bacterial antigens due to the solvent exposed nature of the sole Trp residue of these proteins. Using this method for rRTA however, we observed a continual red shift in Trp emission indicating that with time, the protein was gradually unfolding on the adjuvant surface. We also noted that the shift was much more rapid and extreme when storage occurred at an elevated temperature (40 vs. 4 ^{o}C). The efficacy of the material stored at 4 vs. 40 ^{o}C was evaluated in an animal study. The results indicated that despite inducing similar antibody levels, the adsorbed product stored at 40 ^{o}C was not protective, while the 4 ^{o}C incubated material was. This result suggested that the results of the fluorescence assay may correlate with the efficacy of the vaccine. Thus, we conducted accelerated excipient screening of the adsorbed antigen to

identify compounds which might slow or impede the loss of biological activity. We were unable to identify any promising excipient candidates, but instead examined the possibility that an elevated pH on the adjuvant surface might be the source of physical alterations observed of the surface adsorbed protein [3]. We then used a previously documented technique [3] to reduce the surface pH by treatment with phosphate anion. We found that rRTA unfolding was significantly reduced by this surface modification. Unfortunately, the presence of phosphate resulted in a decreased adsorption capacity of the adjuvant causing much of the protein to remain free in solution. Given the noted instability of rRTA in solution, we attempted to decrease the unbound portion by increasing the aluminum hydroxide content and optimizing the phosphate concentration to achieve the greatest stabilization with the least surface desorption. By these actions, we were able to identify a stable, adsorbed rRTA formulation, and proposed animal studies to evaluate the efficacy of the potential product.

6.2 Future Directions

With respect to the continued development of the three bacterial antigens $MxiH^{\Delta 5}$, $PrgI^{\Delta 5}$ and $BsaL^{\Delta 5}$, the next key task is to evaluate the efficacy of each in a murine protection study. This type of experiment would involve inoculating mice with appropriate vaccine formulations and subsequently exposing them to the respective pathogens. Although we have shown here that $MxiH^{\Delta 5}$ and $PrgI^{\Delta 5}$ are capable of eliciting a robust antibody response, this may or may not result in protection. This portion of the development process will be one of the most critical for these antigens

because as mentioned in chapter 4, the route of infection used by each of the pathogens differs. As a result, the type of immune response required for protection may also differ. Subsequent to challenge experiments, it may be necessary to investigate the potential for mucosal delivery of these antigens which would require additional animal work as well as formulation development. The aluminum salt adjuvant used here was chosen because it is suitable for intramuscular injection and is currently the only class of vaccine adjuvant approved. Intranasal delivery, however, would require a different adjuvant and therefore additional formulation studies.

With respect to formulation development, there are several possibilities for further improvement. First, we have shown here that administration of an oligomerized needle antigen results in a largely increased immune response over the monomer version, and thus it would be advantageous to examine possible recombinant methods for preparing oligomerized versions in a reproducible manner. Secondly, using the *Shigella* system we have also shown that it may be possible to boost the immune response by administering a bivalent vaccine containing antigens from a single bacterial species. However, we also observed a non-synergistic response when the same experiment was conducted using antigens from the *Salmonella* system. Therefore, further development would be required to evaluate the advantages of this approach for each bacterial system individually. Lastly, it has been suggested that a single multivalent vaccine containing antigens from several bacterial species including *Shigella*, *Salmonella*, and *Burkholderia* may be feasible. This type of formulation would offer several advantages over individual

vaccines such as increased patient compliance and the potential for cross-protection, but thorough immunogenicity studies would be required to confirm this.

Further development of the vaccines would also include toxicology studies to evaluate safety of the vaccine, and field trials of the vaccines in highly affected regions. Furthermore, it may be necessary to lyophilize the formulations in order to ensure biological activity is maintained during transport to developing nations where the vaccines are greatly needed but the cold chain is inadequate.

The rRTA vaccine is in a later stage of development than the bacterial antigens. A formal toxicology study has already been conducted indicating the administration of RiVax® is safe. Therefore, if the phosphate containing formulation is shown to preserve the biological activity of the vaccine, the next step would be to manufacture the vaccine under GMP conditions and proceed with a non-human primate challenge study, a process which is underway under the guidance of DOR Biopharma Inc. The field studies proposed above for the bacterial pathogens are not feasible for this type of formulation due to that fact that intentional exposure to the fatal toxin is obviously unacceptable, and there does not exist a group of people regularly exposed to the toxin. Thus, the first efficacy testing in humans would be the first use of the vaccine, although hopefully this will never be necessary.

I present here work toward the development of several recombinant protein vaccines. Although they share some common characteristics, subunit vaccines vary widely from one another and each presents distinct challenges which must be addressed on a case-by-case basis. The complexity of the immune system and highly dynamic

behavior of macromolecules make it difficult to envision the development of an empirical subunit vaccine formulation strategy, but it seems that if progress continues at the current pace, we may acquire enough data and experience to do so in the relatively near future.

6.3 Bibliography

[1] Norde W. Adsorption of proteins from solution at the solid-liquid interface. Adv Colloid Interface Sci 1986;25(4):267-340.

[2] Peek LJ, Brey RN, Middaugh C. A rapid, three-step process for the preformulation of a recombinant ricin toxin A-chain vaccine. J Pharm Sci 2007;96(1):44-60.

[3] Wittayanukulluk A, Jiang D, Regnier FE, Hem SL. Effect of microenvironment pH of aluminum hydroxide adjuvant on the chemical stability of adsorbed antigen. Vaccine 2004;22(9-10):1172-6.